KU LEUVEN
FACULTEIT GENEESKUNDE
BIOMEDISCHE WETENSCHAPPEN

Notch-1 signaaltransductie en oligodendrocyten dysfunctie in amyotrofe laterale sclerose

(Notch-1 signaling and oligodendrocyte dysfunction in amyotrophic lateral sclerosis)

Masterproef voorgedragen
tot het behalen van de
graad van Master of Science in de
biomedische wetenschappen
door Caroline EYKENS

Promotor: Prof. dr. Wim ROBBERECHT
Faculteit Geneeskunde
Departement Neurowetenschappen
Afdeling Experimentele Neurologie

Leuven, 2013

KU LEUVEN
FACULTEIT GENEESKUNDE
BIOMEDISCHE WETENSCHAPPEN

Notch-1 signaaltransductie en oligodendrocyten dysfunctie in amyotrofe laterale sclerose

(Notch-1 signaling and oligodendrocyte dysfunction in amyotrophic lateral sclerosis)

Masterproef voorgedragen
tot het behalen van de
graad van Master of Science in de
biomedische wetenschappen
door Caroline EYKENS

Promotor: Prof. dr. Wim ROBBERECHT
Faculteit Geneeskunde
Departement Neurowetenschappen
Afdeling Experimentele Neurologie

Leuven, 2013

Acknowledgements

So this is it. Nine months went by and the final words of my thesis will be written in the next couple of minutes. With little confidence and not knowing what to expect, I started this journey. It would have been impossible to realize the work I've delivered without the help of many. I therefore wish to thank those who've helped me through this period.

First of all, I would like to thank my promoter Prof. Dr. Wim Robberecht for believing in me and giving me the opportunity to start this thesis. Thank you for letting me be a member of the Neurobiology lab, for the advice throughout the year and for bringing out the best in me.

Secondly I would like to express my gratitude to my supervisor. Annelies, thank you for the continual guidance and support throughout this work. I could always direct my questions to you and in case of problems, you were there instantly to help me out. You are a very dedicated and hardworking PhD student who is very precise in handling experiments. Thank you for passing on your knowledge to me and teaching me a lot of new skills. During the time we've worked together there were a lot of funny moments, however, at crucial times you took full responsibility. To summarize, I could not have wished for a better supervisor.

I certainly cannot forget to mention the people from the lab. André, Bea, Begga, Elke, Laura, Lawrence, Lien, Lies, Lindsay, Louis, Mieke, Miguel, Nathalie, Nicole, Sara (pequeñita mala/buena), Sarah, Steven, Tom, Veerle, Veronick, Wanda, Wendy: thank you for the unforgettable time in and beyond the lab and for creating an enjoyable atmosphere to work in. There were a lot of amusing situations and also moments in which you couldn't get enough of teasing me. I'm still not fully convinced that it was to 'strengthen me', but I will give you guys the benefit of the doubt.

A person whom I respect a lot and who was always there to keep me motivated is Christine. Thank you for the support and encouraging cards you've given me over the past years. You are an inspiration for a lot of people and you remind me every day why the work delivered by researchers is so important. Thank you for all of this.

I would also like to thank my grandfather, who has taught me to persevere in the most difficult of situations and to keep in mind that there will always be light at the end of the tunnel. You will always be the one person in my life that I admire most. I really regret that you couldn't witness the evolution I went through during the past months and I regret even more that you can't see me graduate. But I know that you've been with me the whole time, watching over my shoulder. I'm sure that you would have been proud of me.

And finally, special thanks to my parents for giving me, amongst other things, the opportunity to study Biomedical Sciences. Mom, I know we've had a lot to deal with over the past years, but thank you for the support and love you've given me. I now realize even more that the warmth and appreciation from people you care about is indispensable to achieve something in life.

Abstract

Background The exact mechanism underlying the neurodegenerative disorder, amyotrophic lateral sclerosis (ALS), is poorly understood. Recently, the concept of ALS as a non-cell autonomous disease has emerged, meaning that other cell-types contribute to motor neuron degeneration. In this study, we focused on oligodendrocytes that degenerate and are replaced by new but dysfunctional oligodendrocytes. Since Notch-1 signaling is described to inhibit oligodendrocyte precursor cell (OPC) differentiation into functional oligodendrocytes, we hypothesize that aberrant Notch-1 activity may contribute to the oligodendrocyte pathology observed in ALS.

Methods We first characterized the Notch-1 expression pattern in the spinal cord of $SOD1^{G93A}$ mice, using immunofluorescent stainings. Secondly, a ubiquitous Notch-1 deletion $SOD1^{G93A}$ model was established through tamoxifen-inducible recombination by CAGCre-ER. We designed primers for genotyping and determined recombination efficiency of CAGCre-ER by means of RT-PCR. In this model, oligodendrocyte function was investigated by immunoblotting MBP and MCT-1, markers for myelination and trophic support. We recorded compound muscle action potentials and quantified the percentage of neuromuscular junction innervation at the gastrocnemius muscle.

Results Notch-1 activation was observed in neurons, oligodendrocytes and OPCs. The designed primers were specific for CAGCre-ER and the recombination efficiency of CAGCre-ER was optimal in the spinal cord. Notch-1 deletion in all cell-types of $SOD1^{G93A}$ mice, resulted into an increase of MBP and MCT-1 expression, higher CMAP amplitudes and an increased number of innervated neuromuscular junctions.

Conclusion Our results suggest that ubiquitous Notch-1 deletion exerts a beneficial effect on oligodendrocyte function, motor neuron survival and muscle innervation in the $SOD1^{G93A}$ mouse model for ALS.

Abbreviations

AD	Alzheimer's disease
Ala	Alanine
ALS	amyotrophic lateral sclerosis
AMPA	Alpha-Amino-3-Hydroxy-5-Methyl-4-Isoxazole Propionic Acid
APH-1	anterior pharynx-defective 1
APP	amyloid precursor protein
Aβ	amyloid β-peptide
bHLH	basic-helix-loop-helix
CAG	cytomegalovirus immediate-early enhancer and chicken β–actin promoter/enhancer
CBF1	C promoter-binding factor 1
CMAP	compound muscle action potential
CMV	cytomegalovirus
CNPase	2', 3'-cyclic nucleotide 3'-phosphodiesterase
CNS	central nervous system
CoRs	co-repressors
COX-2	cyclooxygenase-2
DAPI	4', 6-diamidino-2-phenylindole
EAAT-2	excitatory amino-acid transporter 2
EAE	experimental auto-immune encephalomyelitis
ER	endoplasmic reticulum
FALS	familial amyotrophic lateral sclerosis
FTLD	frontotemporal lobar degeneration
FUS/TLS	Fused in sarcoma and translated in liposarcoma
GABA	Gamma Amino Butyric Acid
GFAP	glial fibrillary acidic protein
Gly	Glycine
GSIs	γ-secretase inhibitors
Hes	Hairy/enhancer of split
Hey	Hairy/enhancer-of-split related with YRPW motif
HRP	horseradish peroxidase
IL2	Interleukin 2
iNOS	inducible nitric oxide synthase
LTP	long-term potentiation
MAG	myelin associated glycoprotein
MAM	Mastermind

MBP	myelin basic protein
MCT-1	monocarboxylate transporter 1
MCTs	monocarboxylate transporters
MS	multiple sclerosis
NECD	Notch extracellular domain
NEXT	Notch extracellular truncation
NG2	nerve-glia factor 2
NICD	Notch intracellular domain
NLS	nuclear localization signal
NMDA	N-Methyl-D-Aspartate
NMJs	neuromuscular junctions
NSCs	neuronal stem cells
OPCs	oligodendrocyte precursor cells
PBS	phosphate buffered saline
PBST	PBS with 0.1 % Triton X-100
PCR	Polymerase chain reaction
PDGFRα	platelet-derived growth factor α
PEN-2	presenilin enhancer 2
PEST	proline, glutamate, serine, threonine
PFA	paraformaldehyde
PLP	proteolipid protein
PNS	peripheral nervous system
PVDF	polyvinylidene difluoride
RAN	repeat-associated non-ATG
RBPjκ	recombination signal sequence-binding protein Jκ
RIPA	Radioimmunoprecipitation Assay
ROS	reactive oxygen species
SALS	sporadic amyotrophic lateral sclerosis
SDS-PAGE	sodium dodecyl sulfate polyacrylamide gel electrophoresis
SOD1	superoxide dismutase 1
TACE	TNF-α-converting enzyme
TARBP	TAR DNA-binding protein
TBS-T	Tris-Buffered Saline and Tween-20
TDP-43	transactivation response region DNA binding protein
T_m	melting temperature
TM	transmembrane
Tx	tamoxifen

Table of contents

1. Introduction

Alzheimer's, Huntington's and Parkinson's disease and amyotrophic lateral sclerosis (ALS) are the four most prevalent neurodegenerative disorders. The number of people suffering from these conditions is continuously increasing because of the growing ageing population. As a consequence, health care instances are put under a large financial pressure and both patient and relatives get to deal with an enormous emotional burden. It becomes almost superfluous to stress the importance of neurobiological research in discovering new targets to slow down and even find a cure for these devastating diseases.

In this study we will focus on ALS, a late-onset progressive neurodegenerative disease affecting motor neurons in spinal cord, brainstem and motor cortex. The clinical presentation is highly variable and disease onset ranges between 50 and 60 years. Patients suffer from muscle atrophy and weakness, spasticity, paralysis and ultimately die within 2 to 5 years after disease onset as no effective treatment is currently available. The incidence of ALS is 8 per 100,000 people whereas the prevalence is only 1 per 100,000 people. In 90 % of ALS cases, referred to as sporadic ALS (SALS), the etiology is unknown. Only for 10 % of ALS patients a disease causing gene has been identified. This so called familial ALS (FALS) form is mainly caused by dominant mutations in *C9ORF72, SOD1, TARBP* and *FUS/TLS*.

Mouse models for human mutant superoxide dismutase 1 (SOD1), that resemble the ALS motor phenotype, have been a very useful tool to elucidate the pathogenesis of ALS. Several proposed toxic mechanisms underlying the observed motor neuron death have emerged from these models. Recently it was shown that SOD1-induced ALS is not merely the result of its action in motor neurons, but also in cells beyond motor neurons such as astrocytes, microglia and oligodendrocytes. This means that the pathogenesis of ALS is non-cell autonomous. In $SOD1^{G93A}$ mice and ALS patients, gray matter oligodendrocytes degenerate prior to disease onset and are replaced by new oligodendrocytes. The newly formed oligodendrocytes are found to be dysfunctional, as the expression levels of the monocarboxylate transporter 1 (MCT-1) and myelin basic protein (MBP), two markers for proper functioning of oligodendrocytes, are decreased. Failure of trophic support to and myelination of the motor neurons might contribute to and aggravate the observed motor neuron death.

We hypothesize that Notch-1 signaling may contribute to ALS pathogenesis, as it is involved in neurogenesis, neurite outgrowth, maintenance of the neuronal stem cell pool in the adult central nervous system (CNS) and proliferation and differentiation of oligodendrocyte precursor cells (OPCs) into mature myelinating oligodendrocytes. Since differentiation of OPCs into functional oligodendrocytes is shown to be impaired in ALS and since Notch-1 is being expressed on OPCs and oligodendrocytes, we hypothesize that aberrant Notch-1 activity may contribute to this failure to generate new fully differentiated, mature and functional oligodendrocytes. This hypothesis is further supported by the evidence of Notch-1 involvement in other neurodegenerative diseases such as Alzheimer's disease and multiple sclerosis. Therefore, we investigated the contribution of Notch-1 in the pathogenesis of ALS by ubiquitously deleting its expression in the $SOD1^{G93A}$ mouse model.

2. Literature

2.1. Amyotrophic lateral sclerosis

2.1.1. Introduction

Amyotrophic lateral sclerosis (ALS) is a neurodegenerative disease characterized by selective loss of both upper motor neurons in motor cortex and brainstem and lower motor neurons in the spinal cord (5). The age of clinical onset is variable but generally ranges between 50 and 60 years (2, 5, 6). Symptoms emerge when the axon retracts and subsequent muscle denervation occurs. Patients suffer from progressive muscle atrophy, generalized weakness, fasciculations and spasticity resulting in loss of executive functions. Current medical practice only offers disease modifying drugs like riluzole, the sole FDA approved drug for ALS that is shown to modestly extend lifespan (7). Also multidisciplinary supportive care, such as ventilatory support in patients with respiratory insufficiency and gastrostomy for those with low vital capacity, represents an important concept of care for ALS patients by ensuring their quality of life (8). Despite these efforts, most patients die within 2 to 5 years after symptom onset as a consequence of respiratory failure, which is the main fatal event (2, 5, 6).

The incidence of ALS is 8 per 100,000 people whereas the prevalence is only 1 per 100,000 people, since most patients die within a handful of years (2, 9). In 90 % of ALS cases, referred to as sporadic ALS (SALS), the etiology is unknown. Only for 10 % of ALS patients an inheritable disease-causing genetic component is apparent (2). This so called familial ALS (FALS) form is clinically indistinguishable from SALS. The only feature that differentiates both forms is the lower mean age of onset in FALS (10).

2.1.2. Genetics

The genetic landscape of ALS is very complex. FALS is mainly caused by autosomal dominant mutations in 12 genes, the most common being *C9ORF72, SOD1, TARBP* and *FUS/TLS* (11).

2.1.2.1. SOD1

About 20 % of all FALS cases have mutations in the Cu, Zn superoxide dismutase 1 (*SOD1*) gene (12). SOD1 is a ubiquitously expressed enzyme involved in free radical scavenging. Until now more than 144, mainly missense, mutations scattered throughout the polypeptide have been described (13). Most of them have reduced SOD1 enzyme activity (for example Asp76Tyr, Asp90Ala, Gly85Arg) but some mutations (for example Gly37Arg, Ala89Val, Gly93Ala) result in normal or slightly reduced SOD1 function (10, 14). The finding of normal functioning SOD1 mutants to be involved in ALS pathogenesis together with the absence of motor degeneration in mice lacking SOD1, has led to the hypothesis that mutant SOD1 facilitates motor neuron death through a toxic gain-of-function rather than a loss-of-function (10, 15).

2.1.2.2. TDP-43 and FUS/TLS

Missense mutations in transactivation response region DNA binding protein (TDP-43), encoded by the TAR DNA-binding protein (*TARBP*) gene, account for 4 % of FALS cases and 2 % of cases diagnosed with SALS (16). Most of the mutations are located in the C-terminal ribonucleoprotein binding domain of the protein (17). TDP-43 shuttles between the nucleus and the cytoplasm and is involved in RNA processing. In most patients with ALS and frontotemporal lobar degeneration (FTLD), TDP-43 is present in cytoplasmic inclusions (18). It remains unclear whether altered TDP-43 nuclear-to-cytoplasmic localization contributes to ALS and FTLD pathogenesis by loss of its nuclear function or a toxic gain-of-function caused by aggregation.

Fused in sarcoma and translated in liposarcoma (*FUS/TLS*) resembles *TDP-43* in its structure and function. Like TDP-43, FUS/TLS is also found in cytoplasmic inclusions and missense mutations accumulate at the C-terminal part (19). *FUS/TLS* mutations are found in 4 % of FALS and 1 % of SALS cases (20). How they contribute to ALS pathology remains to be elucidated.

2.1.2.3. The 9p21 locus

The *C9ORF72* gene on chromosome 9 has recently become a hot topic in ALS research. The gene defect concerns a hexanucleotide-repeat expansion $(GGGGCC)_n$ in its 5' non-coding sequence (21). Normal individuals possess less than 30 repeats, while in ALS patients the repeat can be expanded up to 1,600 times (22). An abnormal expansion is found in about 40 % of FALS cases and in 7 % of patients with SALS (23). The dynamics of the repeat number might explain the heterogeneous clinical presentation in these patients.

The normal function of the C9ORF72 protein is unknown. Several hypotheses have been proposed by which the *C9ORF72* expansion might contribute to ALS pathogenesis. First of all, loss-of-function mutations since the levels of C9ORF72 mRNA are reduced by 50 % in ALS patients (24). Secondly, gain-of-function mutations as RNA foci are observed in neurons of patients with *C9ORF72* mutations (21). Another hypothesis includes repeat-associated non-ATG (RAN) translation which results into pathogenic accumulation of the truncated C9ORF72 protein (25). However, the exact mechanism by which the repeat expansion in *C9ORF72* causes ALS remains to be elucidated.

2.1.3. Animal models of ALS

2.1.3.1. General information

Various transgenic animal models of FALS have been generated (26). Since FALS and SALS are clinically similar, insights provided by these models can be extrapolated to both forms of this disorder. Mutant SOD1 mouse models of FALS have been very useful in discovering new mechanisms underlying ALS

pathogenesis (4). The biggest disadvantage however, is that they only represent 2 % of the total ALS population. Therefore, TDP-43 and FUS/TLS-based models are emerging, but their significance remains uncertain. C9ORF72-based models are currently unavailable as the *C9ORF72* repeat expansion is only discovered last year. Since the repeat underlies about 40 % of all FALS cases, it would be valuable to have such models at one's disposal. Therefore, several research groups are intensively working on the development of C9ORF72-based models. Besides rodent models for ALS, also *Drosophila* and zebrafish models are available, but they reach beyond the scope of this master thesis.

2.1.3.2. Mutant SOD1^{G93A} mouse model

The mutant SOD1^{G93A} mouse model, that develops pathology reminiscent of ALS, is one of the most frequently used models in ALS research and is also used in our laboratory. These mice overexpress the human *SOD1* gene with a substitution of Glycine (Gly) by Alanine (Ala) at position 93 (27). Until the age of 60 days the mice are asymptomatic. Disease onset starts 90 days after birth and is characterized by massive loss of motor neurons. The period between the asymptomatic stage and disease onset is being referred to as the pre-symptomatic stage. During this period, progressive microgliosis (around day 60) and astrocytosis (around day 80) are noticeable. At the symptomatic stage, posterior to disease onset, mice exhibit hind limb weakness and tremulous movements as initial symptoms. Around 140 days of age, referred to as the post-symptomatic stage, major symptoms such as progressive atrophy of hind limb muscles and paralysis occur. Mice show disability of gait, eating and drinking and generally die within 60 days after disease onset (around day 150) (27, 28).

The mechanism underlying the phenotype observed in SOD1^{G93A} mice concerns a toxic gain-of-function of mutant SOD1 (28). This conclusion is based on several findings. First of all, SOD1-induced FALS is inherited in an autosomal dominant fashion (13). Secondly, the severity of clinical ALS features does not correlate with the level of SOD1 activity (29). Thirdly, neither SOD1 knock-out nor SOD1 wild-type overexpressing mice show ALS-like pathology (15). The severity of pathological features observed in SOD1^{G93A} mice depends on transgene copy number (30). Mice carrying high *SOD1^{G93A}* copy numbers display disease pathology with early-onset and rapid progression. On the other hand, mice carrying low *SOD1^{G93A}* copy numbers show late-onset and slow progression (28). The SOD1^{G93A} mice model we use in our laboratory carries 28 copies of the *SOD1^{G93A}* gene and has a disease onset and progression as described above.

For now, mutant SOD1 models are most frequently used for the study of ALS. In spite of being good models, the exact mechanism by which the motor phenotype is being established, remains still uncertain. Several hypotheses like oxidative damage, mitochondrial dysfunction, defects in axonal transport and glial pathology have been proposed. These will be explained in more detail in the next section.

2.2. Current hypotheses for the underlying biology of ALS

The exact mechanism underlying selective motor neuron degeneration in ALS remains a mystery. Insights into the pathogenesis of ALS are mainly derived from transgenic mutant SOD1 mouse models that develop pathology reminiscent of that of ALS (27). Several hypotheses (Figure 1) to explain toxicity have been proposed and a combination of different mechanisms is most likely (4, 9, 31-33). An overview of these putative mechanisms will be given in the next paragraphs.

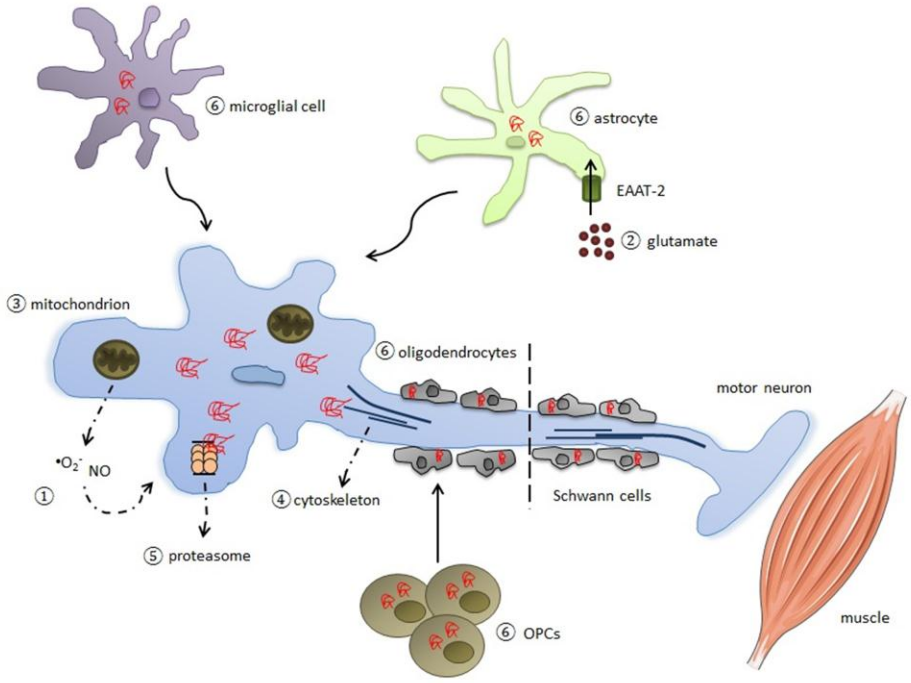

Figure 1. Putative mechanisms of toxicity in ALS pathogenesis. These mechanisms include ① oxidative damage, intracellular accumulation of mutant SOD1 aggregates (), ② glutamate excitotoxicity, ③ mitochondrial dysfunction, ④ defects in axonal transport, ⑤ proteasome inhibition in motor neurons and other cells and ⑥ glial pathology. This illustration is by analogy with (4).

2.2.1. Oxidative stress

SOD1 is a cytoplasmic free radical scavenging enzyme which is ubiquitously expressed. In normal conditions it protects intracellular components from reactive oxygen species (ROS) induced injury, which is a consequence of the imbalance between scavenging and production of ROS. ROS are byproducts of aerobic respiration and arise during mitochondrial oxidative phosphorylation (34). When electron leakage from the respiratory chain occurs, oxygen is left behind in an incomplete reduced state entailing reactive oxygen radicals (35). Cells possess different ROS scavenging pathways to protect themselves against oxidative stress (2). For example catalases, superoxide dismutases and peroxidases that neutralize free radicals (Figure 2a). Also glutathione, vitamin C and vitamin E fulfill a pivotal role as cellular antioxidants.

More than 114 mutations scattered throughout the SOD1 polypeptide have been linked to ALS and account for 2 % of all ALS cases (13). A number of pathological studies report an increase in oxidative damage in *post-mortem* tissue of ALS patients (36). Motor neurons possess high levels of SOD1 protein in their cell body and axonal processes, providing them with a robust defense mechanism against oxidative stress (37). As it is known that the mitochondrial oxidative metabolism is the main source of ROS production, and that motor neurons show a very high mitochondrial activity due to their extraordinary metabolic requirements, it is plausible that this is the reason why motor neurons are so sensitive to injury in presence of mutant SOD1 (38).

No consensus on the mechanism through which mutant SOD1 facilitates motor neuron death has been established yet. There are two lines of evidence in favor of the toxic gain-of-function rather than the loss-of-function hypothesis (39). First, there is the observation that SOD1 knock-out mice do not develop a motor phenotype (15). Second, an X-ray crystallographic study that revealed a structural change in the active cupper site of mutant SOD1 (40). In this way, besides its normal substrate of superoxide anions ($^{\bullet}O_2^-$), also inappropriate substrates like hydrogen peroxide (H_2O_2) and peroxynitrite (^-ONOO) gain access to the mutant enzyme (Figure 2b,c). As a result, reactive hydroxyl radicals ($^{\bullet}OH$) arise, promoting a cascade of oxidative damage (41).

Thus, aberrant oxidative reactions result into an overload of ROS production. This reflects a toxic gain-of-function of mutant SOD1 to be responsible for the pathogenesis of ALS. Despite the attractiveness of the previously mentioned hypotheses, none of them is likely to fully represent the complete spectrum of toxicity in ALS (9, 42, 43).

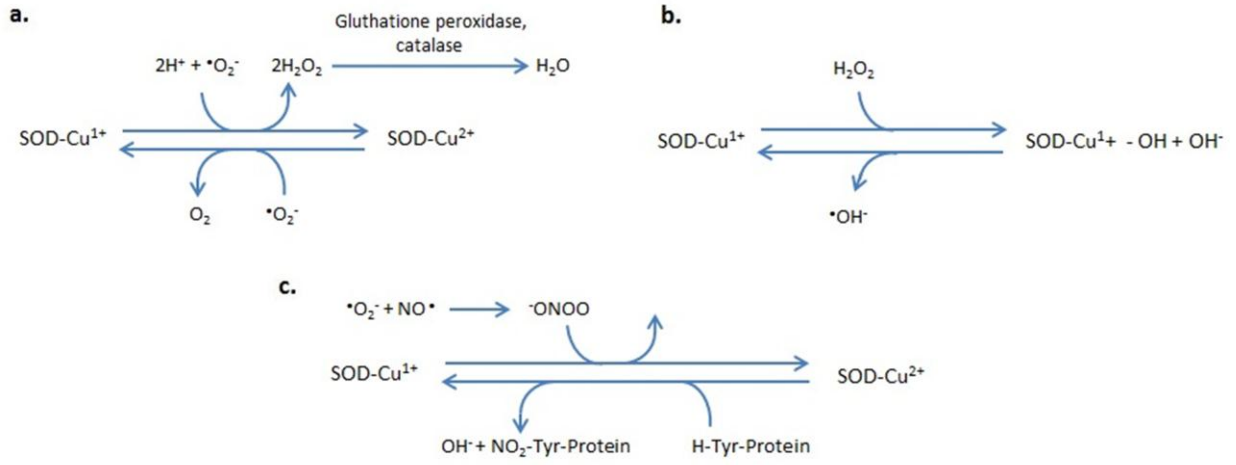

Figure 2a. Normal SOD1 chemistry with superoxide as substrate. SOD1 converts superoxide anions ($^{\bullet}O_2^-$), a naturel byproduct of aerobic metabolism, into hydrogen peroxide (H_2O_2) in a two-step redox reaction. Copper in the active site undergoes a reduction (Cu^{2+}) and re-oxidation reaction (Cu^{1+}) resulting in oxygen (O_2) and hydrogen peroxide (H_2O_2) formation, which is consequently processed by gluthatione peroxidase and catalase to produce water (H_2O). **2b. Peroxidase hypothesis.** Use of hydrogen peroxide (H_2O_2) as an inappropriate substrate by mutant SOD1-Cu^{2+} produces the reactive hydroxyl radical ($^{\bullet}OH$-). **2c. Peroxynitrite hypothesis.** Peroxynitrite, which can spontaneously form superoxide ($^{\bullet}O_2^-$), and nitric oxide ($NO^{\bullet}$), yields Tyrosine (Tyr) nitration when used as a substrate by mutant SOD1. As a result, the function of targeted proteins becomes disrupted. This illustration is by analogy with (2).

2.2.2. SOD1 aggregation

Presence of intracellular protein aggregates or inclusions have been identified in motor neurons and glial cells of mutant SOD1 mice and ALS patients (28, 44). These aggregates appear before disease onset and an accumulation of these aggregates occurs with disease progression. This clearly indicates that occurrence of SOD1 aggregates is an early event in the pathogenesis of ALS (45-47). Toxicity of these aggregates arises through sequestration of essential cellular components, reduced chaperone activity and impairment of the ubiquitin-proteasome system by overloading it with misfolded mutant SOD1 (48-50). The latter explains the presence of ubiquitin-positive aggregates in both FALS and SALS (42, 50, 51).

2.2.3. Glutamate-mediated excitotoxicity

Increased levels of glutamate are detectable in the cerebrospinal fluid of ALS patients, indicating abnormal glutamate handling (52-54). Riluzole is the only FDA approved therapy for ALS and functions by decreasing glutamate toxicity through an unknown mechanism (7, 55, 56).

Overstimulation by glutamate triggers repetitive firing of motor neurons, thereby driving an increased calcium influx through permissive glutamate receptors, such as Alpha-Amino-3-Hydroxy-5-Methyl-4-Isoxazole Propionic Acid (AMPA), N-Methyl-D-Aspartate (NMDA) and kainate receptors (2, 9). When calcium storage within mitochondria and the endoplasmic reticulum (ER) becomes saturated, the resulting increase in intracellular calcium becomes toxic. This process is called excitotoxicity (57). The vicious cycle ultimately results in neuronal damage and death (2, 9). As motor neurons express high levels of the AMPA glutamate receptor, they are very sensitive to this glutamate-induced excitotoxicity. The GluR2 receptor subunit is necessary in the glutamate receptor to lower calcium permeability, thereby providing a protection mechanism against excitotoxicity. However, motor neurons possess a lower proportion of this GluR2 subunit and it is known that ALS patients have a decline in their GluR2 levels, making them even more vulnerable to excitotoxicity (58).

Rapid removal of synaptic glutamate by the excitatory amino-acid transporter 2 (EAAT-2) is critical in preventing excitotoxicity (2). EAAT-2 is expressed on the processes of astrocytes surrounding the motor neurons (4). Substantial loss of this glial transporter in the motor cortex and spinal cord of mutant SOD1 mice and ALS patients has been reported (45, 59-62). Ceftriaxone, a β-lactam antibiotic that stimulates EAAT-2 expression, delayed disease onset and prolonged life span in mutant SOD1 mice (63). These observations underline the importance of rapid synaptic glutamate removal through EAAT-2 in preventing excitotoxicity.

2.2.4. Mitochondrial dysfunction

Mitochondrial dysfunction contributes to the phenotype of many neurodegenerative diseases (4). In motor neurons and muscles of ALS patients and mutant SOD1 mice, mitochondrial abnormalities such as

vacuolization and swelling are seen at pre-symptomatic stages (64-69). Therefore, mitochondria seem to be primary targets for mutant SOD1 mediated damage, delivering an important contribution to disease initiation (70, 71). Several mechanisms for this toxicity have been proposed, including clogging of mitochondrial importers and disturbance of calcium buffering (32). As a result, normal levels of glutamatergic stimulation can yield secondary excitotoxicity (72). The latter also fits within the proposed excitotoxic mechanism contributing to neuronal damage (73). Disruption of energy metabolism also renders an explanation for toxicity, since motor neurons possess very high metabolic requirements due to their enormously long axon. This feature makes them vulnerable to oxidative stress and the development of an energy deficit (74). Administration of creatine, enhancing the mitochondrial energy storage capacity, extended the survival in mutant SOD1 mice but was ineffective in human clinical trials (75-78). However, no consensus on the energy disturbance hypothesis has been obtained, since the electron transport chain was reported to be either unchanged or altered (4). Lastly, mitochondria are the main gatekeepers of apoptosis, as they release cytochrome c through their transition pore and thereby initiate cell death (79). Apoptosis is known to be the mechanism by which motor neurons die in mutant SOD1 mice, so the correlation with mitochondrial dysfunction is quite obvious.

2.2.5. Impairment of axonal transport

Motor neurons possess very long axons that necessitate a robust cytoskeleton. Neurofilaments are the major components of the cytoskeleton and play a role in the maintenance of cell shape and more importantly in axonal transport (33). Motor neurons are very dependent on this axonal transport because of their enormous metabolic needs and very long axons. In this context, the delivery of mitochondria is very indispensable to meet local energy requirements and this is established through the neurofilaments (80).

Also components synthesized within the cell body, such as proteins and cell organelles, need to be delivered to axons and synapses by means of axonal transport (81). If not, axons start wearing off and neurons become jeopardized (82).

Abnormal assembly and misaccumulation of neurofilaments in the cell body and proximal axons of motor neurons is one of the hallmarks of ALS pathology (83). SOD1 mutants have also been shown to slow down both anterograde and retrograde transport (81, 84). The impairment of axonal transport is observed prior to disease onset (85).

2.2.6. Involvement of non-neuronal cells

A growing number of studies support the hypothesis that ALS is a non-cell autonomous disease (4, 31, 86, 87). The cellular neighborhood, especially mutant SOD1 expressing glial cells, does matter in motor neuron death. This concept will be explained in section 2.3.

2.3. Non-cell autonomous death of motor neurons in ALS

Contrary to what has been thought for a long time, ALS is a non-cell autonomous disease. This means that besides motor neurons, other cell types play a role in the pathogenesis of ALS as well. The motor neuron degeneration seen in ALS is not only the result of the action of mutant SOD1 within the motor neurons, but results also from the mutant SOD1 expression in the non-neuronal cells neighboring the motor neurons, such as astrocytes, microglial cells, oligodendrocytes and nerve-glia factor 2 (NG2) glial cells, thereby aggravating the motor neuron damage (Figure 3) (4, 31, 88, 89). This discovery is based on two observations. First of all, the observation that mutant SOD1 expression only within motor neurons is not sufficient to cause ALS-like disease in mice (90-92). One could argue that the level of mutant SOD1 expression in this set-up was insufficient to cause neurodegeneration. However, higher mutant SOD1 expression levels only resulted in pathogenic changes at very late time points. Secondly, the observation that selective expression of mutant SOD1 in astrocytes or microglia, gave no signs of motor neuron pathology neither (90, 93). The notion that motor neuron death is non-cell autonomous was supported by an experiment with chimeric mice, in which normal cells were combined with cells carrying mutant SOD1 (94). These mice showed a significantly extended survival. All this taken together led to the hypothesis that simultaneous expression of mutant SOD1 in both the motor neurons and the non-neuronal cells surrounding the motor neurons is necessary to induce motor neuron degeneration.

To unravel which cells are impaired by mutant SOD1 and how this impairment contributes to disease onset and progression, mutant *SOD1* was excised in a cell-specific way using the Cre-Lox recombination system (86, 95). The recombination findings and pathogenic properties of the CNS cells of interest will be discussed in the next paragraphs.

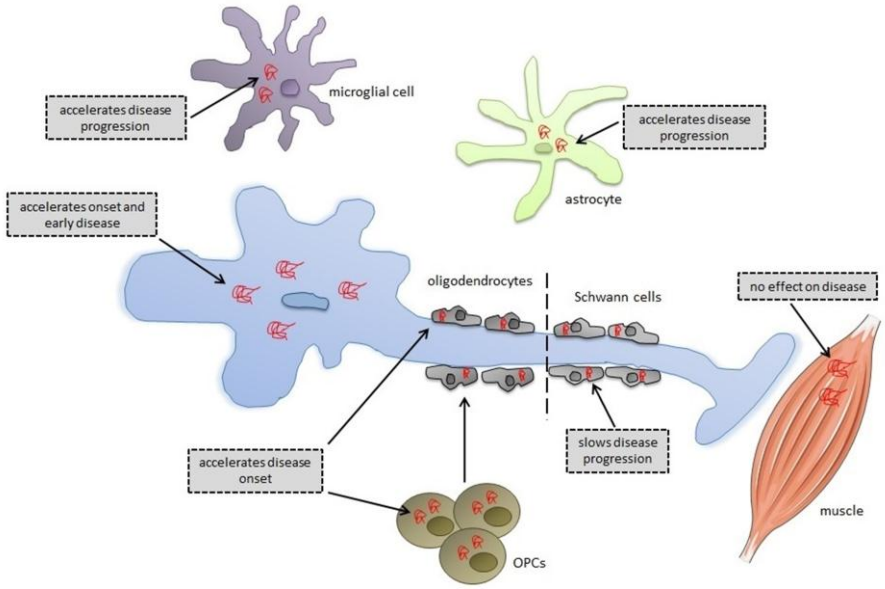

Figure 3. **ALS is a non-cell autonomous disease**. Expression of mutant SOD1 (SOD1) in motor neurons directs disease onset and early disease development. Also non-neuronal cells surrounding the motor neurons contribute to ALS pathogenesis via SOD1-mediated toxicity. The presence of mutant SOD1 in microglial cells and astrocytes accelerates disease progression, whereas disease onset remains unchanged. Surprisingly, Schwann cells expressing mutant SOD1 were found to slow down disease progression. Mutant SOD1 expressing oligodendrocyte precursor cells (OPCs) and oligodendrocytes accelerate disease onset and shorten survival. Mutant SOD1 within muscles does not affect ALS onset, nor ALS progression. This illustration is by analogy with (4).

2.3.1. Motor neurons

To examine to what extend mutant SOD1 within motor neurons contributes to disease pathogenesis, experiments were conducted with floxed mutant SOD1 mice expressing Cre-recombinase under the control of the Islet-1 promoter (86, 95). This permits selective deletion of mutant *SOD1* within motor neuron progenitors. This resulted into a significant delay of disease onset and early progression (pre-symptomatic stage) with 18 and 31 days respectively. However, no alterations in later disease progression were observed (4, 86). So the mutant SOD1 damage within motor neurons determines disease onset and early progression, whereas other cell types are responsible for later disease progression (described below).

2.3.2. Microglia

Microglial cells are the macrophages of the CNS and constantly survey the environment for damaging factors. They can exert deleterious (M1 microglia) and benign (M2 microglia) effects depending on their microenvironment (96-98). When encountering a pathogenic insult, they shift from the surveying to the activated state and release neurotoxic molecules (87). They also produce cyclooxygenase-2 (COX-2) that in turn stimulates cytokine synthesis, resulting in a vicious cycle of neuroinflammation (99).

In ALS, strong microglial proliferation and activation occur. This so-called microgliosis is already present in the ventral horn of the spinal cord prior to motor neuron loss (100, 101). The number of activated microglia escalates during disease progression until end-stage and concomitant infiltration of T-cells and cytotoxic T-cells occurs (102). This creates a neurotoxic environment for motor neurons, contributing to their death.

Pharmacological inhibition of microglial activation with minocycline in mutant SOD1 mice slowed down disease progression and increased survival, whereas COX-2 inhibitors only prolonged survival (103-106). Selective deletion of mutant *SOD1* in microglia by using Cre-recombinase under control of the microglia specific CD11b promoter delayed later disease progression. Early disease progression remained unchanged but survival was significantly extended with 99 days (86, 95). This is why microglia are thought to drive rapid disease progression during the later disease stage by reacting to the initial motor neuron damage and thereby aggravating it (4).

2.3.3. Astrocytes

Astrocytes are star-shaped glial cells present in the brain and spinal cord. They fulfill two main functions in motor neuron maintenance. Firstly, they provide metabolic support to motor neurons by delivering nutrients like lactate (107). Secondly, astrocytes protect motor neurons against excitotoxicity by rapid removal of glutamate from the synaptic clefts. This is accomplished by EAAT-2 transporter which is expressed on the processes of the astrocyte (4, 31). EAAT-2 levels are reduced in the CNS of ALS patients and also in the spinal cords of mutant SOD1 mice and rats (45, 59, 61, 108). As a result, the glutamate

concentration increases in the synaptic clefts. AMPA and NMDA receptors on motor neurons become overstimulated, leading to excitotoxicity-induced motor neuron death (61). This EAAT-2 loss however is not caused by mutant SOD1, reflecting non-cell autonomous damage to astrocytes (95).

Astrocytosis is a process elicited by neuronal injury or neurodegeneration (109). In mutant SOD1 mice, astrocytes are at rest at the asymptomatic stage and become hypertrophic and activated together with the start of motor neuron loss. As disease progresses, astrocytes become even more reactive (87, 100, 110). Typically for astrocytosis is the upregulation of the glial fibrillary acidic protein (GFAP), and unlike microgliosis, reactive astrocytes do not proliferate (110, 111) and astrocytosis is not restricted to the ventral horn but also occurs in the dorsal horn and in the brain (112, 113).

The functional crosstalk between astrocytes and microglia is also an important concept in ALS pathogenesis (31). Astrocytes enhance the production of inducible nitric oxide synthase (iNOS) in microglia, promoting generation of deleterious nitrogen species (95, 114). So damage within astrocytes amplifies the inflammatory response of the microglia. In this way motor neurons are further damaged and disease progression is accelerated (95).

Experimental evidence for astrocytic contribution to disease progression came from floxed SOD1 mice expressing Cre-recombinase under the control of the astrocyte specific GFAP promoter (4, 94, 95). In these mice mutant *SOD1* is deleted selectively from the astrocytes, resulting into delay of microglial activation and consequently a slower disease progression. Overall survival was also extended with 60 days (86, 95).

2.3.4. Schwann cells

Schwann cells are the myelinating cells of the peripheral nervous system (PNS). Mutant SOD1 overexpression only within Schwann cells had no effect on locomotion, neuronal loss or axonal degeneration (115). In contrast, selective excision of mutant *SOD1* from Schwann cells yielded unexpected results. Disease onset remained unchanged whereas disease progression was significantly accelerated (116). This means that expression of mutant SOD1 in Schwann cells has a protective effect on ALS progression.

2.3.5. Oligodendrocytes and NG2 glial cells

In the concept of ALS as a non-cell autonomous disease, mainly astrocytes and microglia have been studied. Recently, an article was published demonstrating that *SOD1* excision in oligodendrocytes and NG2-expressing oligodendrocyte precursor cells delayed disease onset and prolonged survival (117). These experiments indicate that SOD1 expression within both cell types accelerates motor neuron degeneration. The role of oligodendrocytes in the pathogenesis of ALS is nowadays a hot topic, and will be explained in more detail in section 2.4.

2.4. Oligodendrocytic dysfunction in ALS

2.4.1. Oligodendrocytes

Oligodendrocytes are post-mitotic cells that promote rapid impulse propagation throughout the CNS by insulating axons with myelin (88, 89, 118). Their function is analogous to that of Schwann cells in the PNS. A single oligodendrocyte creates a multilayered myelin sheath by wrapping its cell membrane several times around up to fifty axons (118). Structural proteins, like myelin basic protein (MBP) and proteolipid protein (PLP), ensure compaction of the multilayered myelin sheath (119).

Myelination is not restricted to embryonic development, but also occurs during postnatal life. *Post-mortem* studies revealed that the formation of insulating myelin sheaths continues up to a person's 30s and possibly beyond (120). Also under conditions of injury or degeneration, remyelination is observed. For example in spinal cord injury, ependymal cells lining the central canal differentiate into myelinating oligodendrocytes. The latter migrate towards the site of the injury, trying to remyelinate the naked axons which are vulnerable for degeneration (121). Another example is multiple sclerosis (MS), a neurodegenerative disease in which the axonal myelin sheath is damaged after an immune attack. After an acute phase of demyelination, oligodendrocytes try to remyelinate the axons (122).

Having axons exceeding a length of more than one meter, motor neurons possess a high metabolic need. Since axons are only exposed to extracellular metabolites at the nodes of Ranvier, specialized transport systems are needed to provide trophic support (88). Lactate, pyruvate and ketone bodies are being transported by monocarboxylate transporters (MCTs) (123). Neurons express MCT-2 whereas glial cells express both MCT-1 and MCT-4 (124, 125). Nevertheless, MCT-1 is the most prominent transporter in the CNS and oligodendroglia form the major site of MCT-1 expression (126). In this way oligodendrocytes are the main metabolic providers of lactate to axons through the MCT-1 transporter (127).

Impairment of proper functioning of oligodendrocytes is known to contribute to the pathogenesis of neurological disorders, such as multiple sclerosis (MS) and leukodystrophies (128). Recent findings show oligodendrocytes to be also dysfunctional in ALS (88, 89) . This will be discussed in section 2.4.3.

2.4.2. NG2 glial cells

For long time, it was thought that oligodendrocytes themselves ensure remyelination at sites of demyelination. However, these cells are not able to divide as they are post-mitotic and therefore oligodendrocytes must be derived from precursor cells (129, 130). NG2 cells, marked by nerve-glia factor 2 proteoglycan and platelet-derived growth factor α (PDGFRα), are the oligodendrocyte precursor cells (OPCs) of the CNS and form a reservoir for the generation of new oligodendrocytes throughout life (131, 132). They are equally distributed in gray and white matter and still proliferate in the adult organism in response to mechanical CNS injury, excitotoxicity and demyelination (133). OPCs are able to mobilize to damaged regions and are found in demyelinated regions (134). Their function in the undamaged CNS is

still unclear. Given their expression of Gamma Amino Butyric Acid (GABA) and AMPA receptors and since their processes make intimate contact with the nodes of Ranvier and synapses, they are thought to influence neuronal activity (135-137).

The turnover rate of adult OPCs is slower compared with perinatal OPCs and the exact stimuli for differentiation remain unknown (138). *In vitro* experiments suggest OPCs to be multipotent cells that can differentiate into oligodendrocytes, neurons and astrocytes (139, 140). *In vivo* models however do not support this observation and found their lineage potential to be restricted to the oligodendrocytes (131).

The differentiation pathway of NG2 cells comprises several steps (141). Each step is characterized by typical cell morphology and specific molecular markers (Figure 4). Both need to be taken into account when evaluating the cell type identity, since markers can sometimes be inadequate. In ALS the differentiation of OPCs is compromised, as will be discussed in 2.4.3.

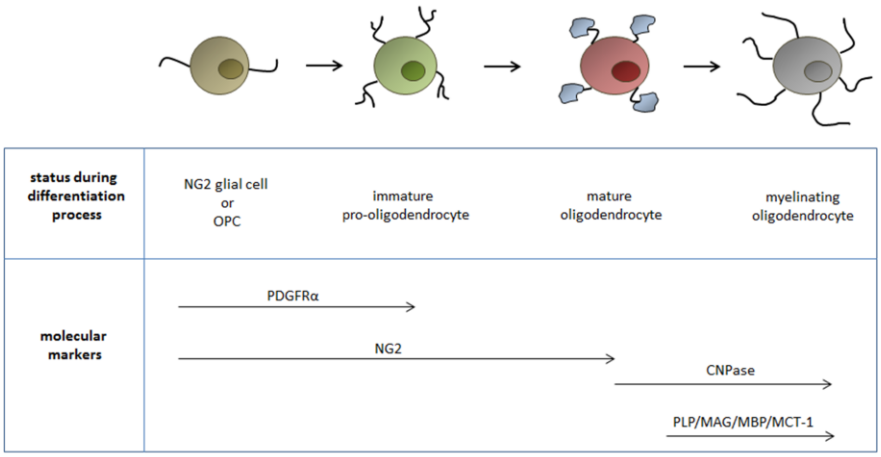

Figure 4. Oligodendroglial lineage scheme. During differentiation from oligodendrocyte precursor cells (OPCs) to oligodendrocytes, a morphological transformation takes place. Bipolar NG2 cells evolve into immature pro-oligodendrocytes bearing multiple processes, mature oligodendrocytes and finally functional myelinating oligodendrocytes. Together with this morphological change there is also a sequential expression of molecular markers: platelet-derived growth factor α (PDGFRα) in progenitors and pro-oligodendrocytes, nerve-glia factor 2 (NG2) proteoglycan in progenitors and (pro-) oligodendrocytes; 2', 3'-cyclic nucleotide 3'-phosphodiesterase (CNPase) in mature (myelinating) oligodendrocytes; monocarboxylate transporter 1 (MCT-1) and most of the myelin components, such as myelin associated glycoprotein (MAG), myelin basic protein (MBP) and proteolipid protein (PLP), in myelinating oligodendrocytes.

2.4.3. Impaired OPC differentiation and dysmorphic oligodendrocytes in ALS

In spinal cords of ALS patients and mutant SOD1 mice, oligodendrocyte pathology can be observed. Grey matter oligodendrocytes undergo morphological and functional changes (88, 89, 142). They degenerate and die even before motor neuron loss is present and this process of deterioration continues during disease progression (117). Nevertheless, the number of oligodendrocytes remains constant since their

loss is compensated by enhanced proliferation and differentiation of OPCs. The newly formed oligodendrocytes however, are dysmorphic, which means they have an enlarged cell body with an increased number of processes (89). They also fail to fully maturate as is indicated by their reduced MCT-1 and MBP expression levels (88, 89). No reduction of other oligodendrocytic markers, like myelin associated glycoprotein (MAG) and 2', 3'-cyclic nucleotide 3'-phosphodiesterase (CNPase), was observed since the number of oligodendrocytes remains unchanged (89).

Oligodendroglia form the major site of MCT-1 expression and thus constitute one of the most important cell types that nourish neurons with lactate (127). The expression of the MCT-1 lactate transporter is affected by the presence of mutant SOD1 species and the reduction of MBP can be explained in terms of this MCT-1 loss (89). Lactate, produced by astrocytes and transported by MCT-1, is not only being used by oligodendroglia to provide trophic support to motor neurons it also serves as a substrate for lipogenesis in oligodendrocytes to synthesize and maintain the lipid-rich myelin membrane in the CNS (127, 143-145). So with the loss of MCT-1, metabolic support of motor neurons, as well as myelination of motor neuron axons is affected. In this way, oligodendrocytes contribute to death of motor neurons in a non-cell autonomous way as described previously (88, 89, 146).

The cause of these changes in oligodendroglia remains unknown. Several signaling cascades have been described to inhibit myelination, for example Notch and Wnt signaling (147). For the Notch pathway, there is evidence to play a role in the timing of oligodendrocyte differentiation (89, 148). Experiments with Notch-1 expressing oligodendrocytes and OPCs from rat optic nerves showed a decline in the expression of the Notch-1 ligand, called Jagged-1, during periods of active myelination *in vivo*. OPCs transfected *in vitro* with constitutively activated Notch, fail to differentiate into MBP-positive oligodendrocytes and retain the bipolar morphology of OPCs (148, 149). Notch-1 inhibits oligodendrocyte differentiation by uncoupling OPC proliferation and differentiation (Figure 5). In this context, it is hypothesized that Notch is responsible for the OPCs to be arrested at an early stage of differentiation in ALS (148). Therefore the number of oligodendrocytes remains constant but they appear to be immature and are dysfunctional (89). The Notch signaling pathway will be discussed in more detail in section 2.5.

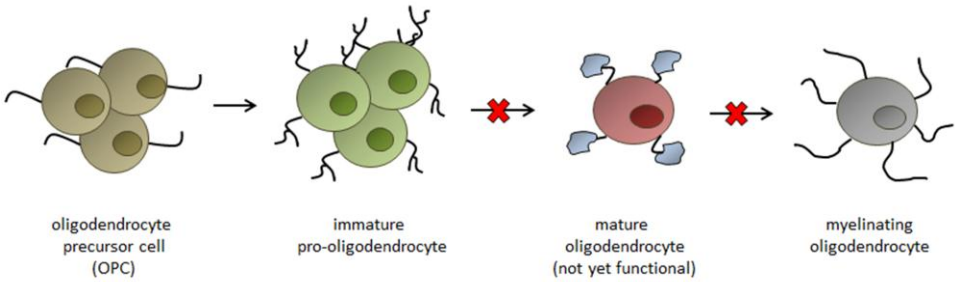

Figure 5. Notch-1 inhibits OPC differentiation into mature and functional oligodendrocytes. Since oligodendrocytes are post-mitotic cells that are not able to divide, they derive from a reservoir of oligodendrocyte precursor cells (OPCs). OPCs are kept in a proliferative state for maintenance of the precursor pool and OPC differentiation is directed by several cues. For example, binding of Notch-1 to its ligand inhibits differentiation (red crosses) of oligodendrocyte precursor cells (OPCs) into mature and functional oligodendrocytes. As a result, the number of immature and thus dysfunctional oligodendrocytes increases while the overall number of oligodendrocytes remains constant (3).

2.5. Notch signaling

The Notch signaling pathway orchestrates numerous developmental processes including differentiation, proliferation, maturation and function of several cell types (150-152). Notch-mediated signals have a pleiotropic outcome and are strictly controlled in terms of intensity and duration (153). Although Notch signaling is mainly known for its involvement in cell fate decisions and morphogenesis during embryonic development, accumulating evidence suggests a role for this pathway in postnatal life (122). For example, stem cell maintenance in the CNS and adult tissue homeostasis (154). Malfunction of Notch signaling is linked to multiple human disorders such as cancer, Alagille syndrome and spondylocostal dysostosis (152, 155). More importantly, aberrant Notch function has recently emerged as a major player in the pathogenesis of several neurodegenerative diseases, as described in section 2.5.3 (156).

2.5.1. Overview of the Notch signaling pathway

Notch signaling is triggered by direct contact between the Notch receptor on one cell and its ligand on a neighboring cell (Figure 6) (157). In mammals four Notch receptors (Notch-1, -2, -3, -4) and five Notch ligands (Delta-like-1, -3, -4 and Jagged-1, -2) have been identified (152, 157, 158). Notch receptors are heterodimeric single-pass transmembrane proteins. They are composed of an extracellular and intracellular domain, connected by the transmembrane domain (TM). In this study we will focus on the Notch-1 receptor.

Following ligand binding, the Notch receptor undergoes a conformational change, allowing a proteolytic cleavage to occur. As shown in Figure 6, two consecutive proteolytic cleavage steps take place. The first cleavage (S2) is mediated by the ADAM10 metalloprotease, also known as TNF-α-converting enzyme (TACE) (158). The Notch extracellular domain (NECD) is released from the membrane and subsequently undergoes transendocytosis in the ligand expressing cell (122). The lagging membrane tethered intracellular domain, called Notch extracellular truncation (NEXT), serves as a substrate for the second cleavage (S3) which is mediated by the γ-secretase complex. This complex contains presenilin as catalytic component and three co-factors: nicastrin, PEN-2 (presenilin enhancer 2) and APH-1 (anterior pharynx-defective 1) (159). As a result, the Notch intracellular domain (NICD) is released and is translocated to the nucleus by means of its nuclear localization signal (NLS). NICD itself cannot bind directly to the DNA and therefore forms a transcriptional complex with the nuclear protein Mastermind (MAM) and C promoter-binding factor 1 (CBF1), also known as recombination signal sequence-binding protein Jκ (RBPjκ) (153, 160). CBF1 is surrounded by co-repressors (CoRs) that are being displaced after NICD binding. This allows the NICD/MAM/CBF1 complex to bind to the promoter of downstream Notch target genes, hereby switching on their transcription (161).

The main Notch targets are basic-helix-loop-helix (bHLH) genes belonging to the Hairy/enhancer of split (*Hes*) and Hairy/enhancer-of-split related with YRPW motif (*Hey*) gene families (162). Hes-1, -5, -7 and Hey-1, -2 are best characterized in mammals. These proteins act as transcriptional repressors, especially of genes that are required for cell differentiation (163). Although the number of target genes is limited,

the effect of Notch activation is pleiotropic. For example enhancement of proliferation in some situations and induction of apoptosis in other situations (161).

Termination of Notch signaling is mediated through SEL-10, an E3 ubiquitin ligase. SEL-10 attaches a ubiquitin label to the proline, glutamate, serine, threonine (PEST) domain of NICD. In this way, NICD is transformed into a substrate for subsequent proteosomal degradation (164). The resulting negative regulation of Notch signaling is crucial, as sustained NICD accumulation can be deleterious.

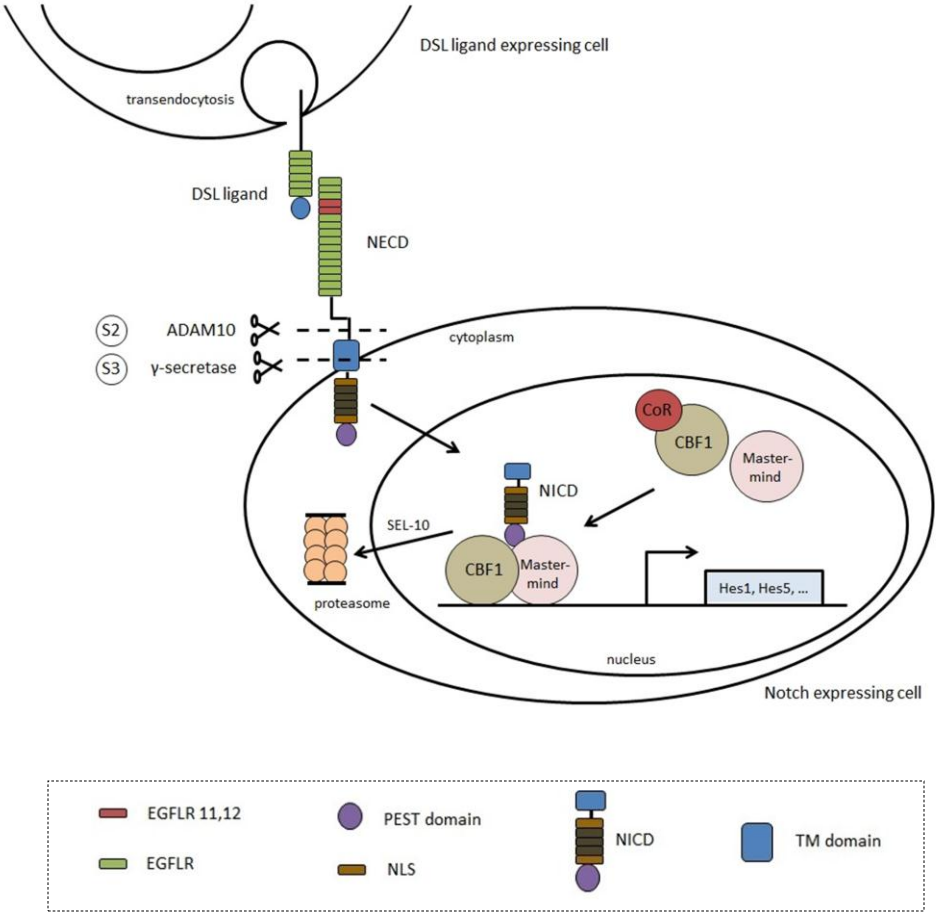

Figure 6. Overview of the Notch signaling pathway. Binding of the DSL (Delta, Serrate, LAG2) ligand on one cell to the extracellular epidermal growth factor-like repeats (EGFLR) 11 and 12 of the Notch receptor on the other cell results in a conformational change of this receptor. The first cleavage (S2) is mediated by the ADAM10 metalloprotease. The Notch extracellular domain (NECD) is released from the membrane and subsequently undergoes transendocytosis in the ligand expressing cell. The lagging membrane tethered intracellular domain, called Notch extracellular truncation (NEXT), undergoes the second cleavage (S3) which is mediated by the γ-secretase complex. As a result, the Notch intracellular domain (NICD) is cleaved off and sequestered to the nucleus by the nuclear localization signal (NLS). NICD cannot bind directly to DNA and therefore forms a complex with two transcriptional co-factors, namely the nuclear protein Mastermind (MAM) and C promoter-binding factor 1 (CBF1). NICD binding removes the co-repressors (CoRs) attached to CBF1. The NICD/MAM/CBF1 complex binds to the promoter of target genes belonging to the hairy/enhancer of split (*Hes*) and Hairy/enhancer-of-split related with YRPW motif (*Hey*) gene families. Hes proteins repress transcription of especially genes involved in differentiation and proliferation. Termination of Notch signaling is mediated through the SEL-10, an E3 ubiquitin ligase. SEL-10 attaches a ubiquitin label to the proline, glutamate, serine, threonine (PEST) sequence of NICD thereby transforming it into a substrate for subsequent proteosomal degradation.

2.5.2. Notch in the CNS

2.5.2.1. Embryonic development

During neurogenesis, neurons and glia are generated from proliferating neuronal stem cells (NSCs) in the ventricular zone (165). In the developing nervous system, sufficient numbers of neurons are necessary for the formation of neuronal circuits. Therefore strict regulation of proliferation, differentiation and survival of NSCs is required (151). Notch signaling warrants the NSC reservoir by maintaining these cells in a proliferative state (self-renewal), whereas Notch inhibition promotes cell cycle arrest and neuronal differentiation (166, 167). Formation of astrocytes is mediated through inhibition of pro-neuronal genes by Notch-mediated activation of *Hes* genes (168).

2.5.2.2. Postnatal life

Notch-1 expression is not only restricted to the embryonic stages but also persists in the adult CNS where it regulates a variety of processes, explained in this paragraph (169, 170).

Similar with embryonic development, Notch-1 also controls neurogenesis and maintenance of the NSC pool during adulthood. Notch-mediated signals avoid premature cell cycle exit of NSCs, thereby preventing premature depletion of the stem cell reservoir (171, 172).

Neurons in the mature CNS are capable of remodeling their neurites. These modulations comprise neurite outgrowth or retraction and strengthening of existing synapses (173-175). A number of studies found that Notch-1 activation inhibits neurite outgrowth and even causes their retraction, whereas Notch-1 inhibition promotes neurite extension (176, 177). Involvement of Notch-1 in axonal retraction is very important for this study, since axonal retraction is the earliest event during the pathogenesis of ALS.

Notch signaling is also involved in long-term potentiation (LTP). LTP is a long-lasting strengthening of existing synapses and is thought to be the mechanism underlying memory formation (151). Mice bearing a 50 % reduction of Notch expression, showed impaired LTP responses (178). Since synaptic plasticity is assumed to be the mechanism underlying learning and memory, a link between Notch signaling and Alzheimer disease evolved (159, 179). This will be discussed in section 2.5.3.

2.5.2.3. Oligodendrocyte specification and differentiation

Both during embryonic development and post-natal life, Notch-1 activity promotes specification of neuronal precursor cells to adopt an oligodendrocytic fate (180). The oligodendrocyte precursor pool is then also further regulated by Notch-1, which keeps the OPCs in an undifferentiated state and stimulates their proliferation (148). In this way maintenance of the OPC pool is being guaranteed during development and throughout life.

2.5.3. Notch in neurodegeneration

2.5.3.1. Alzheimer's disease

Alzheimer's disease (AD) is characterized by amyloid β-peptide (Aβ) accumulation and by the degeneration of neurons in brain regions involved in learning and memory (181). Neurotoxic Aβ is generated upon cleavage of the amyloid precursor protein (APP) by γ-secretase, the same enzyme that processes Notch-1 (182). This knowledge taken together with the role of Notch-1 in learning and memory implicated a potential link between Notch-1 signaling and AD pathogenesis (159, 179). In *post-mortem* brains of AD patients, the levels of Notch-1 are two-fold higher compared with controls (170). This increased Notch-1 activity might contribute to neurodegeneration through apoptosis induction and inhibition of neurite outgrowth (183, 184). Nevertheless, the exact contribution of Notch-1 to AD pathogenesis still needs to be elucidated (185, 186).

2.5.3.2. Multiple Sclerosis

MS is a disease of the CNS characterized by an autoimmune and neurodegenerative component (187). Acute MS lesions show infiltration of T cells and macrophages but also demyelination, axonal damage and loss of oligodendrocytes. Chronic active lesions contain high numbers of immature oligodendrocytes, but the latter fail to remyelinate naked axons after the immune attack (122). Since Notch signaling controls development and function of both immune and glial cells, the pathway is thought to be involved in both components of the MS pathogenesis (122).

Firstly, T cell activation and differentiation of $CD4^+$ T cells into the Th1 lineage are important events in the pathogenesis of MS. Th1 cells secrete pro-inflammatory mediators in response to MHC presented myelin self-antigens. Notch-1 promotes Th1 polarization but the mechanisms underlying this process remains unclear (122). Nevertheless, in this way Notch signaling constitutes an inflammatory environment in which oligodendrocytes and myelinated axons become damaged.

Secondly, as a consequence of the immune attack, remyelination of naked axons in required. In MS lesions, myelin repair is often ineffective despite the high number of OPCs that accumulate in these lesions. It has also been shown that MS lesions express components of the Notch-1 signaling pathway, such as Jagged-1 on astrocytes and Notch-1 and Hes-5 on OPCs (188). Interestingly, in remyelinated lesions Jagged-1 was found to be absent (122). All these observations taken together implicate that Notch-1 signaling blocks OPC differentiation into mature and functional oligodendrocytes, thereby impairing remyelination.

Additional evidence for the role of Notch in MS pathogenesis came from experimental autoimmune encephalomyelitis (EAE) mice treated with γ-secretase inhibitors (GSIs), the most commonly used Notch inhibitors. These mice showed less severe inflammation and enhanced remyelination (189). Therefore Notch signaling might represent a novel therapeutic target in MS.

2.5.3.3. Ischemic stroke

Notch signaling enhances several neurodegenerative mechanisms linked with ischemic stroke. For example, Notch-1 enhances apoptotic signaling cascades in neurons and exacerbates inflammatory processes in microglial cells and leukocytes (184). In this way, Notch-1 has a negative effect on brain damage and functional outcome after an ischemic stroke event.

A study revealed γ-secretase to be transiently activated after stroke, leading to increased Notch-1 cleavage and subsequently elevation of NICD levels. Mice treated with GSIs displayed less stroke-induced brain damage and an improved functional outcome (184). However, better understanding of Notch-1 involvement in different cell types contributing to stroke pathology is desirable. In this way, therapeutic strategies targeting Notch-1 can be developed for the treatment of stroke.

2.5.3.4. ALS

No articles have been published so far about the role of Notch-1 in ALS. Recently, oligodendrocyte pathology has been described in the $SOD1^{G93A}$ mouse model (89, 117). Gray matter oligodendrocytes were shown to degenerate prior to disease onset, impairment of OPC differentiation was observed and the expression of two functional markers, MBP and MCT-1, was decreased. Based on these articles and the knowledge of Notch-1 involvement in cellular differentiation, neurite outgrowth and other neurodegenerative diseases, we want to investigate the involvement of Notch-1 signaling in the pathogenesis of ALS.

2.6. Aims of the study

Starting from the hypothesis that Notch-1 might be involved in the pathogenesis of ALS, we will focus on three main topics. First of all, the characterization of the Notch-1 expression pattern in ALS. Secondly, the characterization of the mouse model for deletion of Notch-1 signaling in ALS, and lastly the evaluation of the effects of Notch-1 deletion on motor neuron degeneration, muscle innervation and functioning of the oligodendrocytes.

2.6.1. Characterization of Notch-1 expression in the $SOD1^{G93A}$ mouse model of ALS

First of all, we want to characterize the cells that express the Notch-1 receptor in $SOD1^{G93A}$ mice. Doing so, we hope to clarify several questions. First of all, which cell types express Notch-1 and is there a difference in Notch-1 expression between $SOD1^{G93A}$ and $SOD1^{WT}$ mice?

2.6.2. Characterization of the mouse model for ubiquitous deletion of Notch-1 in $SOD1^{G93A}$ mice

In the next part of this master thesis, we will try to unravel to what extend Notch-1 signaling contributes to ALS pathogenesis. In order to do so, we will switch off Notch-1 expression ubiquitously in $SOD1^{G93A}$ mice by tamoxifen-inducible CAGCre-ER mediated recombination. This model needs to be characterized. Therefore we want to design specific primers for the genotyping of this CAGCre-ER line, as different Cre-ER mouse lines are available in our laboratory. Further, we also want to define the recombination efficiency of CAGCre-ER, which will give us an idea of the amount of *Notch-1* excision in our mouse model.

2.6.3. Evaluation of the effects of Notch-1 deletion on motor neuron degeneration and function of the oligodendrocytes in $SOD1^{G93A}$ mice

As Notch-1 is known to be involved in the differentiation of OPCs into fully mature and functional oligodendrocytes, it would be of interest to investigate first of all the effects of Notch-1 deletion on the functionality of oligodendrocytes. This will be done by looking at the protein expression levels of two functional markers, namely MBP and MCT-1. Axon myelination and innervation will also be investigated by measuring the compound muscle action potential (CMAP), being indicative for the nerve conduction velocities of the motor neurons. The potential beneficial effect of Notch-1 deletion on preserving the motor neurons through better myelination of their axons and more trophic support will be explored via hanging wire and accelerated rotarod. In this context, also the number of innervated neuromuscular junctions at the level of the gastrocnemius muscle will be evaluated.

3. Experimental work

3.1. Materials and methods

3.1.1. Mouse models

Animal housing and ethics statement

Mice were housed in the 'KU Leuven' animal facilities with a 12-hour light-dark cycle at a temperature of 20 °C. Animals were given free access to standard rodent chow and water and were helped with their food and fluid intake at the end of their disease. All animals received care in accordance to The Principles of Laboratory Animal Care formulated by the National Society for Medical Research and the Guide for the Care and Use of Laboratory Animals published by the National Institutes of Health (NIH publication no. 86-23, revised 1996). Protocols were designed to minimize animal discomfort and all experiments were approved by the Ethical Committee for Animal Research of the 'Katholieke Universiteit Leuven', Belgium.

$SOD1^{WT}$ and $SOD1^{G93A}$ mice

Human wild-type SOD1 overexpressing mice [B6SJL-Tg(SOD1)2Gur/J; stock number: 002297] carry the normal allele of the human *SOD1* gene. This strain serves as a control for human mutant SOD1 overexpressing mice [B6SJL-Tg(SOD1*G93A)1Gur/J; stock number: 002726]. These mice harbor a substitution of glycine to alanine at codon 93 of the human *SOD1* gene which is driven by its endogenous human SOD1 promoter. $SOD1^{G93A}$ mice develop pathology reminiscent of ALS in humans due to loss of motor neurons from the spinal cord. Until approximately 60 days of age mice are asymptomatic. During the pre-symptomatic period, progressive microgliosis (around day 60) and astrocytosis (around day 80) are noticeable. Disease onset starts 90 days after birth and is characterized by massive loss of motor neurons. At the symptomatic stage, mice exhibit hind limb weakness and tremulous movements as initial symptoms. Around 140 days of age, referred to as the post-symptomatic stage, major symptoms such as progressive atrophy of hind limb muscles and paralysis occur. Mice show disability of gait, eating and drinking and generally die within 60 days after disease onset (around day 150) (27, 28). End-stage is determined as the time point when the $SOD1^{G93A}$ mice are not able any more to turn on their belly within 10 seconds, when laying on their back. Both mouse strains were purchased from The Jackson Laboratory.

CAGCre-ER mice

CAGCre-ER mice [B6.Cg-Tg(CAG-cre-Esr1)5Amc/J; stock number: 004682] were purchased from The Jackson Laboratory. These transgenic mice possess a Cre-mediated recombination system that is driven by a chimeric promoter of the cytomegalovirus immediate-early enhancer and chicken β–actin

promoter/enhancer (CAG). When crossbred with mice carrying a gene flanked by two LoxP sites, the floxed genes will be deleted in almost all cell types after tamoxifen administration (Sigma, St-Louis, MO, 200 mg/kg/day, via oral gavage during four consecutive days). The Cre-ER fusion protein consists of Cre-recombinase fused to the mutant G525R estrogen receptor. This form binds 4-hydroxytamoxifen but not 17β-estradiol, its naturel ligand. In the absence of tamoxifen, Cre-ER is restricted to the cytoplasm and cannot exert its recombinase activity (Figure 7a). Only after tamoxifen administration, Cre-ER translocates to the nucleus, where it excises the floxed genes (Figure 7b). By using this tamoxifen-inducible Cre-recombination system, we are able to delete a gene at a desired time-point, in this study at the age of 60 days (asympomatic). The recombination efficiency of the CAGCre-ER mouse equals 82 % in spinal cord and 76 % in brain.

Notch-1$^{Lox/Lox}$ mice

Notch-1$^{Lox/Lox}$ mice [B6.129X1-Notch1^{tm2Rko}Grid/J; stock number: 007181] were purchased from The Jackson Laboratory. These transgenic mice possess the *Notch-1* gene of which exon 1 is flanked by LoxP sites. When crossbred to Cre-ER mice, exon 1 of the *Notch-1* gene is deleted after tamoxifen administration and this occurs only within the Cre-expressing cells (Figure 7b). This conditional knock-out approach enables the generation of mice in which the Notch-1 receptor activity can be spatially and temporally regulated.

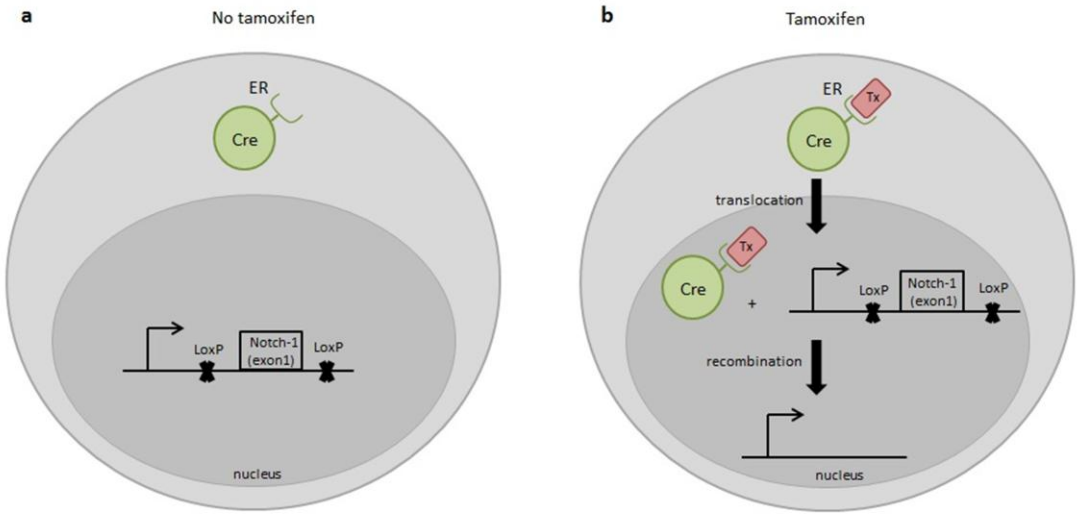

Figure 7. The tamoxifen inducible Cre-LoxP recombination system. a. In this study, Cre-ER is under control of the CAG promoter, which enables the expression of Cre-ER in almost all the cell types. In the absence of tamoxifen (Tx), Cre-ER is restricted to the cytoplasm and consequently no recombination takes place and the Notch-1 receptor continues to be expressed. **b.** After tamoxifen administration, Cre-ER translocates to the nucleus, where it catalyzes recombination between the two LoxP sites flanking exon 1 of the *Notch-1* gene. Exon 1 is excised and thereby Notch-1 expression is deleted in almost all cell types.

3.1.2. Characterization of Notch-1 expression in the SOD1^{G93A} mouse model

Immunofluorescent staining

SOD1^{G93A} (n=3) and SOD1^{WT} (n=3) mice at the age of 130 days were anesthetized with 10 % Nembutal (Ceva chemicals, Hornsby, NSW, Australia) and transcardially perfused with 1X Dulbecco's phosphate buffered saline (PBS) (Sigma-Aldrich, St. Louis, USA) and 4 % paraformaldehyde (PFA). The lumbar region of the spinal cord was dissected, further post-fixated with 4 % PFA for 2 hours on ice and dehydrated overnight in a 30 % sucrose solution at 4 °C. After imbedding the spinal cord in Tissue-Tek O.C.T compound (Sakura, Antwerp, Belgium), 20 µm thick frozen sections were cut on a cryostat (Leica, Wetzlar, Germany). Sections were hydrated with 1X PBS, permeabilized with 0.1 % Triton X-100 (Sigma-Aldrich, St. Louis, USA) in PBS (PBST) and blocked during 1 hour with 10 % normal donkey serum (Sigma-Aldrich, St. Louis, USA) in PBST. The sections were incubated during 1 hour with the primary and secondary antibodies shown in Table 1, diluted 1/200 and 1/500 respectively, in PBST with 10 % normal donkey serum.

Table 1. Antibodies used for immunofluorescent staining

Target	Antibody	Species reactivity	Supplier	Catalogue n°	Secondary antibody
Neurons	anti-NeuN	Mouse	Milipore Billerica, MA, USA	MAB377	Alexa-555-conjugated donkey anti-mouse IgG Invitrogen, Carlsbad, CA
Oligodendrocytes	anti-CC-1	Mouse	Abcam Cambridge, MA, USA	Ab16794	
NG2 glia	anti-NG2	Mouse	Milipore Billerica, MA, USA	MAB5384	
Microglia	anti-CD11b	Rat	AbD Serotec Oxford, UK	MCA74G	Alexa-555-conjugated goat anti-rat IgG Invitrogen, Carlsbad, CA
Astrocytes	anti-GFAP	Mouse	Sigma-Aldrich St. Louis, USA	G3893	Alexa-555-conjugated donkey anti-goat IgG Invitrogen, Carlsbad, CA
Notch-1	Notch-1 anti-activated	Rabbit	Abcam Cambridge, MA, USA	Ab8925	Alexa-488-conjugated donkey anti-rabbit IgG Invitrogen, Carlsbad, CA

In between the two antibody incubation steps, sections were washed three times with PBST. After mounting the sections with 4', 6-diamidino-2-phenylindole DAPI-containing Vectashield (Vectorlabs Inc., Burlinglame, CA), sections were analyzed under a fluorescence microscope (Zeiss Imager M1, Jena,

Germany) with Axiovision software (Zeiss, Jena, Germany). Images were processed using the ImageJ software (National Institutes of Health, Bethesda, MD, USA).

3.1.3. Mouse model for ubiquitous deletion of Notch-1 in SOD1^{G93A} mice

3.1.3.1. Mouse genotyping

Primer design

Primers for genotyping CAGCre-ER mice were designed with the Primer 3.0 interface (http://frodo.wi.mit.edu/). The sequence of the primers synthesized was: 5'-CAAGTACGCCCCCTATTGAC-3' (forward) and 5'-TTCTGCTTCACTCTCCCCAT-3' (reverse). The size of the amplicon was 163 bp.

Genomic DNA isolation

For genotyping PCR analysis, genomic DNA was purified from mouse tail tissue of no longer than about 0.5-1 cm. Tail biopsies were incubated with 75 µl of lysis buffer (25 mM NaOH, 0.2 mM EDTA, pH 12.0) for 45 minutes at 95 °C. Lysis was terminated by adding 75 µl of neutralization buffer (40 mM Tris-HCl, pH 6.0-7.0).

Polymerase chain reaction (PCR)

PCR was performed in 20 µl reactions containing 2X DreamTaq Green PCR Master Mix (Thermo Fisher Scientific, Reskilde, Denmark), 0.5 µM of each primer and 2 µl of extracted genomic DNA. The amplification was performed under following cycling conditions (Applied Biosystems 2720 Thermal Cycler, Foster City, CA, USA): 94 °C for 5 minutes (initial denaturation) followed by 32 cycles of 94 °C for 30 s (denaturation), 54.6 °C for 30 s (annealing) and 72 °C for 45 s (elongation). Cycling was followed by a final extension step at 72 °C for 7 minutes. The sequence of the forward (Fw) and reverse (Rv) primers used were as follows:

CAG Fw: 5'-CAAGTACGCCCCCTATTGAC-3' ; Rv: 5'-TTCTGCTTCACTCTCCCCAT- 3'

IL2 Fw: 5'-GTAGGTGGAAATTCTAGCATCATCC-3' ; Rv: 5'-CTAGGCCACAGAATTGAAAGATCT-3'

Interleukin 2 (IL2) was used as an internal control to check whether the PCR reaction had taken place. No template (H_2O) control was used to verify that the obtained PCR bands were not derived from contaminations. The PCR products were run on a 2 % agarose gel (20 µl/lane) at 126 mV in TAE buffer (Lonza Braine SA, Braine-l'Alleud, Belgium) containing 40 mM Tris-acetate, 1 mM EDTA, pH 8.0. Bands were stained using GelGreen™ (Biotium Inc., Hayward, USA) and visualized using the BioDoc-It imaging system (UVP, Upland, CA).

DNA gel extraction, purification and sequencing

DNA from CAGCre-ER mice (n=3) was purified from the 2 % agarose gel using the GenElute™ Gel Extraction Kit (Sigma-Aldrich, St. Louis, USA) following manufacturer's instructions. DNA concentration was quantified by a NanoDrop ND-1000 spectrophotometer (NanoDrop Technologies, DE, USA). Purified DNA was sent for bi-directional sequencing (LGC Genomics, Berlin, Germany). Sequence alignment was performed using the EMBOSS Needle interface for pairwise nucleotide alignment (http://www.ebi.ac.uk/Tools/psa/emboss_needle/nucleotide.html).

Primer specificity testing

Tail tips from following Cre-ER mouse lines (n=3 per line), summarized in Table 2, were isolated and genotyped as described above. Also non-transgenic mice were included as a negative control.

Table 2. Different Cre-ER mouse lines used for primer specificity testing

Cre-ER mouse line	Site of recombination
PDGFRα	Oligodendrocyte precursor cells
PLP	Oligodendrocytes
FoxJ1	Ependymal cells
Nestin	Sub-ependymal cells
CX30	Activated astrocytes
GFAP	Astrocytes
Thy1	Motor neurons
Vacht	Cholinergic neurons
CAG	Almost all cell types

3.1.3.2. Recombination efficiency of Notch-1$^{Lox/Lox\ and\ Lox/-}$ :: CAGCre-ER mice

Crossbreeding

For the study of the recombination efficiency of CAGCre-ER, we crossbred Notch-1$^{Lox/Lox}$ mice with CAGCre-ER mice. Recombination efficiency was determined in Notch-1$^{Lox/Lox}$ CAGCre-ER mice, Notch-1$^{Lox/-}$ CAGCre-ER mice and Notch-1$^{Lox/Lox\ or\ Lox/-}$ mice. From each genotype 3 mice were treated with tamoxifen and 3 mice were left untreated. Tamoxifen (Sigma, St-Louis, MO, 200 mg/kg/day) was administered via oral gavage for four consecutive days.

Quantitative Real-Time PCR

After a 1-week washout period posterior to tamoxifen administration, mice were anesthetized with 10 % Nembutal (Ceva chemicals, Hornsby, NSW, Australia) and transcardially perfused with 1X PBS (Sigma-Aldrich, St. Louis, USA). Spinal cord, brain, sciatic nerve, gastrocnemius and liver were rapidly dissected and collected in lysis matrix D tubes (MP Biomedicals, Brussels, Belgium). Samples (n=3 per tissue, per genotype) were immediately snap frozen to prevent RNase activity and stored at -80 °C until further use. Total RNA was extracted using TriPure (Roche, Basel, Switserland) and isopropanol purification. RNA concentrations were determined by a NanoDrop ND-1000 spectrophotometer (NanoDrop Technologies, DE, USA) with 260/280 ratios of 1.8-2.2 considered acceptable. Complementary DNA (cDNA) was synthesized from 1 µg total RNA using the Superscript^{TM} III First-Strand Synthesis Mastermix kit (Invitrogen, Carlsbad, CA). Residual RNA was removed upon RNaseH treatment for 30 minutes at 37 °C. Quantitative Real-Time PCR reactions were performed on 5 µl cDNA (1/200) using TaqMan Universal PCR master mix (Invitrogen, Carlsbad, CA) and following commercially available TaqMan gene expression assays (Applied Biosystems, Foster city, CA, USA): Mm00627185_m1 (Notch-1), Mm99999915_g1 (GAPDH), Mm00446968_m1 (HPRT), Mm00839493_m1 (Polr2a) and 4352341E (ACTB). Samples were run in triplicate in a 96-well plate and thermal cycling was performed on a StepOne-Plus Real-Time PCR system (Applied Biosystems, Foster city, CA, USA) using a standard (~40 minutes) amplification protocol. The resulting amplification curves were further analyzed by the $\Delta\Delta C_t$ method. Briefly, the threshold cycle (C_t) is the number of PCR cycles required for the probe fluorescence signal to exceed background level. The difference between the C_t of the target gene and the C_t of the best fitting reference gene C_t, is being referred to as ΔC_t. GeNorm analysis was performed with qBase Plus software (Biogazelle) in order to determine the best fitting reference genes. $\Delta\Delta C_t$ is obtained by subtracting the ΔC_t of a control sample ($Notch^{Lox/Lox\ or\ Lox/-}$), defined as calibrator sample, from the ΔC_t of other samples ($Notch^{Lox/Lox}$ :: CAGCre-ER and $Notch^{Lox/-}$ :: CAGCre-ER). The $2^{-\Delta\Delta Ct}$ formula was used to calculate relative Notch-1 expression levels. Recombination efficiency was defined as the percentage change of Notch-1 expression levels from the control group. Statistical analysis was done using a one-way ANOVA ($p < 0.05$) and Tukey's post-hoc test. Data are presented as mean ± SEM

3.1.4. Evaluation of the effects of Notch-1 deletion on motor neuron degeneration and function of the oligodendrocytes in SOD1^{G93A} mice

Crossbreeding

For the study of the effects of Notch-1 deletion in the SOD1^{G93A} mouse model, Notch-1$^{Lox/Lox}$ mice were crossbred with CAGCre-ER mice and with SOD1^{G93A} mice, to generate triple transgenic Notch-1$^{Lox/-}$ :: CAGCre-ER :: SOD1^{G93A} mice. After tamoxifen administration at the age of 60 days (Sigma, St-Louis, MO, 200 mg/kg/day, via oral gavage, during four consecutive days), the expression of Notch-1 is deleted in all cell types. Notch-1$^{Lox/-}$ :: SOD1^{G93A} mice were used as control.

3.1.4.1. Assessment of oligodendrocyte functionality

Western Blot

Notch-1$^{Lox/-}$ :: CAGCre-ER :: SOD1^{G93A} and Notch-1$^{Lox/-}$ :: SOD1^{G93A} mice were anesthetized with 10 % Nembutal (Ceva chemicals, Hornsby, NSW, Australia) and transcardially perfused with 1X PBS (Sigma-Aldrich, St. Louis, USA) at the age of 130 days. Lumbar spinal cords (n=2 per genotype) were dissected and collected in lysis matrix D tubes (MP Biomedicals, Brussels, Belgium). Samples were snap frozen in liquid nitrogen and stored at −80 °C until use. To prepare lysates, frozen samples were immersed in Radioimmunoprecipitation Assay (RIPA) lysis buffer containing 50 mM Tris-HCl (pH 7.5), 150 mM NaCl, 1 % NP-40, 0.5 % Na-deoxycholic acid, 0.5 % SDS supplemented with EDTA free protease inhibitor cocktail (Complete, Roche, Mannheim, Germany). Homogenization was done three times with the MagNA lyser oscillator (Roche, Mannheim, Germany) at 6,500 rpm for 30 seconds. Lysates were kept on ice for one hour and consequently centrifuged at 4 °C for 20 minutes at 13,200 rpm. Protein concentration of the resulting supernatant was determined with the BCA protein assay kit (Pierce, Rockford, USA). Equal amounts of protein (30 µg) were loaded onto a 10 % (for MCT-1 blot) or 15 % (for MBP blot) SDS–polyacrylamide (SDS-PAGE) gel. After electrophoresis, separated proteins were transferred to a polyvinylidene difluoride (PVDF) membrane (Millipore, Overijse, Belgium) by a semi-dry transfer apparatus (TE70XP, Hoefer, San Fransisco, California) at 180 mA for 1.45 hours. The membrane was then blocked with 5 % skimmed milk in Tris-Buffered Saline containing 10 mM Tris–HCl (pH 7.5), 150 mM NaCl and 1 % Tween-20 (TBS-T) for 1 hour at room temperature. For immunodetection, blots were rinsed with TBS-T and incubated overnight with primary antibodies against MBP (goat, 1/10,000; Santa Cruz, sc-13912) and MCT-1 (chicken, 1/1000; Millipore, AB1286). After washing the membranes with TBST and incubating them for 1 hour with the appropriate horseradish peroxidase (HRP)-conjugated secondary antibody (1/5000; Santa Cruz Biotechnology Inc., California, USA), protein bands were visualized using enhanced chemiluminescence (ECL substrate; Pierce, Rockford, USA). The same procedure was followed for the endogenous GAPDH protein (goat, 1/2,000; Ambion, AM4300) that was used as a loading control. Blots were scanned using the ImageQuant LAS 4000 Biomolecular Imager (GE Healthcare, Waukesha, WI) and band intensities were quantified using ImageJ software (National Institutes of Health, Bethesda, MD, USA). Statistical analysis was done using an unpaired T-test ($p < 0.05$). Data are presented as mean ± SEM.

3.1.4.2. Animal behavior and motor performance evaluation

Accelerating rotarod

An accelerating rotarod treadmill (UGO Basile, VA, Italy) was used to assess the motor performance, which is measured as the time the mouse can stay on the rod (Figure 8a). Before tamoxifen administration (60 days of age), mice were trained for one week to get acquainted with the motorized rod and baseline motor performance was monitored. After the training period and before tamoxifen administration at the age of 60 days, the rotarod measurements were started. The rotational speed of the cylinder was gradually increased from 4 to 40 rpm over a period of 5 minutes. Each mouse was given three attempts and testing was done once a week until they were sacrificed. The data shown are the averages of all three trials per sessions ± SEM. Statistical analysis was done using a one-way ANOVA at each time-point ($p < 0.05$) and Tukey post-hoc testing. Data are presented as mean ± SEM.

Hanging wire test

The hanging wire test was used to assess hind- and forelimb muscular strength. All mice started this test before tamoxifen administration (60 days of age) and continued until they were sacrificed. Each mouse was placed on the grid of a conventional housing cage where after it was gently turned upside down (Figure 8b). The inverted lid was held approximately 60 cm above the soft cage bedding to avoid injuries. Mice had to hold on to the grid for a maximum period of 60 seconds and time upon falling was recorded. A score of zero seconds was assigned when the mouse fell off instantaneously. The hanging wire test was performed twice a week with a time interval of at least two days between each measurement. Statistical analysis was done using a one-way ANOVA at each time-point ($p < 0.05$) and Tukey post-hoc testing. Data are presented as mean ± SEM.

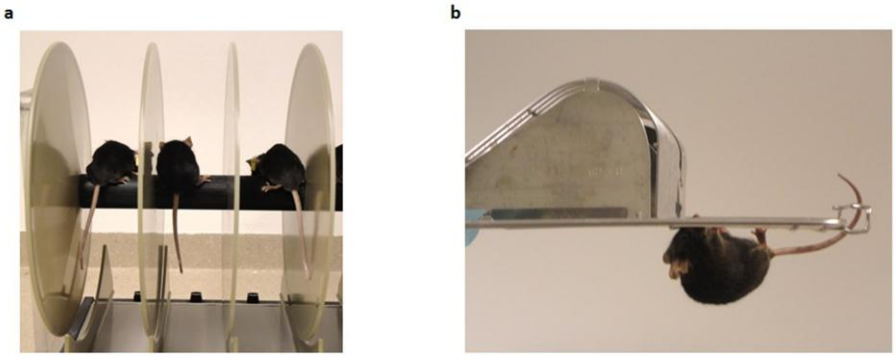

Figure 8. a. Accelerating rotarod. An accelerating rotarod was used to asses motor performance. The rotational speed of the cylinder was gradually increased from 4 to 40 rpm over a period of 5 minutes. Each mouse was given three attempts and the time until the mouse fell off the rod was recorded. **b. Hanging wire test.** The hanging wire test was used to assess hind- and forelimb muscular strength. Each mouse was placed on the grid of a conventional housing cage where after it was gently turned upside down. Mice had to hold on to the grid for a maximum period of 60 seconds and time upon falling was recorded.

3.1.4.3. Compound muscle action potential (CMAP) recordings

Mice were anesthetized using isoflurane (Halocarbon Laboratories, River Edge, NJ) delivered in a mixture of O_2 (flow of each 2,3 l/min, 1 bar O_2) at 3 % concentrations for both induction and maintenance of anesthesia. Body temperature was maintained at 37 °C using a heating pad (Physitemp Instruments Inc., New Jersey, USA). With the animals under anesthesia and fixed in a ventral prone position, compound muscle action potential (CMAP) measurements were conducted with an EMG monitoring set-up (Medelec Vickers/Modul, Brooksville, USA). All 0.4-mm electrodes (Technomed Europe, Maastricht, Netherlands) were inserted subcutaneously and were positioned as shown in Figure 9a. For stimulation, the cathode (white) was placed at the level of the sciatic notch, whereas its reference anode (blue) was positioned 1 cm caudally to the anode. The recording electrode (yellow) was inserted into the gastrocnemius muscle, whereas its reference electrode (red) was placed on the Achilles tendon. The ground electrode (green) was randomly fixed at a position of choice. Stimulation intensity of the sciatic nerve was gradually increased until the supramaximal CMAP amplitude was obtained. Most of the electric stimuli ranged between 2-13 mA. The CMAP amplitude (mV) was determined as the distance between the base and top of the waveform, whereas the latency (ms)was defined as the distance between stimulation and the beginning of the provoked action potential (Figure 9b). Measurements were repeated three times and were carried out once a week, only on the right gastrocnemius muscle. CMAP recordings started before tamoxifen administration (60 days of age) and continued until mice were sacrificed. Statistical analysis was done using a one-way ANOVA at each time-point ($p < 0.05$) and Tukey post-hoc testing. Data are presented as mean ± SEM.

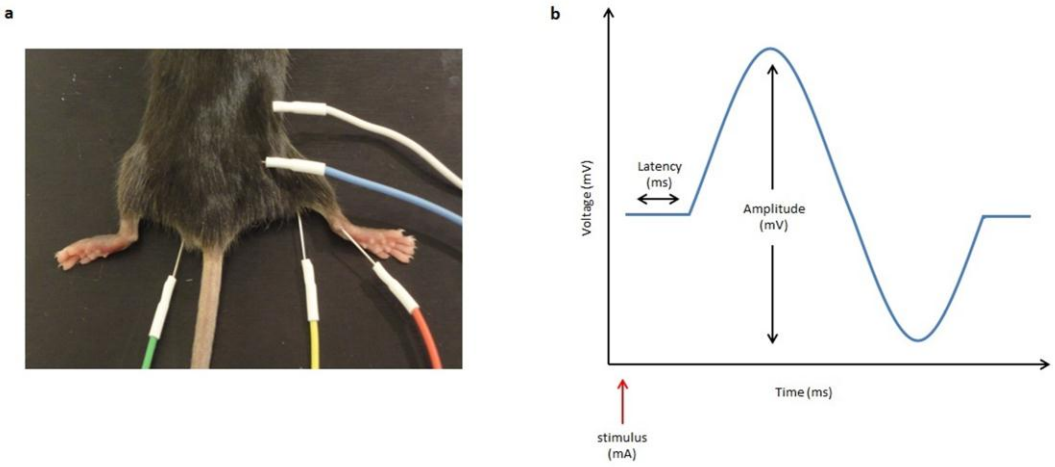

Figure 9. a. Electrode placement on the mouse. White: stimulating electrode (cathode), blue: stimulating reference electrode (anode), yellow: recording electrode, red: recording reference electrode, green: ground electrode. The active stimulating and recording electrodes were paired together with a reference electrode, which acts as a concentric needle electrode for these recordings. **b. Graphical representation of compound muscle action potential (CMAP).** After stimulation of the sciatic nerve at the level of the spinal cord, individual gastrocnemius muscle fibers become depolarized. As a result, the muscle contracts and this evoked motor response is called a CMAP. The latency reflects the delay by which the stimulus is delivered to the muscle fibers and reflects axonal myelination. Prolonged latencies point to slower conduction velocities and demyelination. The height of the nerve conduction amplitude is a representation of how many axons innervate the gastrocnemius muscle. Reduction of this amplitude yields the degree of muscle denervation.

3.1.4.4. Muscle innervation

Neuromuscular junction staining

Notch-$1^{Lox/-}$ :: CAGCre-ER :: $SOD1^{G93A}$ and Notch-$1^{Lox/-}$ :: $SOD1^{G93A}$ mice were anesthetized with 10 % Nembutal (Ceva chemicals, Hornsby, NSW, Australia) followed by dissection of the gastrocnemius muscle. Samples (n=2 per genotype) were instantly frozen in isopentane, cooled by immersion in liquid nitrogen. After embedding the muscles in Tissue-Tek O.C.T compound (Sakura, Antwerp, Belgium), 20 µm thick longitudinal sections were made. Sections were washed twice with 1X PBS (Sigma-Aldrich, St. Louis, USA) for 5 minutes and blocked with 5 % normal donkey serum (Sigma- Aldrich, St. Louis, USA) in PBST for 1 hour at room temperature. To visualize neuromuscular junctions, sections were simultaneously incubated with Alexa-555-conjugated α-bungarotoxin (1/5,000, Invitrogen, Carlsbad, CA, B35451) and Alexa-488-conjugated NF-200 (1/500, Cell Signaling Technologies, Danvers, MA, USA, #80245) diluted in PBST for 2 hours at room temperature. Sections were washed twice with PBST for 5 minutes and mounted with DAPI-containing Vectashield (Vectorlabs Inc., Burlinglame, CA). Fluorescent stains were visualized with a Zeiss Axio Imager M1 microscope (Carl Zeiss, Jena, Germany), using the monochrome AxioCam Mrm camera.

Quantification of neuromuscular junctions

A total of 100 neuromuscular junctions was counted from at least 4 sections of gastrocnemius from 130-day-old mice (n=2 per genotype). The innervation level of neuromuscular junctions was determined by the overlap of NF-200 (green) and α-bungarotoxin (red). We considered fully innervated junctions to have an overlap of at least two NF-200 branches (Figure 10, left), partially innervated junctions to have an overlap of only one NF-200 branch (Figure 10, middle) and denervated junctions to show no overlap of NF-200 with α-bungarotoxin (Figure 10, right). Statistical analysis was performed using an unpaired T-test ($p < 0.05$). Data are presented as mean ± SEM.

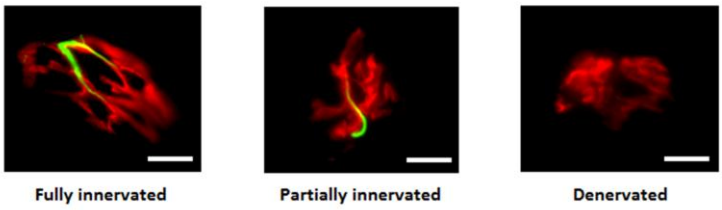

Figure 10. Criteria for interpreting neuromuscular junction innervation. NF-200 (green) and α-bungarotoxin (red) are used as pre- and post-synaptic markers for the visualization of neuromuscular junctions. **Left.** Fully innervated junctions must have an overlap of at least two NF-200 branches with α-bungarotoxin. **Middle.** Partially innervated junctions have an overlap of only one NF-200 branch with α-bungarotoxin. **Right.** Denervated junctions show no overlap of NF-200 with α-bungarotoxin. Scale bar, 20 µm.

3.2. Results

3.2.1. Characterization of Notch-1 expression in the SOD1^{G93A} mouse model revealed co-localization of Notch-1 with neurons, oligodendrocytes and NG2 glial cells.

To characterize the Notch-1 signaling cascade, we performed immunofluorescent stainings on the lumbar spinal cord of the commonly used SOD1^{G93A} mouse model and control SOD1^{WT} mice.

Immunofluorescent double-labeling of activated Notch-1 with cell type specific markers, such as NeuN for neurons, CC-1 for oligodendrocytes, NG2 for oligodendrocyte precursor cells, CD11b for microglia and GFAP for astrocytes, was conducted at the age of 130 days, and also at disease end-stage for NG2 glial cells. The antibody used in this experiment was specific for Notch-1 and only recognized the cleaved (activated) form of the receptor (NICD), as the epitope is only exposed after γ-secretase cleavage. Besides Notch-1 activation, also Notch-1 expression could be detected at the same time, as no γ-secretase cleavage occurs without the presence of the full receptor.

Notch-1 immunoreactivity was observed in both SOD1^{G93A} and SOD1^{WT} mice in neurons (Figure 11) and oligodendrocytes (Figure 12a), but not in astrocytes and microglia (Figure 12b,c). The situation in the NG2 glial cells is more complicated, as described below.

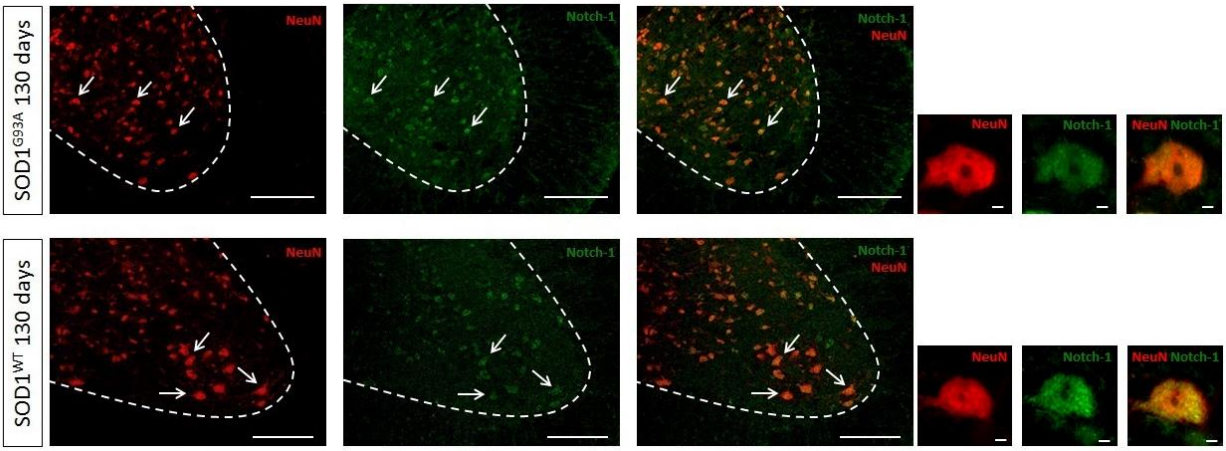

Figure 11. Notch-1 activation was observed in neurons. Notch-1 activation (green) was observed in neurons (NeuN, red) in both SOD1^{G93A} and SOD1^{WT} mice at the age of 130 days. The ventral horn of the spinal cord was marked by the dotted line. Arrows indicated co-localization. The enlargements on the right confirmed this overlap. Scale bars were 100 µm (large pictures on the left) and 5 µm (small pictures on the right).

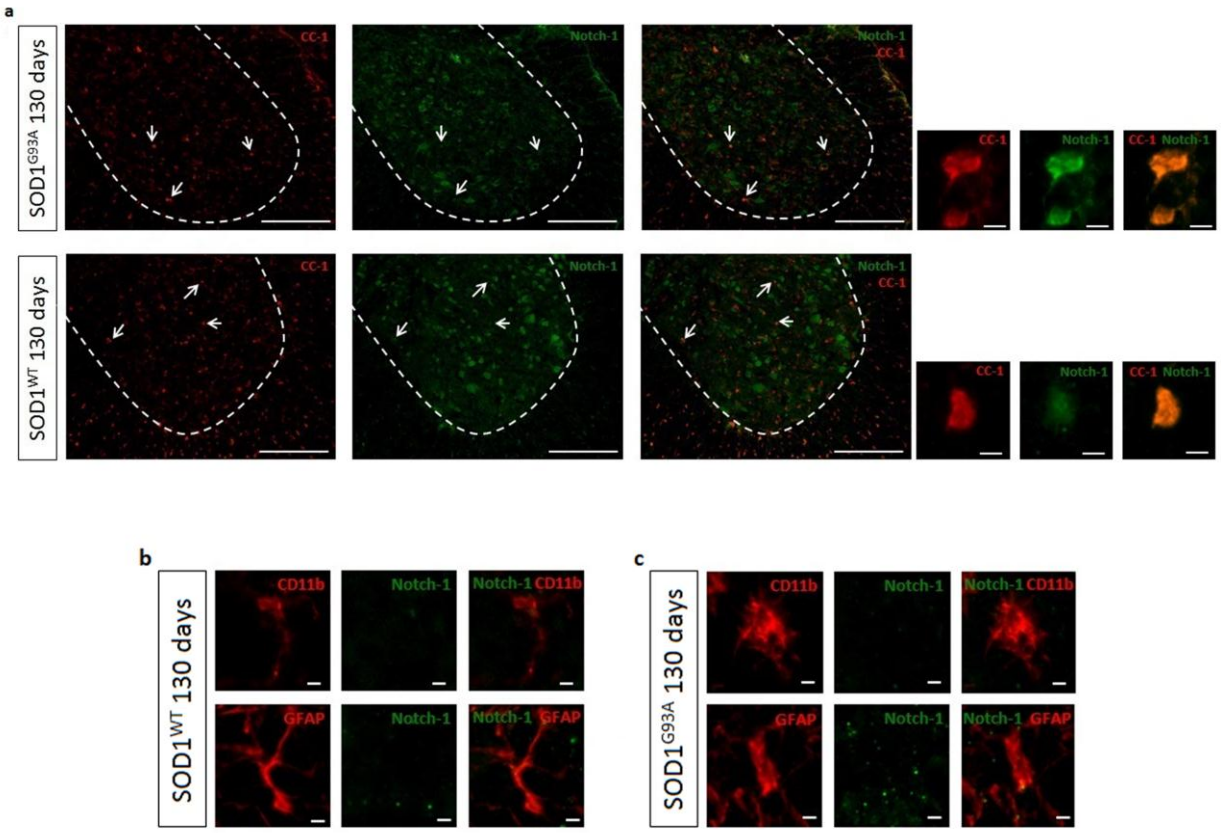

Figure 12. Notch-1 activation was observed in oligodendrocytes but was absent in astrocytes and microglia. a. Notch-1 activation (green) was observed in oligodendrocytes (CC-1, red) in both $SOD1^{G93A}$ and $SOD1^{WT}$ mice at the age of 130 days. The ventral horn of the spinal cord was marked by the dotted line. Arrows indicated co-localization. The enlargements on the right confirmed this overlap. Scale bars were 100 µm (large pictures on the left) and 5 µm (small pictures on the right). **b-c.** No co-localization of Notch-1 (green) could be observed in astrocytes (GFAP, red), nor in microglia (CD11b, red) in **b**. $SOD1^{WT}$ mice and **c.** $SOD1^{G93A}$ at the age of 130 days. Scale bars were 5 µm.

$SOD1^{WT}$ nor $SOD1^{G93A}$ mice displayed Notch-1 immunoreactivity in NG2-positive cells until the age of 130 days (Figure 13 upper and middle panel). When we looked at end-stage however, extensive co-localization of Notch-1 and NG2 labeling could be observed, indicating that Notch-1 activation was abundantly present in these cells (Figure 13, bottom panel). The density of NG2-positive cells was observed to be increased at end-stage compared with 130 days of age, possibly reflecting enhanced proliferation of these cells at disease end-stage.

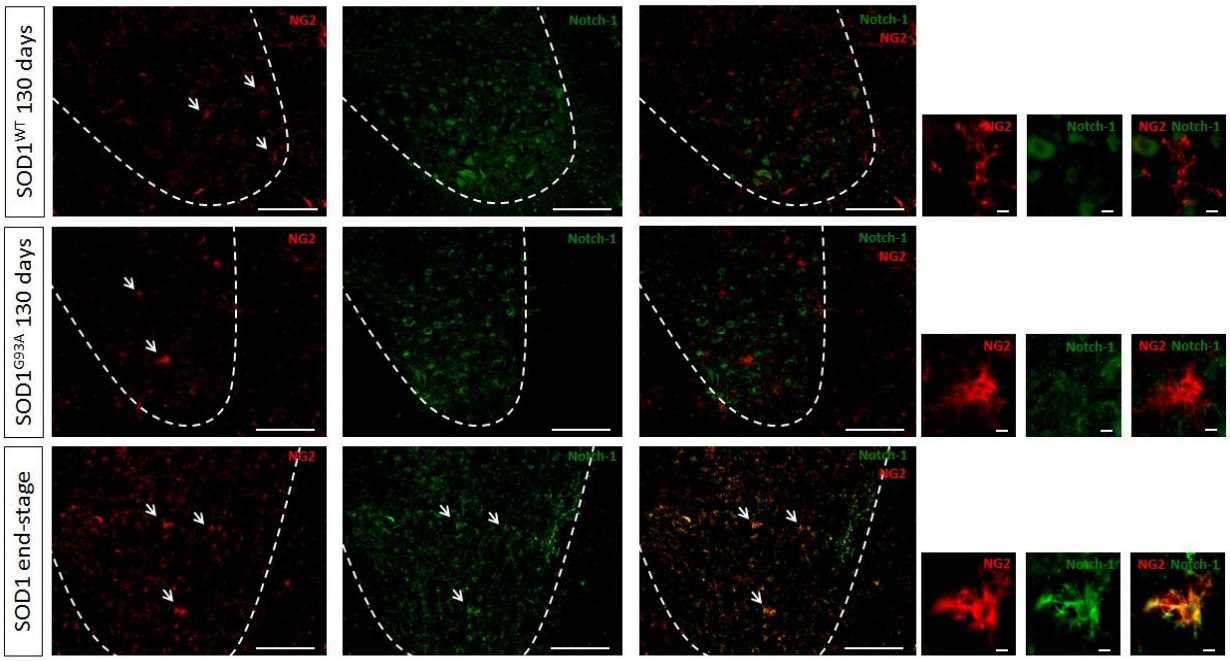

Figure 13. Notch-1 activation was only present in NG2-positive cells at disease end-stage. Upper and middle panel. Co-localization of Notch-1 (green) with the NG2 marker (red) was not observed in both $SOD1^{WT}$ and $SOD1^{G93A}$ mice at the age of 130 days. Arrows indicated labeling with only the NG2 marker. The enlargements on the right confirmed that there was no overlap of Notch-1 with NG2 in both $SOD1^{WT}$ and $SOD1^{G93A}$ mice at the age of 130 days. **Bottom panel.** At disease end-stage, massive Notch-1 labeling was observable in NG2-positive cells as indicated by the arrows. The enlargements on the right confirmed this overlap. Also strong proliferation of NG2-positive cells was observed at disease end-stage. The ventral horn of the spinal cord was marked by the dotted line. Scale bars were 100 µm (large pictures on the left) and 5 µm (small pictures on the right).

To summarize, Notch-1 activation was clearly observable in the lumbar spinal cord of both $SOD1^{G93A}$ mice and $SOD1^{WT}$ mice, and this in neurons and oligodendrocytes, but not in astrocytes and microglia. In NG2 glial cells, Notch-1 activity was not present in $SOD1^{G93A}$ and $SOD1^{WT}$ mice until the age of 130 days. At disease end-stage however, massive co-localization of Notch-1 with NG2-positive cells was observed, indicating that Notch-1 activation was up-regulated towards disease end-stage. In the present study, no absolute quantification of the number of NG2 glia was conducted. The increased density of NG2-positive cells observed at end-stage however, may indicate that enhanced proliferation took place.

It is known that, by end-stage of the disease, NG2-positive cells exhibit the highest rate of proliferation and differentiation into oligodendrocytes, but the latter are dysfunctional. This, together with the observation of extensive activation of Notch-1 towards disease end-stage, is in line with our hypothesis that aberrant Notch-1 activity may prevent oligodendrocyte differentiation into functional and myelinating oligodendrocytes. This hypothesis was investigated by deleting the Notch-1 receptor ubiquitously by means of the tamoxifen-inducible CAGCre-ER in order to get a general overview of the effects of Notch-1 deletion on the pathogenesis of the $SOD1^{G93A}$ mouse model, as will be discussed in the next chapters. In the near future, cell-specific Notch-1 deletion experiments in oligodendrocytes (PLPCre-ER) and OPCs (PDGFRαCre-ER) will also be investigated.

3.2.2. Characterization of the mouse model for ubiquitous deletion of Notch-1 in SOD1^{G93A} mice

Notch-1 signaling is important during development and postnatal life. As Notch-1 knock-out mice are embryonically lethal, we used a tamoxifen inducible knock-out approach. The advantage of this approach is that we can delete the Notch-1 receptor at a desired time-point, and thereby overcome embryonic lethality and undesired developmental defects. In this study, we used CAGCre-ER mice, a mouse line that expresses the Cre-recombinase in almost all cell types (1), and induced recombination with tamoxifen at the age of 60 days. First of all we wanted to characterize this model, by developing CAGCre-ER specific primers for genotyping and by assessing the recombination efficiency of CAGCre-ER. This is necessary to be able to correctly interpret the effects of Notch-1 deletion in ALS, described in section 3.2.3.

3.2.2.1. Genotyping of CAGCre-ER mice

3.2.2.1.1. Design of CAGCre-ER specific primers for genotyping

As several Cre-ER transgenic mouse lines are available in the lab, the design of Cre-specific primers was necessary. In this study we used CAGCre-ER mice and therefore we designed primers that are specific for CAGCre-ER.

The Cre-recombinase expression in these mice is driven by the chimeric promoter of the cytomegalovirus (CMV) immediate-early enhancer and chicken β-actin promoter/enhancer (CAG). Since this construct is not naturally present in mice, we decided to design the forward primer (5'-CAAGTACGCCCCCTATTGAC-3', T_m = 59.45 °C) against nucleotide 78-197 of the CMV enhancer whereas the reverse primer (5'-ATGGGGAGAGTGAAGCAGAA-3', T_m = 59.80 °C) was designed against nucleotide 8-37 of the chicken β-actin promoter/enhancer (Figure 14). Both primers had an optimal length of 20 bp and their GC content was 50 %, which lies perfectly within the range of 40-60 %. Melting temperatures (T_m) ranging between 52 °C and 58 °C generally produce the best PCR results. Our melting temperatures slightly exceeded this range, but temperatures lower than 65 °C are still acceptable.

Figure 14. Localization of CAGCre-ER specific primers. Primers were designed against the sequence of the chimeric promoter of the cytomegalovirus (CMV) immediate-early enhancer and chicken β-actin promoter/enhancer (CAG). The forward primer (5'-CAAGTACGCCCCCTATTGAC-3', T_m = 59.45 °C) was located at the 78-197 nucleotide position of the CMV enhancer. The reverse primer (5'-ATGGGGAGAGTGAAGCAGAA-3', T_m = 59.80 °C) was located at the 8-37 nucleotide position of the chicken β-actin promoter/enhancer.

The amplification was performed under following cycling conditions (Figure 15, left panel): 94 °C for 5 min (initial denaturation) followed by 32 cycles of 94 °C for 30 s (denaturation), 54.6 °C for 30 s (annealing) and 72 °C for 45 s (elongation). Cycling was followed by a final extension step at 72 °C for 7 min. The choice of the temperatures for the PCR protocol is based on the standard protocol: 94 °C (denaturation), T_m - 5 °C (annealing) and 70-72 °C (elongation). For annealing we used a temperature of 54.6 °C, as the optimal annealing temperature is 5 °C below the average of the melting temperatures T_m of the primer pair that is being used ((59.45 °C + 59.80 °C)/2 – 5 °C = 54.6 °C). The size of the amplicon was 163 bp, as shown in Figure 15 (right panel).

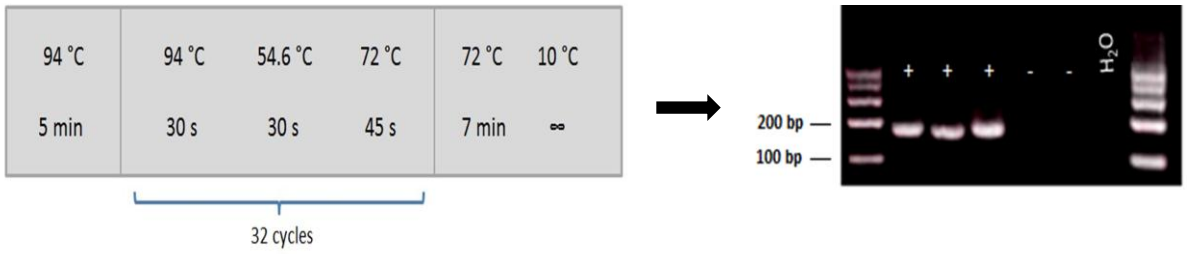

Figure 15. Left panel. PCR cycling protocol for the CAGCre-ER specific primers. The amplification was performed under following cycling conditions: 94 °C for 5 min (initial denaturation) followed by 32 cycles of 94 °C for 30 s (denaturation), 54.6 °C for 30 s (annealing) and 72 °C for 45 s (elongation). Cycling was followed by a final extension step at 72 °C for 7 min. **Right panel. Amplicon produced by the CAGCre-ER specific primers.** The size of the amplicon was 163 bp and a band was only visible in the CAGCre-ER (+) lanes, but not in the negative control lanes (-) and water lane (H_2O).

3.2.2.1.2. Sequence alignment of the PCR product confirmed that the right fragment has been amplified

To check whether the proper product is amplified during the polymerase chain reaction (PCR), we extracted the amplification products from the agarose gel and sent them for bi-directional sequencing to LGC Genomics (Berlin, Germany). Forward and reverse sequencing results were both aligned to the sequence of the CAG promoter, by means of the EMBOSS Needle interface for pairwise nucleotide sequence alignment.

Forward primer sequencing result

In figure 16 the alignment of the sequencing result based on the forward primer is shown. The first forty to fifty base pairs, starting from the forward primer (yellow) on, are generally not sequenced. This was stated by the company. The alignment shows only two gaps (-), but no mismatches (.). So a perfect a perfect alignment of the forward sequencing result could be concluded.

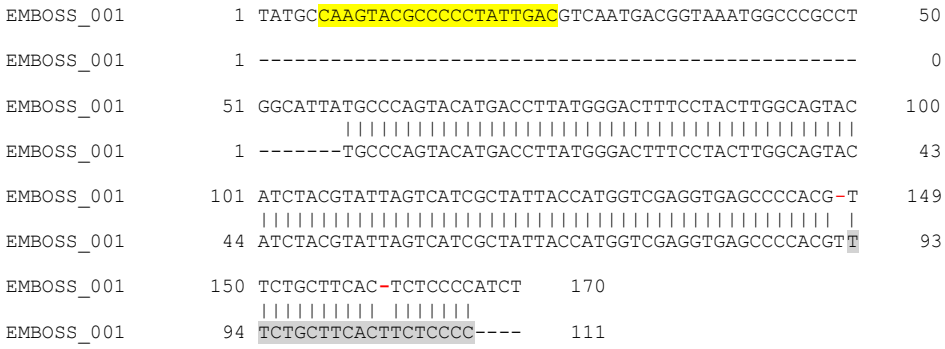

Figure 16. Alignment of the forward sequencing result and the chimeric CAG promoter sequence. Forty to fifty base pairs starting from the forward primer (yellow) are traditionally not being sequenced. The sequencing results showed a perfect alignment from forward (yellow) to reverse (gray) primer. Only two gaps (-), but no mismatches (.) were found.

Reverse primer sequencing result

Equivalently to the forward sequencing result, also the reverse primer sequencing result shows perfect alignment, as is visible in the sequence readout below (Figure 17). As described previously, the first forty to fifty base pairs starting from the reverse primer (grey) are not sequenced and the alignment from the reverse (gray) to the forward (yellow) primer only show one gap (-) and one mismatch (.).

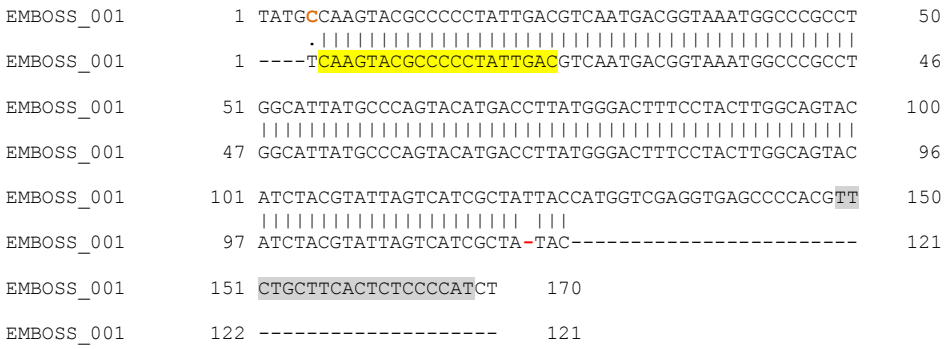

Figure 17. Alignment of the reverse sequencing result and the chimeric CAG promoter sequence. Forty to fifty base pairs starting from the reverse primer (gray) are traditionally not being sequenced. The sequencing results showed a perfect alignment from reverse (gray) to forward (yellow) primer. Only one gap (-) and one mismatch (.) were found.

Based on these data about the forward and the reverse sequencing and the alignment, we can state that the product that has been amplified is correct. We can conclude successful CAG promoter specific primer design.

3.2.2.1.3. Primer specificity testing on several Cre lines showed no aspecific DNA amplification

In order to exclude the possibility that our designed CAGCre-ER specific primers hybridize to DNA of other Cre lines, we tested our CAG primer set on all Cre lines available in the lab (Figure 18). Only CAGCre-ER showed a clearly positive band at the height of 163 bp, whereas the other Cre lines did not show any band. IL2 was used as an internal control to ensure that the PCR reaction really had taken place. This control protected us from dealing with false negative results. Primer dimers were visible as a 30-50 bp smear with moderate intensity. Primer dimers are a by-product of the PCR reaction and arise when primer molecules hybridize to each other. The experiment was done in triplicate (only one out of three results is depicted) and we can conclude that no other Cre line showed false positive results (Figure 18).

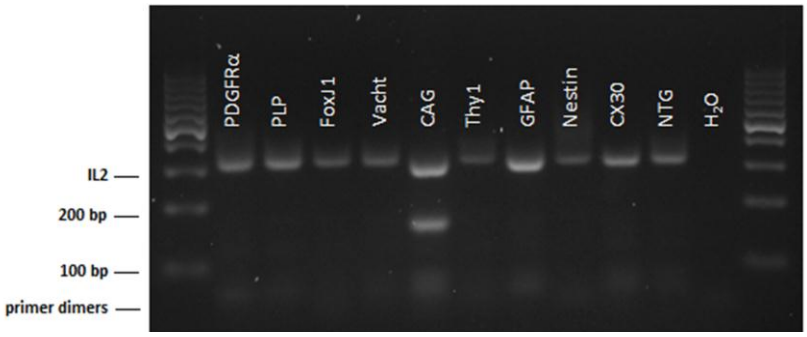

Figure 18. The designed CAG primer set is specific for CAGCre-ER. The CAG-specific primers only amplify a product for CAGCre-ER mice. No product is amplified in other Cre-ER^{TM} lines, nor in transgenic mice (NTG). Following Cre-ER lines were tested: PDGFRαCre-ER: oligodendrocyte precursor cells , PLPCre-ER: oligodendrocytes, FoxJ1Cre-ER: ependymal cells, VachtCre-ER: cholinergic neurons, CAGCre-ER: almost all cell types, Thy1Cre-ER^{TM}: motor neurons, GFAPCre: astrocytes, NestinCre-ER: subependymal cells, CX30Cre-ER: activated astrocytes. IL2 was used as an internal control. Primer dimers were visible as smears with low intensity at the height of 30-50 bp.

Taken together, both sequencing results and the primer testing on several Cre lines indicated that the primers we designed for the genotyping of the CAGCre-ER mice are specific for the CAG promoter. We can state that the designed CAG primers (Forward 5'-CAAGTACGCCCCCTATTGAC-3' ; reverse 5'-ATGGGGAGAGTGAAGCAGAA-3') are suited for further use as a genotyping tool in our laboratory.

3.2.2.2. Recombination efficiency of Notch-1$^{Lox/Lox\ and\ Lox/-}$ :: CAGCre-ER mice

3.2.2.2.1. The Notch-1 Real-Time PCR assay has an optimal amplification efficiency

The PCR amplification efficiency depicts the overall performance of a Real-Time PCR assay. A premise to apply the $\Delta\Delta C_t$ method for quantification is that the amplification efficiencies of the assays used is ranging between 90-100 %. Otherwise calculations of relative concentrations will be inaccurate, yielding delusive results (190). A sensitive method to check the efficiency of the assay of interest is to look how the obtained C_t values vary with template dilution.

In this set-up, we only checked the amplification efficiency of the Notch-1 assay, as the reference assays are commonly used in our laboratory and are considered as very good, as they have an efficiency of approximately 100 %. Figure 19 shows the results of the dilution experiment, in which a cDNA preparation from the liver of a mouse control sample was diluted over a 1000-fold range. Each dilution, done in triplicate, was amplified by using the Notch-1 assay. A standard curve of the logarithm of the cDNA concentration versus Ct was plot, from which the slope can be converted into a value for amplification efficiency by using following the equation:

$$E = (10^{-1/slope} - 1) \times 100$$

Normally, the efficiency (E) of the PCR should range between 90–100 % which equals a slope of about -3.32. This means that the amount of amplicon doubles with each cycle and thus a 10-fold increase will be obtained every 3.32 cycles ($\log_2 10 = 3.32$). In the case of our Notch-1 assay, the slope of the standard curve amounted -3.36 (Figure 19), suggesting an efficiency of 98.33 %. This value is near to 100 % so the $\Delta\Delta C_t$ method for the relative quantification of Notch-1 mRNA can be applied when using this Notch-1 assay.

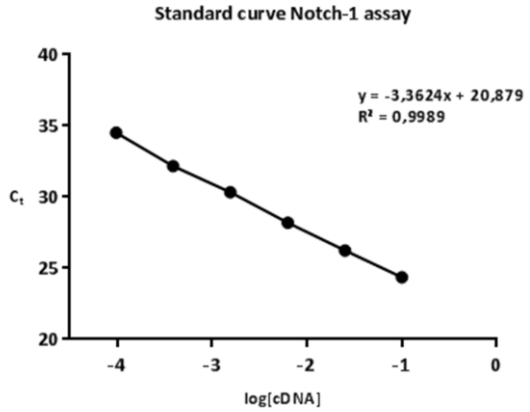

Figure 19. Standard curve of the Notch-1 assay. The amplification efficiency of the Notch-1 target gene by using the Notch-1 assay was examined using real-time PCR and TaqMan detection. cDNA was synthesized from 1 µg total RNA isolated from the liver of a mouse control sample. Each dilution, done in triplicate, was amplified using the Notch-1 assay. The highest concentration was derived from 1 µg of total RNA and dilutions were made over a 1000-fold range. The data were fit using linear regression analysis (n=3).

3.2.2.2.2. The recombination efficiency of CAGCre-ER in various tissues delivered satisfying results

As described above, it is mandatory to know to what extend the expression of the Notch-1 receptor is deleted in the various tissues with the tamoxifen-inducible CAGCre-ER. The knowledge about the amount of Notch-1 expression remaining after recombination in the various tissues of our Notch-1 deletion $SOD1^{G93A}$ mouse model, helps us to correctly interpret the observed phenotype in these mice. To quantify the changes in Notch-1 expression, as a result of ubiquitous CAGCre-ER-mediated recombination, we performed Real-Time PCR. Brain, spinal cord, sciatic nerve, gastrocnemius and liver samples from $Notch^{Lox/Lox}$ :: CAGCre-ER, $Notch^{Lox/-}$ :: CAGCre-ER and $Notch^{Lox/-}$ samples (n=3 per genotype) were collected one week after tamoxifen (Tx) administration and Notch-1 expression was analyzed. In this experiment, one of the $Notch^{Lox/-}$ mice, that also received tamoxifen, was used as a 100 % Notch-1 expression calibrator sample for $\Delta\Delta C_t$ quantification.

The RT-PCR results (Figure 20) showed that high levels of recombination were achieved in all of the tested tissues. Spinal cord, an important tissue in our study, displayed a recombination efficiency of 25 % in the $Notch^{Lox/-}$ :: CAGCre-ER group and 82 % in the $Notch^{Lox/Lox}$ :: CAGCre-ER group (Figure 20a). Sciatic nerve (Figure 20b) and gastrocnemius muscle (Figure 20c) also demonstrated good recombination results, as the efficiencies range between 40-45 % for the $Notch^{Lox/-}$ :: CAGCre-ER group and 70-75 % for the $Notch^{Lox/Lox}$ :: CAGCre-ER group, when compared to control mice ($Notch\text{-}1^{Lox/-}$).

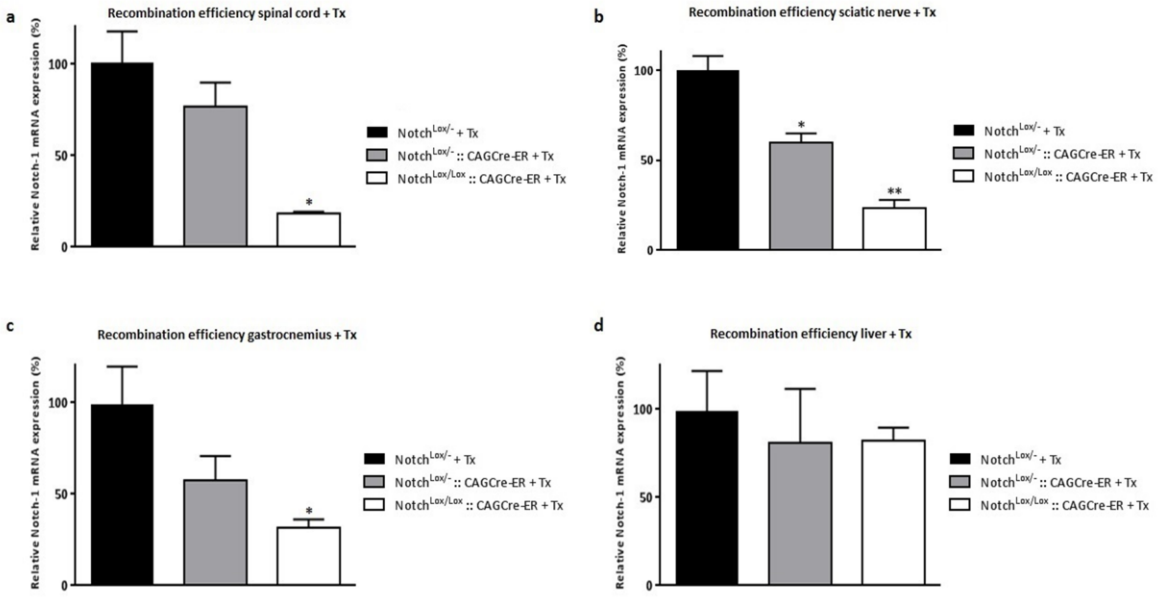

Figure 20. CAGCre-ER recombination efficiency in spinal cord, sciatic nerve, gastrocnemius and liver. a. Tamoxifen (Tx) induced recombination in spinal cord resulted in 25 % Notch-1 excision for $Notch^{Lox/-}$ :: CAGCre-ER and 82 % for $Notch^{Lox/Lox}$ :: CAGCre-ER mice. **b.** Sciatic nerve displayed 41 % Notch-1 excision for $Notch^{Lox/-}$ :: CAGCre-ER and 77 % for $Notch^{Lox/Lox}$ :: CAGCre-ER mice. **c.** Recombination in the gastrocnemius muscle amounted 43 % Notch-1 excision for $Notch^{Lox/-}$ CAGCre-ER and 69 % for $Notch^{Lox/Lox}$ CAGCre-ER mice. **d**. Liver showed unexpected results. Almost no recombination (19 % for $Notch^{Lox/-}$ :: CAGCre-ER and 18 % for $Notch^{Lox/Lox}$ :: CAGCre-ER) was observed, in accordance to literature (1). Data are shown as mean ± SEM (n=3 per genotype). Statistical differences as compared with $Notch^{Lox/-}$ + Tx are given as $*P < 0.05$, $**P < 0.001$; one-way ANOVA; Tukey's post-hoc analysis.

The results obtained from liver samples were surprising (Figure 20d). Only low and almost equivalent (19 % for Notch$^{Lox/-}$ :: CAGCre-ER and 18 % for Notch$^{Lox/Lox}$ :: CAGCre-ER) levels of recombination could be observed between groups, despite the fact that CAGCre-ER is known for its activity in almost all cell types. When looking in literature, we found that only low levels of recombination are evident in the liver, as in agreement with our results (1). This knowledge however, had no consequences for our mouse model as we were particularly interested in nervous system tissues.

Brain displayed a recombination efficiency of 49 % in the Notch$^{Lox/-}$ :: CAGCre-ER group and 76 % in the Notch$^{Lox/Lox}$ :: CAGCre-ER group, when compared to control mice (Figure 21a).

We also performed an experiment without tamoxifen administration, in order to exclude the effects from the different genotypes (without recombination) on the expression of Notch-1. When looking at the brain samples for example, no significant differences in brain Notch-1 expression between the groups were observed (Figure 21b), allowing us to conclude that the genotype by itself has no effect on the expression of Notch-1.

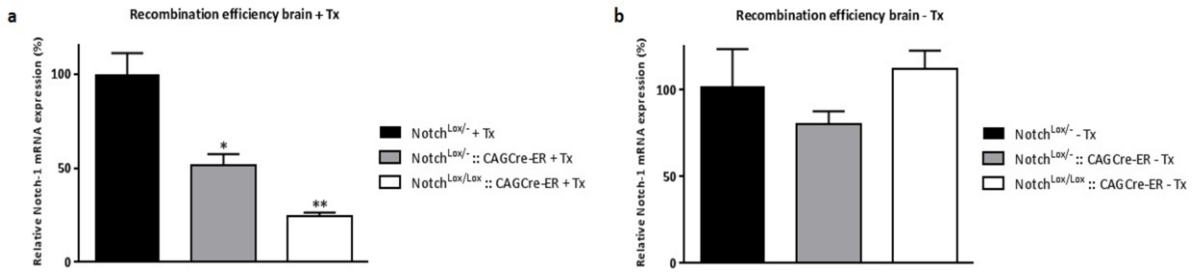

Figure 21. CAGCre-ER recombination efficiency in brain. a. Tamoxifen induced recombination in brain resulted in 49 % Notch-1 excision in Notch$^{Lox/-}$ :: CAGCre-ER and 76 % for Notch$^{Lox/Lox}$ :: CAGCre-ER mice. **b.** Mice that did not receive tamoxifen displayed comparable basal levels of Notch-1 expression. Data are shown as mean ± SEM (n=3 per genotype). Statistical differences as compared with **a.** Notch$^{Lox/-}$ + Tx, one-way ANOVA; Tukey's post-hoc analysis, *P < 0.05, **P < 0.001; as compared with **b.** Notch$^{Lox/-}$ - Tx, one-way ANOVA, P < 0.05.

Taken together, these results indicate that the transgenic CAGCre-ER line allows efficient modulation of Notch-1 gene activity in spinal cord, brain, sciatic nerve and gastrocnemius. Only liver tissue displayed low levels of recombination, as clearance of tamoxifen takes place.

3.2.2.2.3. Gel analysis of the RT-PCR product confirmed assay specificity for Notch-1

The Notch-1 assay description states that the product amplified by RT-qPCR has a length of approximately 83 bp. To confirm this and to assess the specificity of the Notch-1 assay, we visualized the RT-PCR product through agarose gel electrophoresis.

RT-PCR products from control Notch$^{Lox/-}$ (Ctrl), Notch$^{Lox/-}$ :: CAGCre-ER (HZ) and Notch$^{Lox/Lox}$ :: CAGCre-ER (KO) mice that received tamoxifen (Tx) were included in this experiment. The results showed that the amplified product from all three conditions was localized near the 100 bp region (Figure 22). This is in accordance with the 83 bp length proposed in the assay description. Also the proper controls were included during RT-PCR: no template control, no reverse transcription control (no RT) and no amplification. In the no template lane, no band was visible, as no cDNA was added during the qPCR reaction. The no RT lane neither displayed a band, indicating the absence of genomic DNA contamination. In the no amplification condition, no bands and no primer dimers were visible, as no assay was added to this condition (Figure 22).

No difference in band intensity between the HZ, KO and Ctrl groups was observed. This is because in RT-PCR, DNA amplification stops when a certain threshold of fluorescence has been reached. This threshold is the same for all of the different samples, even when they do not possess the same amount of target DNA to start with. Therefore, no difference in RT-PCR product intensity was observed between the three groups.

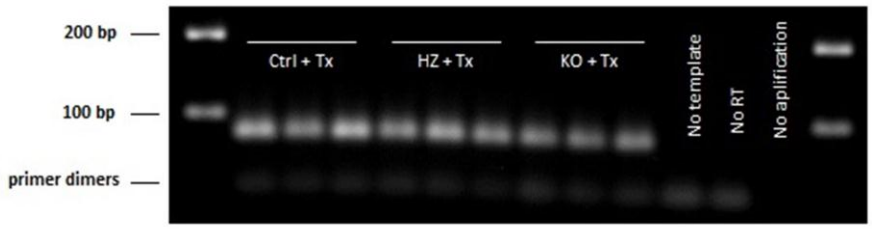

Figure 22. Gel analysis of the Notch-1 assay amplicon. RT-qPCR products of Notch$^{Lox/-}$ (Ctrl), Notch$^{Lox/-}$ :: CAGCre-ER (HZ) and Notch$^{Lox/Lox}$ :: CAGCre-ER (KO) mice that received tamoxifen (Tx) were visualized through agarose gel electrophoresis. No template, no reverse transcription (no RT) and no amplification controls were included during qPCR. The amplicon was localized near the 100 bp region for all three genotypes and equals the proposed 83 bp amplicon length. The negative controls do not display a band.

These results confirmed the specificity of the Notch-1 assay used for the assessment of the recombination efficiency of the Notch-1$^{Lox/Lox \text{ and } Lox/-}$ :: CAGCre-ER mice used throughout this study. The assay did not aspecifically amplify genomic DNA, confirming that the assay is exon spanning as stated by description.

In conclusion, CAGCre-ER specific primers will allow us to genotype CAGCre-ER mice in a specific way and the assessment of CAGCre-ER recombination efficiency has learnt us how much Notch-1 expression still remains present after recombination. Thanks to these measures, we now know that we can correctly interpret and explore the effect of Notch-1 deletion in ALS.

3.2.3. Evaluation of the effects of Notch-1 deletion on motor neuron degeneration and function of oligodendrocytes in SOD1^{G93A} mice

3.2.3.1. Assessment of oligodendrocyte function: Notch-1 deletion corrects function of oligodendrocytes in SOD1^{G93A} mice

Recent studies suggest that the function of oligodendrocytes is disrupted in SOD1^{G93A} mice, as the expression of MCT-1 and MBP, two oligodendrocytic markers for metabolic support and myelin formation, is shown to be reduced along with disease progression (88, 89).

It is known from literature that Notch-1 signaling is involved in the process of proliferation and differentiation of oligodendrocyte precursor cells into fully mature and functional oligodendrocytes (148).

Our hypothesis states that aberrant Notch-1 activity may prevent oligodendrocytes to fully mature into functional, myelinating and supportive oligodendrocytes. Therefore, we wanted to investigate whether Notch-1 deletion results into a rescue of the MBP and MCT-1 levels in SOD1^{G93A} mice, implicating an improvement of trophic support and myelination by oligodendrocytes.

To this end, we investigated the expression levels of MBP and MCT-1 proteins in lumbar spinal cords of Notch$^{Lox/-}$ :: CAGCre-ER :: SOD1^{G93A} mice (n=2) and Notch$^{Lox/-}$ :: SOD1^{G93A} mice (n=2) that received tamoxifen at the age of 60 days. Only two mice per genotype were available, so the main purpose was to look for trends in the expression levels of both proteins. The immunoblots for MBP and MCT-1 showed respectively a 32 % and 45 % increase in MBP and MCT-1 expression for the Notch$^{Lox/-}$ :: CAGCre-ER :: SOD1^{G93A} group, compared to the Notch$^{Lox/-}$ :: SOD1^{G93A} group (Figure 23).

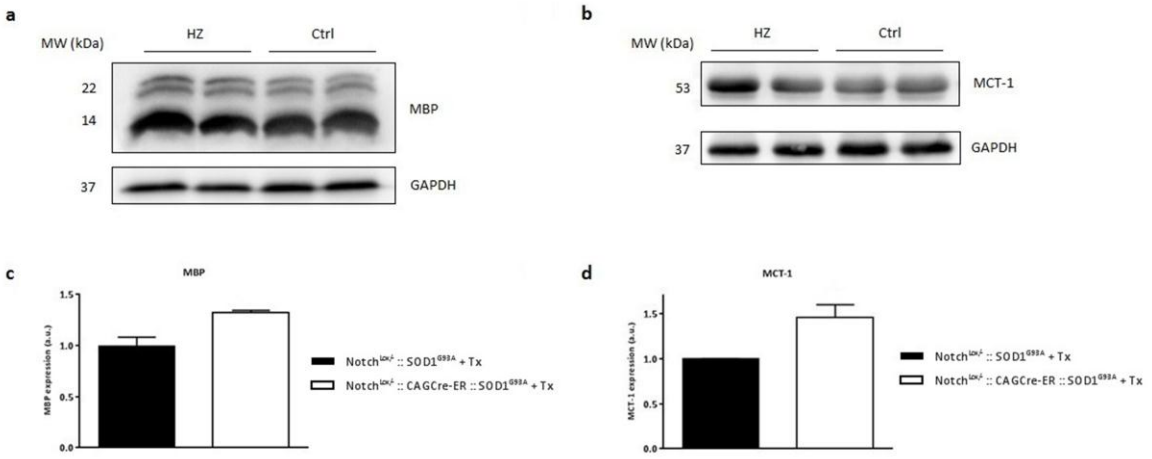

Figure 23. Notch-1 deletion results into better oligodendrocyte function. Western blot for **a.** MBP, a marker for myelin formation by oligodendrocytes, and for **b.** MCT-1, a marker for trophic support by oligodendrocytes. (HZ = Notch$^{Lox/-}$ :: CAGCre-ER:: SOD1^{G93A} + tamoxifen, Ctrl = Notch$^{Lox/-}$ :: SOD1^{G93A} + tamoxifen). **The quantification of c.** the expression levels of MBP and **d.** the expression levels of MCT-1 showed a possible rescue of the levels of MBP and MCT-1. **c.** A 32 % increase of MBP (p=0.06) was observed in the Notch$^{Lox/-}$ :: CAGCre-ER :: SOD1^{G93A} mice, compared with the Notch$^{Lox/-}$ :: SOD1^{G93A} mice. **d.** A 45 % increase of MCT-1 (p=0.08) was detected in the Notch$^{Lox/-}$ :: CAGCre-ER :: SOD1^{G93A} group, when compared to the Notch$^{Lox/-}$ :: SOD1^{G93A} group. Data are shown as mean ± SEM (n=2 per genotype). Only the bottommost MBP band was used for quantification. Statistical analysis was done using unpaired T-test ($p < 0.05$).

Surprisingly, despite the limited number of mice per group, p-values of 0.06 for MBP and 0.08 for MCT-1 could already be obtained, indicating that there is clearly a trend for increased MBP and MCT-1 expression levels in Notch$^{Lox/-}$ :: CAGCre-ER :: SOD1^{G93A} mice, when compared to control mice. These results implicate that Notch-1 deletion exerts a beneficial effect on myelination and neurotrophic support of the oligodendrocytes. Therefore, the experiment certainly has to be repeated in the future with an increased number of mice per group, in order to confirm whether the observed trend is truly significant.

3.2.3.2. Animal behavior and motor performance evaluation

3.2.3.2.1. Compound muscle action potential (CMAP) recording was more sensitive than rotarod and hanging wire to evaluate disease evolution and motor performance in SOD1^{G93A} mice

In order to evaluate disease evolution and function of the motor unit in SOD1^{G93A} mice in the most sensitive way, we assessed different methods: hanging wire, rotarod and compound muscle action potential (CMAP) recording.

Normally, disease onset is determined as the time-point of failure on hanging wire and rotarod. The SOD1^{G93A} mice in our experiment only started to fail the hanging wire test at the age of approximately 130 days, while motor neuron degeneration (disease onset) starts around 90 days of age (Figure 24a). Rotarod results showed no significant difference between SOD1^{G93A}, SOD1^{WT} and non-transgenic mice (Figure 24b)

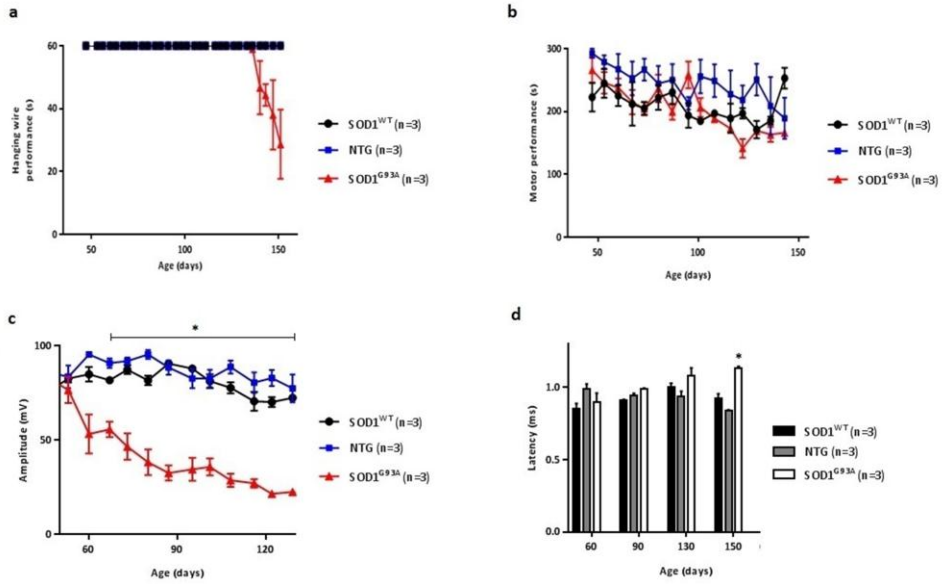

Figure 24. Sensitivity testing of the hanging wire test, rotarod and compound muscle activity recording. a. SOD1^{G93A} mice only started to fail the hanging wire test at the age of approximately 130 days. **b.** No difference during weekly testing on rotarod performance of non-transgenic (NTG), SOD1^{WT} and SOD1^{G93A} mice was observed. **c.** CMAP recordings revealed an enormous amplitude drop in SOD1^{G93A} at the age of 60 days and this decline continued during disease progression. **d.** Subtle differences in latencies were observed, with a trend of increase in SOD1^{G93A} mice. Data are shown as mean ± SEM (n=3 per genotype). Statistical differences of SOD1^{G93A} mice, as compared to NTG and SOD1^{WT} mice are given as $*P < 0.05$; one-way ANOVA; Tukey's post-hoc analysis.

CMAP recordings on the other hand, revealed an enormous amplitude drop at the age of 60 days, reflecting that at this time-point oligodendrocyte and motor neuron pathology had already initiated (Figure 24c). This decline in amplitude continued during disease progression. The increase in CMAP latencies of SOD1^{G93A} was only significant (p=0.001) at the age of 153 days. Changes in nerve conduction latency however are very subtle and difficult to detect. Despite this, a trend of increase for latencies was observable in SOD1^{G93A} mice.

From these results, we can conclude that CMAP recording is the most sensitive way to monitor disease evolution. Failure on the hanging wire test was only present at late disease stage and rotarod showed no significant difference in performance between the groups. We therefore decided to use CMAP recordings to evaluate disease evolution in the Notch-1 $^{Lox/Lox}$ :: CAGCre-ER :: SOD1^{G93A} mice, Notch-1 $^{Lox/-}$ :: CAGCre-ER :: SOD1^{G93A} mice and Notch$^{Lox/- \text{ and } Lox/Lox}$ :: SOD1^{G93A} mice, as described in the next section.

3.2.3.2.2. Notch-1 deletion results into a rescue of the CMAP amplitudes of SOD1^{G93A} mice

At protein level, an increase in MBP en MCT-1 expression was observed in Notch$^{Lox/-}$ :: CAGCre-ER :: SOD1^{G93A} mice. To investigate whether this improvement in trophic support en myelination of motor neurons was translated into a better outcome at the electrophysiological level, CAMPs were recorded from the gastrocnemius muscle after electrical stimulation at the sciatic notch.

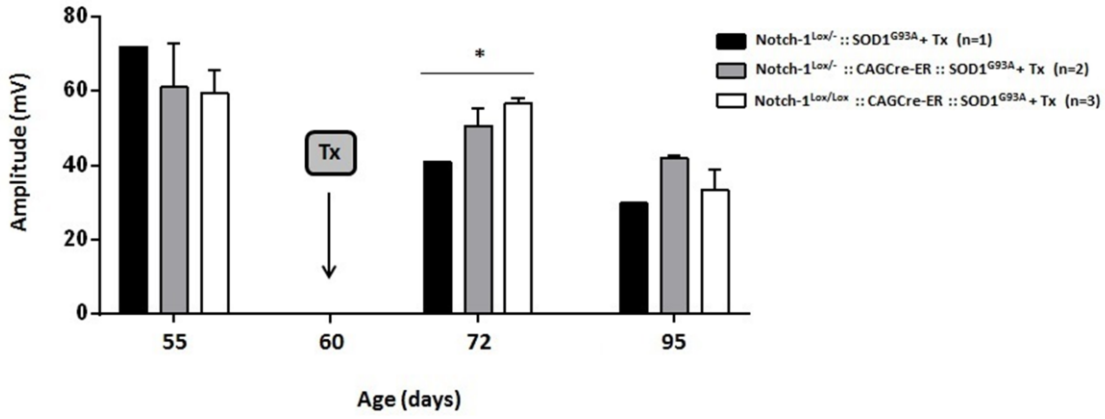

Figure 25. Deletion of Notch-1 results into a rescue of the CMAP amplitudes of SOD1^{G93A} mice. At the age of 55 days, before tamoxifen (Tx) administration, all three different genotype groups display equivalent CMAP amplitudes. After tamoxifen administration (day 60), Notch-1 $^{Lox/Lox}$ :: CAGCre-ER :: SOD1^{G93A} mice and Notch-1 $^{Lox/-}$ :: CAGCre-ER :: SOD1^{G93A} mice showed higher CMAP amplitudes at pre-symptomatic age (day 72) and at disease onset (day 95), as compared with Notch$^{Lox/- \text{ and } Lox/Lox}$ mice**.** Data are shown as mean ± SEM. Statistical differences as compared to Notch$^{Lox/- \text{ and } Lox/Lox}$ :: SOD1^{G93A} mice are given as *P < 0.05; one-way ANOVA; Tukey's post-hoc analysis.

By measuring the compound muscle action potential (CMAP), we observed that CMAP amplitudes were higher in Notch-1 $^{Lox/Lox}$ :: CAGCre-ER :: SOD1^{G93A} mice and Notch-1 $^{Lox/-}$ :: CAGCre-ER :: SOD1^{G93A} mice,

when compared to Notch$^{Lox/-\ and\ Lox/Lox}$ :: SOD1^{G93A} mice. At the age of 55 days, before tamoxifen administration, all three different genotype groups display equivalent CMAP amplitudes (Figure 25). After tamoxifen administration at day 60, mice that were homozygous and heterozygous for Notch-1 deletion, possessed higher CAMP amplitudes as compared with the controls, and this already at the pre-symptomatic (day 75) age and also at disease onset (day 95) (Figure 25). No significant differences in CMAP latencies were observed between de different groups at the different ages (data not shown).

The improvement of the CMAP amplitudes when Notch-1 is deleted in all cell types (Notch-1 $^{Lox/Lox}$ :: CAGCre-ER :: SOD1^{G93A} mice and Notch-1 $^{Lox/-}$ :: CAGCre-ER :: SOD1^{G93A} mice) indicated an improvement of the connectivity of the neuromuscular unit. The changes in CMAP latency were very subtle and difficult to detect, but a tendency of decrease could be observed in case of Notch-1 deletion, pointing to better nerve conduction in the periphery.

3.2.3.2.3. Notch-1 deletion results into an improved muscle innervation in SOD1^{G93A} mice

From the western blots for MBP and MCT-1, we can conclude that Notch-1 exerts a deleterious effect on motor neuron trophic support and myelination. CMAP amplitudes were also shown to be improved upon Notch-1 deletion, pointing to a better preservation of the motor unit. Taken together with the fact that Notch-1 is known to cause axon retraction, we wanted to investigate the effect of Notch-1 deletion on muscle innervation in SOD1^{G93A} mice.

To this end, we quantified the innervation of the neuromuscular junctions (NMJs) of the gastrocnemius muscle using α-bungarotoxin and NF-200 staining and quantified the number of fully innervated, partially innervated and denervated NMJs. Our results revealed a significant 22 % increase in the number of fully innervated NMJs in Notch$^{Lox/-}$ :: CAGCre-ER :: SOD1^{G93A} mice (n=2) compared with Notch$^{Lox/-}$ :: SOD1^{G93A} mice (n=2) (Figure 26a). No significant difference in the number of partially innervated NMJs was observed (Figure 26b). Figure 26c, shows a tendency to a decrease in the number of denervated NMJs, when Notch-1 is deleted. More mice per group are needed to confirm these data.

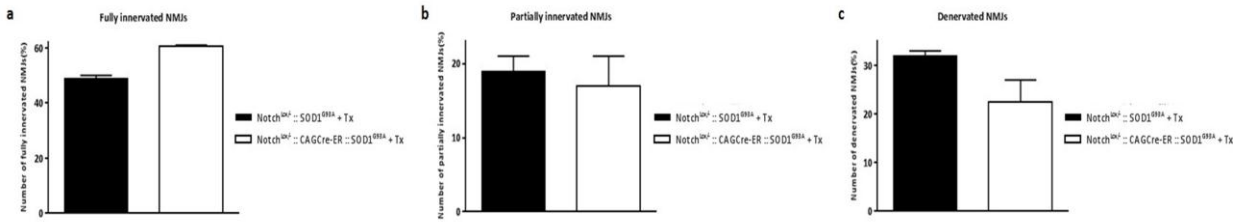

Figure 26. Deletion of Notch-1 improves muscle innervation in SOD1^{G93A} mice. a. The number of fully innervated neuromuscular junctions (NMJs) was significantly increased in Notch$^{Lox/-}$ :: CAGCre-ER :: SOD1^{G93A} mice. **b.** The number of partially innervated NMJs of Notch$^{Lox/-}$ :: CAGCre-ER :: SOD1^{G93A} mice was comparable to that of Notch$^{Lox/-}$ :: SOD1^{G93A} mice **c.** A tendency of a decrease in the number of denervated NMJs could be observed between groups. Data are shown as mean ± SEM (n=2 per genotype). Statistical differences as compared with Notch$^{Lox/-}$ :: SOD1^{G93A} are given as *P < 0.001; unpaired T-test ($p < 0.05$).

These results show that Notch$^{Lox/-}$ :: CAGCre-ER :: SOD1^{G93A} mice possess more fully innervated and less denervated NMJs, compared to Notch$^{Lox/-}$ :: SOD1^{G93A} mice. This observation is in line with the better CMAP recordings, as described previously.

Taken together, our data suggest that Notch-1 deletion in all cell types in the SOD1^{G93A} mouse model result into better myelination of and better trophic support to motor neurons and consequently into an improvement of the preservation of the NMJs. Possibly, this might slow down disease progression and prolong survival.

4. Discussion

In ALS research, the mutant SOD1^{G93A} mouse model, that develops pathology reminiscent of ALS, is one of the most frequently used models and has also been used throughout this study. These mice overexpress the human *SOD1* gene with a substitution of Glycine by Alanine at position 93 (27). Human wild-type SOD1 overexpressing mice, that carry the normal allele of the human *SOD1* gene, serve as a control as they do not develop ALS-like pathology and have a normal lifespan. During the disease course of SOD1^{G93A} mice, several pathological changes occur in the ventral horn of the spinal cord. At the pre-symptomatic stage, signs of neuroinflammation, a process wherein microgliosis and astrocytosis play a key role, are already present (87). At this stage, also degeneration of gray matter oligodendrocytes is already noticeable (89, 117). All of these reactive glial changes occur prior to disease onset and actively contribute to motor neuron degeneration. This is considered as the non-cell autonomous component of the pathogenesis of ALS, meaning that cells beyond the motor neurons contribute to the observed motor neuron death (4, 31, 95). Recently, our laboratory and an independent research group published that oligodendrocytes degenerate in the spinal cord gray matter of ALS mice, already prior to disease onset, whereupon they are being replaced by new oligodendrocytes, as NG2 glia sense this loss of oligodendrocytes and increase their proliferation and differentiation rate (89, 117). However, the newly formed oligodendrocytes were shown to be dysfunctional, as they are not fully mature (89, 117). Also in *post-mortem* spinal cord tissue of ALS patients, degenerating oligodendrocytes were found to be present (117), thereby strengthening the importance of the study of oligodendrocytes in the pathogenesis of ALS.

Based on these findings, we made the assumption that the rescue of oligodendrocyte dysfunction may result into beneficial and protective effects on the motor neurons. Notch-1 signaling is known to be involved in the process of proliferation and differentiation of NG2 glia into mature and functional oligodendrocytes (148). This, together with the knowledge that Notch-1 signaling blocks oligodendrocyte maturation and therefore causes remyelination failure in MS pathology (122, 188), led to the hypothesis that aberrant Notch-1 activity may contribute to the observed oligodendrocyte dysfunction in ALS.

In order to test our hypothesis we started with the characterization of Notch-1 expression and activation in the spinal cord of SOD1^{G93A} and SOD1^{WT} mice at the age of 130 days. Immunofluorescent co-stainings, showed no Notch-1 immunoreactivity in microglia and astrocytes in both ALS mice and controls. In oligodendrocytes and neurons of SOD1^{G93A} and SOD1^{WT} mice, we could clearly observe Notch-1 expression and activation. Notch-1 signaling was found to be present in both dorsal and ventral horn and also in both gray and white matter.

The presence of Notch-1 in oligodendrocytes has mainly been described under pathological conditions, for instance in MS lesions (122, 188). On the other hand, the presence of Notch-1 in the oligodendrocytes of SOD1^{WT} mice can be explained by the fact that the Notch-1 activity in oligodendrocytes is needed to keep them in a terminally differentiated state. Mainly Sox-10 has been investigated in this regard, however in keratinocytes it has been shown that Notch-1 induces terminal differentiation through down-regulation of c-myc (191, 192).

The finding of Notch-1 expression in (motor) neurons is in accordance with several findings in literature, as Notch-1 was found *in vitro* to be constitutively expressed at low level in post-mitotic neurons and *in vivo* in mature neurons in the adult mouse and human brain (170, 176).
Interestingly, we observed the expression of Notch-1 in NG2 glia to change with disease progression: until the age of 130 days no Notch-1 expression could be observed in the NG2 glia in $SOD1^{G93A}$ mice, whereas at disease end-stage, Notch-1 was found in NG2 glia. In $SOD1^{WT}$ mice no Notch-1 immunoreactivity was found in NG2 glia at any age. Although no absolute quantifications were performed, enhanced proliferation of these cells was noticeable, which is in accordance with literature that by end-stage, NG2-positive cells exhibit the highest rate of proliferation and differentiation into oligodendrocytes (89, 117). The presence of Notch-1 in NG2 glia has already been described to inhibit oligodendrocyte precursor cell differentiation into mature and functional oligodendrocytes (122, 148). This, together with our observation of extensive Notch-1 activation in NG2-positive cells at end-stage, and the knowledge that the newly formed oligodendrocytes are dysfunctional (89, 117), might implicate that Notch-1 signaling plays a role in the oligodendrocyte pathology observed in ALS, as we hypothesize that aberrant Notch-1 activity in ALS may prevent oligodendrocyte differentiation into mature and functional oligodendrocytes.

To evaluate whether this assumption is true, we investigated the effect of ubiquitous Notch-1 deletion in the $SOD1^{G93A}$ model. We used CAGCre-ER mice, a mouse line that expresses the Cre-recombinase in almost all cell types (1), and induced recombination with tamoxifen at the age of 60 days. Spinal cord, an important tissue in our study, displayed a recombination efficiency of 82 % in homozygous Notch-1 knock-out mice and 25 % in heterozygous Notch-1 knock-out mice. No absolute percentages of recombination for CAGCre-ER are found in literature, but efficient dose-dependent excision has been described throughout the central nervous system (1). The efficiency of recombination in other tissues, such as the gastrocnemius muscle, sciatic nerve and brain, ranged between 70-75 % for homozygous Notch-1 knock-out mice and 40-50 % for heterozygous Notch-1 knock-out mice. With the knowledge of the exact amount of Notch-1 excision in all of these tissues, we next evaluated whether deletion of Notch-1 in $SOD1^{G93A}$ mice influenced myelination and trophic support provided by oligodendrocytes.

Oligodendroglia are considered to be the major site of MCT-1 lactate transporter expression and thus constitute one of the most important cell types that nourish neurons with lactate (88). This transported lactate is also used by the oligodendrocytes themselves, in order to be able to produce MBP, a structural protein of the myelin sheath (127, 144). Therefore, MCT-1 and MBP protein expression levels in the lumbar spinal cord were used as a read-out for oligodendrocyte functionality. Notch-1 deletion was induced at the age of 60 days through tamoxifen administration and mice were sacrificed at the age of 130 days (symptomatic stage). By immunoblotting for MCT-1 and MBP, we found MCT-1 and MBP levels to be increased with 45 % and 32 % respectively, compared with age-matched $SOD1^{G93A}$ mice. In $SOD1^{G93A}$ mice, it has already been shown that the expression level of these two markers decreases along with disease progression and in ALS patients a 50 % decline in MCT-1 expression has been observed (88, 89). Up to now, the exact mechanism causing this drop in MBP and MCT-1 levels was unknown. Our results demonstrate that by ubiquitous deletion of the Notch-1 receptor, a rescue of both functional markers could be obtained, suggesting an important role of Notch-1 signaling in the function of

oligodendrocytes. In our laboratory, immunoblotting for MBP and MCT-1 was already performed on RBP knock-out mice and a rescue of the MBP and MCT-1 levels was observed (unpublished data). Since the RBP protein is common to Notch-1,-2, -3 and -4 signaling pathways, it was unclear which of the four cascades had caused the observed effect. This study with the Notch-1 knock-out SOD1^{G93A} mouse model, gives a slight indication that the Notch-1 signaling pathway could possibly be the foundation of the observed effect, as similar results were obtained. To be fully sure that the effect was indeed solely mediated through Notch-1 signaling, similar experiments with Notch-2, -3 and -4 knock-out mice have to be conducted in the near future. Since motor neurons are highly dependent of MCT-1 lactate transport to meet their metabolic needs, the observed increase in MCT-1 levels may contribute to improved (motor) neuron survival and maintenance of their axon function (117). The increased MBP levels point to a better myelination of axons, thereby enhancing the integrity of the neuromuscular unit.

To evaluate whether the improvements at the level of the oligodendrocyte function observed on western blot could be translated into a better outcome at the level of the motor neuron and its muscle innervation, compound muscle action potentials (CAMPs) were recorded from the gastrocnemius muscle. The motor neuron is part of a neuronal circuit, comprising the motor neuron cell body in the CNS and its axon as a part of the PNS, which forms synapses with for example the gastrocnemius muscle. Although CMAP recordings give information about the axonal loss and conduction velocity in the periphery, the improvement of motor neuron support in the CNS can lead to better outcomes in the periphery, given the connectivity of this neuronal circuit.

CMAP recordings in SOD1^{G93A} mice revealed a drop of the amplitude at the age of 60 days to approximately 30 mV, reflecting that at this time-point peripheral axonal loss had already initiated. This can be due to the loss of motor neurons in the ventral horn of the spinal cord, or as a consequence of the dying-back mechanism in ALS. According to this mechanism, axonal degeneration starts in the periphery at the distal axon end and moves towards the motor neuron cell bodies. The neuromuscular junctions already start to degrade, while the motor neuron cell bodies in the CNS are still intact (193). The SOD1^{G93A} mice with ubiquitous Notch-1 deletion however, still displayed an amplitude of approximately 60 mV at 72 days of age, and scored better on CMAP recordings during disease progression, pointing to a better connectivity of the neuromuscular junctions. The changes in CMAP latency were very subtle and difficult to detect, but a tendency of decrease could be observed in Notch-1 knock-out mice, indicating better nerve conduction in the periphery. This suggests two possible explanations, as Notch-1 is deleted in all cell-types. First of all, the negative influence of Notch-1 signaling on the oligodendrocytes results into a harmful environment for the motor neurons, with a lack of trophic support, and consequently axon retraction takes place. A second possible explanation is that Notch-1 may have a negative influence at the level of the neuromuscular junctions, thereby explaining the better CMAP measurements in the periphery in SOD1^{G93A} mice with ubiquitous Notch-1 deletion. The knowledge that Notch-1 is expressed in Schwann cells (194) and in the gastrocnemius muscle, together with the fact that Notch-1 is known to cause axon retraction, suggests that the effects seen in the PNS might have been mediated through Notch-1 deletion at the level of the NMJs from the gastrocnemius muscle that result into better innervation.

To evaluate whether Notch-1 deletion may have a beneficial impact on the communication between the gastrocnemius muscle and the synapse forming axons, the number of innervated neuromuscular junctions was quantified using α-bungarotoxin and NF-200 staining. The number of innervated NMJs was increased in $SOD1^{G93A}$ mice with ubiquitous Notch-1 deletion, as expected by the improvement of CMAP amplitudes. Since we used CAGCre-ER mice in this study, Notch-1 was deleted from all cell-types. Therefore, the possibility exist that the observed effect may not merely be a result of better myelination and trophic support in the CNS, but can also be attributed to better preservation of the axons and neuromuscular junctions in the periphery, as Notch signaling is known to be present in Schwann cells and the gastrocnemius muscle (194). To further elucidate this issue and in order to be able to assign a certain effect to a specific cell-type, cell-specific knock-out experiments will be conducted in the near future.

Although more mice are needed to confirm all of the observations, these exciting discoveries are already a strong indication of the relation between the Notch-1 signaling pathway and the proper function of oligodendrocytes, motor neuron survival and muscle innervation.

5. Conclusion and future perspectives

Based on our results in the SOD1^{G93A} mouse model, we can conclude the involvement of Notch-1 signaling in the pathogenesis of ALS. By ubiquitously deleting the Notch-1 receptor with CAGCre-ER, we showed beneficial effects on myelination and trophic support, as a recovery of MBP and MCT-1 levels was observed. Consequently, this resulted into better preservation of the neuromuscular unit, as higher CMAPs were recorded and an improvement of the innervation of the NMJs was detected. Possibly, all of these effects may slow down disease progression and prolong survival. In this study we did not investigate the effect on survival, as the amount of available triple transgenic mice was limited and because we sacrificed them at the age of 130 days for our functional experiments. Hopefully these data can be extrapolated in the future to ALS patients, as in these patients oligodendrocyte degeneration and a 50 % decline in MCT-1 expression have also been observed (88).

Therefore, Notch-1 signaling may create possibilities for therapeutic intervention. Before getting to this point, a number of additional experiments have to be conducted and some questions need to be answered.

First of all, which effects can we observe by cell-type specifically deleting the Notch-1 receptor instead of ubiquitously? It would be of interest to modulate Notch-1 only in neurons, oligodendrocytes, oligodendrocyte precursor cells (NG2), Schwann cells or in muscle cells by means of the following tamoxifen-inducible Cre-ER lines: Thy1Cre-ER, PLPCre-ER, PDGFRaCre-ER, P0Cre-ER or PGKCre-ER. This will give more information about Notch-1 deletion specifically in one cell-type and the effects on disease onset, disease progression and overall survival of ALS mice. This will be tested in the near future.

It would also be interesting to perform the mirror experiment of Notch-1 deletion, namely Notch-1 overexpression in SOD1^{G93A} mice. This can be achieved by crossbreeding Rosa-lox-stop-lox-NICD mice, in which a LoxP-flanked neomycin stop cassette blocks the overexpression of the active form of Notch-1 (NICD), with Cre-ER and SOD1^{G93A} mice. By administering tamoxifen, Cre-mediated recombination takes place and NICD becomes overexpressed. In this way we can investigate whether a deterioration of MBP and MCT-1 levels, CMAPs and muscle innervation, but also disease acceleration and shortening of overall survival will be obtained by overexpressing Notch-1 in all cell-types and cell-type specifically.

Pharmacological modulation of Notch-1 signaling in the SOD1^{G93A} model of ALS also needs to be conducted to define Notch-1 signaling as a potential therapeutic target. This can be done through intraventricular administration of several agents, such as γ-secretase inhibitors, Notch-1 neutralizing antibodies or antibodies blocking Notch-1 ligands. In this way, side effects of systemic administration are being avoided as Notch-1 is involved in several processes. Currently, the effect of the administration of γ-secretase inhibitors is under investigation.

To conclude, Notch-1 signaling may represent a potential target for therapeutic intervention in ALS and can be promising as well for other neurodegenerative diseases in which Notch-1 is known to be involved, such as Alzheimer's disease, ischemic stroke and multiple sclerosis. Further research on this topic would be of great interest and necessity.

Nederlandse samenvatting

INLEIDING

De ziekte van Alzheimer, Huntington, Parkinson en amyotrofe laterale sclerose (ALS) zijn de vier meest voorkomende neurodegeneratieve aandoeningen. Door de sterk toegenomen levensverwachting en de hieruit voortvloeiende vergrijzing van de bevolking, wordt onze samenleving steeds meer geconfronteerd met deze ziektes. Hierdoor komen zorginstellingen onder grote druk te staan, maar ook de patiënten zelf en hun omgeving krijgen heel wat leed te verwerken. Daarom onderstrepen we hier het belang van het neurobiologisch onderzoek in het vinden van nieuwe therapeutische aangrijpingspunten voor deze vreselijke aandoeningen.

In deze studie vestigen we de aandacht op ALS, een progressieve neurodegeneratieve aandoening waarbij selectief de motor neuronen in het ruggenmerg, de hersenstam en de motor cortex worden aangetast. De klinische presentatie is vrij variabel en de ziekte begint meestal rond de leeftijd van 50 à 60 jaar. Patiënten krijgen te maken met spierzwakte en atrofie, onwillekeurige spierbewegingen, verlamming en overlijden binnen de 2 à 5 jaar na het begin van de ziekte, aangezien er nog geen effectieve therapie beschikbaar is. ALS heeft een prevalentie van 1 per 100.000 mensen en de incidentie bedraagt 8 per 100.000 mensen vermits de meeste patiënten binnen 5 jaar na diagnose overlijden. Bij 90 % van de ALS patiënten, genaamd sporadische ALS (SALS), is de onderliggende oorzaak niet gekend. In slechts 10 % van de gevallen is er een genetische component aanwezig. Deze zogenaamde familiale ALS (FALS) vorm wordt voornamelijk veroorzaakt door dominante mutaties in *C9ORF72, SOD1, TARBP* en *FUS/TLS*.

Ongeveer 20 % van de FALS patiënten heeft mutaties in het superoxide dismutase 1 (*SOD1*) gen. SOD1 is een enzym dat betrokken is in het opruimen van vrije zuurstof radicalen en komt in bijna alle celtypes tot expressie. Het beschermt de cel tegen oxidatieve stress, maar het is nog niet duidelijk of een verlies of toename van deze functie leidt tot het afsterven van motor neuronen.

Het $SOD1^{G93A}$ muismodel is een nuttig diermodel in het neurobiologisch onderzoek naar ALS. Deze muizen brengen het humane *SOD1* gen, waarbij Glycine vervangen is door Alanine op positie 93, tot overexpressie. Hierdoor ontwikkelen ze een pathologie die lijkt op die van ALS. Verschillende studies hebben aangetoond dat de door mutant SOD1-geïnduceerde FALS vorm, niet het resultaat is van alleen maar de aanwezigheid van het mutante SOD1 in de motor neuronen. Het mutante SOD1 moet tegelijkertijd ook aanwezig zijn in naburige niet-neuronale cellen zoals astrocyten, microglia en oligodendrocyten. Dit komt erop neer dat, in tegenstelling tot wat men voor lange tijd dacht, ALS een niet-cel autonome ziekte is.

Oligodendrocyten zijn post-mitotische cellen die instaan voor een snelle prikkelgeleiding doorheen het centraal zenuwstelsel, door de axonen te voorzien met een myeline schede. Deze schede is opgebouwd uit structurele proteïnes zoals ‘myelin basic protein’ (MBP) en ‘proteolipid protein’ (PLP). Myelinisatie gebeurt niet enkel tijdens de embryonale ontwikkeling, maar wordt ook verdergezet tijdens het postnatale leven wanneer schade of neurodegeneratie zich voordoen. Oligodendrocyten hebben niet enkel een myeliniserende functie, maar bevoorraden de motor neuronen ook met lactaat via de

monocarboxylaat transporter 1 (MCT-1) om hen zo in hun hoge metabole noden te voorzien. Aangezien oligodendrocyten post-mitotisch zijn en dus niet kunnen delen, worden deze cellen gevormd uit een reservoir van oligodendrocyt precursor cellen (OPCs), de zogenaamde NG2 glia. De OPCs migreren naar de plaats van schade en differentiëren tot oligodendrocyten in verschillende stappen (Figuur 4).

Bij $SOD1^{G93A}$ muizen en ALS-patiënten degenereren de oligodendrocyten in de grijze stof nog voor het begin van de ziekte, waarna ze worden vervangen door nieuwe oligodendrocyten. Deze nieuwgevormde oligodendrocyten bleken echter dysfunctioneel te zijn, aangezien de expressieniveaus van MBP en MCT-1, twee functionele markers voor de oligodendrocyten, gedaald zijn. Het falen van myelinisatie en trofische ondersteuning van de motor neuronen zou kunnen bijdragen tot de waargenomen motor neuron sterfte en deze zelfs verergeren.

OPZET VAN DEZE STUDIE

Onze hypothese stelt dat Notch-1 signaaltransductie een rol zou kunnen spelen in de pathogenese van ALS. De cascade is namelijk betrokken in onder meer neurogenese, neuriet uitgroei, het behouden van het neuronale stamcelreservoir in het volwassen centraal zenuwstelsel en ook de proliferatie en differentiatie van oligodendrocyt precursor cellen (OPC) tot volwassen en myeliniserende oligodendrocyten. Vermits men heeft aangetoond dat bij ALS de differentiatie van deze OPCs tot volwassen oligodendrocyten niet goed verloopt en vermits Notch-1 tot expressie komt op OPCs en oligodendrocyten, ontstond de hypothese dat afwijkende Notch-1 activatie zou kunnen bijdragen tot het falen van de aanmaak van nieuwe én functionele oligodendrocyten. Deze hypothese wordt verder ondersteund door het bewijs dat Notch-1 signaaltransductie betrokken is in andere neurodegeneratieve aandoeningen zoals de ziekte van Alzheimer en multiple sclerose. Daarom willen we dan ook in deze studie de bijdrage van Notch-1 signaaltransductie in de pathogenese van ALS nagaan door Notch-1 expressie te verwijderen in bijna alle weefsels van het $SOD1^{G93A}$ model. Om het effect van Notch-1 deletie na te gaan in het $SOD1^{G93A}$ model, zullen we in verschillende stappen tewerk gaan (zie 'experimenteel werk en resultaten')

INTERMEZZO: OVERZICHT VAN NOTCH-1 SIGNAALTRANSDUCTIE

Binding van de DSL (Delta, Serrate, LAG2) ligand met de Notch receptor, resulteert in een conformationele verandering van deze receptor (Figuur 6). De eerste klieving wordt gemedieerd door α-secretase, waardoor het extracellulaire deel van de Notch receptor (NECD) wordt vrijgelaten dat vervolgens transendocytose ondergaat in de cel waarop de ligand gelokaliseerd is. De tweede transmembranaire klieving wordt uitgevoerd door het γ-secretase complex en het Notch intracellulaire domein (NICD) wordt vrijgezet. NICD transloceert naar de kern, waar het een complex vormt met twee transcriptiefactoren: het nucleair proteïne Mastermind (MAM) en C promoter-binding factor 1 (CBF1). Het NICD/MAM/CBF1 complex bindt de promoter van doelwit genen, waaronder *Hes* genen. Deze genen inhiberen de differentiatie en proliferatie van verschillende celtypes. Het beëindigen van de Notch-1 signaaltransductie wordt gemedieerd door het SEL-10 ligase, een E3 ubiquitin ligase. SEL-10 hecht een ubiquitine label vast aan de proline, glutamaat, serine, threonine (PEST) sequentie van NICD, waardoor het omgevormd wordt tot een substraat voor afbraak door het proteasoom.

EXPERIMENTEEL WERK EN RESULTATEN

Het in kaart brengen van Notch-1 expressie in het SOD1^{G93A} muismodel toonde co-lokalisatie aan van Notch-1 met neuronen, oligodendrocyten en NG2 glia

Om te identificeren welke celtypes Notch-1 receptor expressie en activatie vertonen, hebben we immunofluorescente kleuringen uitgevoerd. Vriescoupes van het lumbale ruggenmerg van 130 dagen oude SOD1^{G93A} en SOD1^{WT} muizen werden fluorescent gekleurd met antilichamen gericht tegen Notch-1 en verschillende merkers zoals NeuN voor neuronen, CC-1 voor oligodendrocyten, NG2 voor oligodendrocyt precursor cellen. In deze laatst genoemde cellen, werd de Notch-1 kleuring ook uitgevoerd tijdens terminale fase van de ziekte.

Notch-1 expressie en activatie werd waargenomen in zowel het SOD1^{G93A} als het SOD1^{WT} muismodel in neuronen (Figuur 11) en oligodendrocyten (Figuur 12a), maar niet in astrocyten en microglia (Figuur 12b,c). In NG2 cellen was de situatie iets ingewikkelder. Noch SOD1^{G93A} muizen en noch SOD1^{WT} muizen vertoonden Notch-1 expressie op de leeftijd van 130 dagen (Figuur 13 boven en midden). Wanneer we op de eindfase van de ziekte keken daarentegen, zagen we extensieve co-lokalisatie van het Notch-1 en NG2 fluorescente signaal. Dit toont aan dat Notch-1 activatie alomtegenwoordig aanwezig was in deze cellen (Figuur 13, onder).

De ontworpen primers waren specifiek voor CAGCre-ER en de recombinatie efficiëntie van CAGCre-ER in verschillende weefsels was bevredigend

Eerst hebben we het muismodel waarin Notch-1 in alle weefsels wordt verwijderd volledig gekarakteriseerd. Dit om er zeker van te zijn dat de interpretatie van de waargenomen effecten in dit model wel degelijk correct zijn.

Primer ontwerp

De expressie van Cre-recombinase in ons muismodel, is onder controle van de chimere promoter van de 'cytomegalovirus (CMV) immediate-early enhancer' en de 'chicken β-actin promoter/enhancer' (CAG). Dit construct is van nature niet aanwezig in eender welke muis, daarom hebben we de voorwaartse primer (5'-CAAGTACGCCCCCTATTGAC-3', T_s = 59,45 °C) ontworpen tegen nucleotide 78-197 van de CMV enhancer en de achterwaartse primer (5'-ATGGGGAGAGTGAAGCAGAA-3', T_s = 59,80 °C) werd ontworpen tegen nucleotide 8-37 van de chicken β-actin promoter/enhancer (Figuur 14). De grootte van het geamplificeerde product was 163 bp, zoals getoond wordt in Figuur 15 (rechts).

Om te kijken of het juiste product werd geamplificeerd tijdens de polymerase chain reaction (PCR), hebben we de geamplificeerde producten opgezuiverd uit de agarose gel en deze opgestuurd voor bi-directionele sequencing naar LGC Genomics (Berlijn, Duitsland). De voorwaartse en achterwaartse sequencing resultaten werden gealigneerd met de sequentie van de CAG promoter met behulp van de

EMBOSS Needle interface. Gebaseerd op onze voorwaartse en achterwaartse sequencing resultaten, kunnen we zeggen dat het juiste product door dit primer paar werd geamplificeerd.

Om er zeker van te zijn dat onze primers geen DNA amplificeren in andere Cre muislijnen, hebben we deze uitgetest op alle beschikbare Cre muislijnen die beschikbaar zijn in het labo (Figuur 18). Enkel CAGCre-ER vertoonde een positieve band van 163 bp. IL2 werd gebruikt als interne controle om er zeker van te zijn dat de PCR reactie wel degelijk was opgegaan (Figuur 18). Deze controle beschermde ons ook tegen vals negatieve resultaten.

Op basis van deze resultaten kunnen we zeggen dat de ontworpen primers geschikt zijn voor verder gebruik in het labo.

Recombinatie efficiëntie met RT-PCR

Eerst en vooral zijn we de efficiëntie van onze Notch-1 assay nagegaan om er zeker van te zijn dat we de $\Delta\Delta C_t$ mochten toepassen voor het bepalen van de relatieve Notch-1 mRNA expressie. Een gevoelige methode om de efficiëntie van een assay na te gaan, is te bepalen hoe de verkregen C_t waarden variëren met de verschillende verdunningen van de template. Normaal ligt de efficiëntie van de PCR reactie tussen de 90–100 %, wat overeenkomt met een richtingscoëfficiënt van - 3,32. De richtingscoëfficiënt van onze Notch-1 assay bedroeg - 3,36, wat overeenstemt met een efficiëntie van 98,33 %, wat binnen de grens van 90–100 % lag (Figuur 19). Het PCR product werd achteraf ook op gel gezet en toonde aan dat het juiste fragment tijdens de PCR reactie werd geamplificeerd en gedetecteerd (Figuur 22).

Vervolgens hebben we de recombinatie efficiëntie van de Notch-1 assay bepaald met behulp van RT-PCR, om een idee te krijgen van hoeveel Notch-1 expressie overblijft na CAGCre-ER recombinatie in verschillende weefsels. De resultaten toonden aan dat CAGCre-ER recombinatie efficiëntie modulatie van Notch-1 gen activiteit toelaat in het ruggenmerg (82 %), de hersenen (76 %), de sciatische zenuw (77 %) en de gastrocnemius spier (69 %) (Figuur 20a,b,c en Figuur 21a,b). In de lever daarentegen, was bijna geen recombinatie te bespeuren (18 %), zoals reeds beschreven werd in de literatuur (Figuur 20d).

Notch-1 deletie corrigeert de functie van oligodendrocyten bij SOD1^{G93A} muizen

In een volgende stap hebben we in onze Notch-1 SOD1^{G93A} deletie muizen gekeken naar de MCT-1 en MBP expressieniveaus, twee markers voor oligodendrocyten functie. De immunoblots voor MBP en MCT-1 toonden een 32 % en 45 % stijging in MBP en MCT-1 expressie aan voor de Notch-1 deletie muizen in vergelijking met de controle muizen (Figuur 23a,b). Ondanks het beperkt aantal muizen per genotype, werden nu al p-waarden van 0,06 voor MBP en 0,08 voor MCT-1 behaald. Dit wijst erop dat er een trend is en dat Notch-1 deletie een positief effect uitoefent op de myelinisatie en trofische ondersteuning van motor neuronen door oligodendrocyten. In een volgende stap gingen we na of dit positief effect zich ook vertaalt ter hoogte van de neuromusculaire juncties.

Notch-1 deletie resulteert in een verbetering van de EMG amplitudes bij SOD1^{G93A} muizen

Uit de EMG metingen in het SOD1^{G93A} model hebben we kunnen afleiden dat deze techniek veel gevoeliger is voor het evalueren van de motorische eenheid in vergelijking met de hanging wire test en rotarod (Figuur 24). Daarom hebben we deze techniek dan ook toegepast op onze Notch-1 SOD1^{G93A} deletie muizen.

De controle muizen vertoonden op de leeftijd van 72 dagen een amplitude van 40 mV, wat aantoont dat er zich op dit tijdstip reeds axonaal verlies voordeed in de periferie. De Notch-1 SOD1^{G93A} deletie muizen daarentegen, hadden op deze leeftijd nog een amplitude van 60 mV en in het tijdsverloop hierna presteerden deze muizen ook beter op het gebied van amplitude (Figuur 25). De veranderingen in EMG latenties waren subtiel en moeilijk te meten, maar in de Notch-1 SOD1^{G93A} deletie muizen was er een dalende trend in latenties zichtbaar, wijzend op beter geleiding in de periferie.

Notch-1 deletie resulteert in een verbeterde spierinnervatie bij SOD1^{G93A} muizen

Uit de resultaten van de immunoblots voor MCT-1 en MBP konden we afleiden dat Notch-1 een negatieve invloed uitoefent op de trofische ondersteuning en myelinisatie van motor neuronen. De EMG amplitudes waren verbeterd in de Notch-1 SOD1^{G93A} deletie muizen, wijzend op een verbeterde functie van de neuromusculaire unit. Gegeven deze resultaten en het feit dat Notch-1 gekend is om axon retractie te veroorzaken, wilden we het effect van Notch-1 deletie op de spierinnervatie in de Notch-1 SOD1^{G93A} deletie muizen nagaan.

We telden het aantal geïnnerveerde neuromusculaire juncties (NMJs) van de gastrocnemius spier met behulp van α-bungarotoxin en NF-200 kleuringen. Notch-1 SOD1^{G93A} deletie muizen vertoonden een significante 22 % stijging van het aantal volledig geïnnerveerde NMJs vergeleken met de controle muizen (Figuur 26a). Er was geen significant verschil in het aantal partieel geïnnerveerde NMJs (Figuur 26b) en er was een dalende trend in het aantal gedenerveerde NMJs voor de Notch-1 SOD1^{G93A} deletie muizen (Figuur 26c).

CONCLUSIE

In deze studie hebben we aangetoond dat verwijdering van de Notch-1 receptor in bijna alle weefsels van het SOD1^{G93A} muismodel, een voordelig effect heeft op myelinisatie en trofische ondersteuning van motor neuronen en bijgevolg ook op het behoud van de neuromusculaire unit. Op basis hiervan kunnen we zeggen dat Notch-1 signaaltransductie een rol speelt in de pathogenese van ALS. Notch-1 signaaltransductie zou dus een nieuw therapeutisch aangrijpingspunt kunnen vormen in de strijd tegen ALS. Ook andere neurodegeneratieve aandoeningen met oligodendrocyten pathologie zouden op deze manier behandeld kunnen worden.

References

1. Hayashi S, McMahon AP. Efficient recombination in diverse tissues by a tamoxifen-inducible form of Cre: a tool for temporally regulated gene activation/inactivation in the mouse. Dev Biol. 2002 Apr 15;244(2):305-18.
2. Cleveland DW, Rothstein JD. From Charcot to Lou Gehrig: deciphering selective motor neuron death in ALS. Nat Rev Neurosci. 2001 Nov;2(11):806-19.
3. Lee AG. Myelin: Delivery by raft. Curr Biol. 2001 Jan 23;11(2):R60-2.
4. Boillee S, Vande Velde C, Cleveland DW. ALS: a disease of motor neurons and their nonneuronal neighbors. Neuron. 2006 Oct 5;52(1):39-59.
5. Rowland LP, Shneider NA. Amyotrophic lateral sclerosis. N Engl J Med. 2001 May 31;344(22):1688-700.
6. Mulder DW, Kurland LT, Offord KP, Beard CM. Familial adult motor neuron disease: amyotrophic lateral sclerosis. Neurology. 1986 Apr;36(4):511-7.
7. Hugon J. Riluzole and ALS therapy. Wien Med Wochenschr. 1996;146(9-10):185-7.
8. Gordon PH. Amyotrophic lateral sclerosis: pathophysiology, diagnosis and management. CNS Drugs. 2011 Jan;25(1):1-15.
9. Bruijn LI, Miller TM, Cleveland DW. Unraveling the mechanisms involved in motor neuron degeneration in ALS. Annu Rev Neurosci. 2004;27:723-49.
10. Andersen PM, Nilsson P, Keranen ML, Forsgren L, Hagglund J, Karlsborg M, et al. Phenotypic heterogeneity in motor neuron disease patients with CuZn-superoxide dismutase mutations in Scandinavia. Brain. 1997 Oct;120 (Pt 10):1723-37.
11. Andersen PM, Al-Chalabi A. Clinical genetics of amyotrophic lateral sclerosis: what do we really know? Nat Rev Neurol. 2011 Nov;7(11):603-15.
12. Rosen DR. Mutations in Cu/Zn superoxide dismutase gene are associated with familial amyotrophic lateral sclerosis. Nature. 1993 Jul 22;364(6435):362.
13. Andersen PM. The genetics of amyotrophic lateral sclerosis (ALS). Suppl Clin Neurophysiol. 2004;57:211-27.
14. Andersen PM, Nilsson P, Ala-Hurula V, Keranen ML, Tarvainen I, Haltia T, et al. Amyotrophic lateral sclerosis associated with homozygosity for an Asp90Ala mutation in CuZn-superoxide dismutase. Nat Genet. 1995 May;10(1):61-6.
15. Reaume AG, Elliott JL, Hoffman EK, Kowall NW, Ferrante RJ, Siwek DF, et al. Motor neurons in Cu/Zn superoxide dismutase-deficient mice develop normally but exhibit enhanced cell death after axonal injury. Nat Genet. 1996 May;13(1):43-7.
16. Daoud H, Valdmanis PN, Kabashi E, Dion P, Dupre N, Camu W, et al. Contribution of TARDBP mutations to sporadic amyotrophic lateral sclerosis. J Med Genet. 2009 Feb;46(2):112-4.
17. Chio A, Borghero G, Pugliatti M, Ticca A, Calvo A, Moglia C, et al. Large proportion of amyotrophic lateral sclerosis cases in Sardinia due to a single founder mutation of the TARDBP gene. Arch Neurol. 2011 May;68(5):594-8.

18. Neumann M, Sampathu DM, Kwong LK, Truax AC, Micsenyi MC, Chou TT, et al. Ubiquitinated TDP-43 in frontotemporal lobar degeneration and amyotrophic lateral sclerosis. Science. 2006 Oct 6;314(5796):130-3.

19. Vance C, Rogelj B, Hortobagyi T, De Vos KJ, Nishimura AL, Sreedharan J, et al. Mutations in FUS, an RNA processing protein, cause familial amyotrophic lateral sclerosis type 6. Science. 2009 Feb 27;323(5918):1208-11.

20. Tsai CP, Soong BW, Lin KP, Tu PH, Lin JL, Lee YC. FUS, TARDBP, and SOD1 mutations in a Taiwanese cohort with familial ALS. Neurobiol Aging. 2011 Mar;32(3):553 e13-21.

21. DeJesus-Hernandez M, Mackenzie IR, Boeve BF, Boxer AL, Baker M, Rutherford NJ, et al. Expanded GGGGCC hexanucleotide repeat in noncoding region of C9ORF72 causes chromosome 9p-linked FTD and ALS. Neuron. 2011 Oct 20;72(2):245-56.

22. van der Zee J, Gijselinck I, Dillen L, Van Langenhove T, Theuns J, Engelborghs S, et al. A pan-European study of the C9orf72 repeat associated with FTLD: geographic prevalence, genomic instability, and intermediate repeats. Hum Mutat. 2013 Feb;34(2):363-73.

23. Majounie E, Renton AE, Mok K, Dopper EG, Waite A, Rollinson S, et al. Frequency of the C9orf72 hexanucleotide repeat expansion in patients with amyotrophic lateral sclerosis and frontotemporal dementia: a cross-sectional study. Lancet Neurol. 2012 Apr;11(4):323-30.

24. Gijselinck I, Van Langenhove T, van der Zee J, Sleegers K, Philtjens S, Kleinberger G, et al. A C9orf72 promoter repeat expansion in a Flanders-Belgian cohort with disorders of the frontotemporal lobar degeneration-amyotrophic lateral sclerosis spectrum: a gene identification study. Lancet Neurol. 2012 Jan;11(1):54-65.

25. Zu T, Gibbens B, Doty NS, Gomes-Pereira M, Huguet A, Stone MD, et al. Non-ATG-initiated translation directed by microsatellite expansions. Proc Natl Acad Sci U S A. 2011 Jan 4;108(1):260-5.

26. Robberecht W, Philips T. The changing scene of amyotrophic lateral sclerosis. Nat Rev Neurosci. 2013 Apr;14(4):248-64.

27. Gurney ME, Pu H, Chiu AY, Dal Canto MC, Polchow CY, Alexander DD, et al. Motor neuron degeneration in mice that express a human Cu,Zn superoxide dismutase mutation. Science. 1994 Jun 17;264(5166):1772-5.

28. Shibata N. Transgenic mouse model for familial amyotrophic lateral sclerosis with superoxide dismutase-1 mutation. Neuropathology. 2001 Mar;21(1):82-92.

29. Prudencio M, Hart PJ, Borchelt DR, Andersen PM. Variation in aggregation propensities among ALS-associated variants of SOD1: correlation to human disease. Hum Mol Genet. 2009 Sep 1;18(17):3217-26.

30. Shibata N, Hirano A, Yamamoto T, Kato Y, Kobayashi M. Superoxide dismutase-1 mutation-related neurotoxicity in familial amyotrophic lateral sclerosis. Amyotroph Lateral Scler Other Motor Neuron Disord. 2000 Jun;1(3):143-61.

31. Ilieva H, Polymenidou M, Cleveland DW. Non-cell autonomous toxicity in neurodegenerative disorders: ALS and beyond. J Cell Biol. 2009 Dec 14;187(6):761-72.

32. Rothstein JD. Current hypotheses for the underlying biology of amyotrophic lateral sclerosis. Ann Neurol. 2009 Jan;65 Suppl 1:S3-9.

33. Shaw PJ, Eggett CJ. Molecular factors underlying selective vulnerability of motor neurons to neurodegeneration in amyotrophic lateral sclerosis. J Neurol. 2000 Mar;247 Suppl 1:I17-27.

34. Brand MD, Affourtit C, Esteves TC, Green K, Lambert AJ, Miwa S, et al. Mitochondrial superoxide: production, biological effects, and activation of uncoupling proteins. Free Radic Biol Med. 2004 Sep 15;37(6):755-67.

35. Lambert AJ, Brand MD. Reactive oxygen species production by mitochondria. Methods Mol Biol. 2009;554:165-81.

36. Barber SC, Mead RJ, Shaw PJ. Oxidative stress in ALS: a mechanism of neurodegeneration and a therapeutic target. Biochim Biophys Acta. 2006 Nov-Dec;1762(11-12):1051-67.

37. Pardo CA, Xu Z, Borchelt DR, Price DL, Sisodia SS, Cleveland DW. Superoxide dismutase is an abundant component in cell bodies, dendrites, and axons of motor neurons and in a subset of other neurons. Proc Natl Acad Sci U S A. 1995 Feb 14;92(4):954-8.

38. Quaegebeur A, Carmeliet P. Oxygen sensing: a common crossroad in cancer and neurodegeneration. Curr Top Microbiol Immunol. 2010;345:71-103.

39. Yim MB, Kang JH, Yim HS, Kwak HS, Chock PB, Stadtman ER. A gain-of-function of an amyotrophic lateral sclerosis-associated Cu,Zn-superoxide dismutase mutant: An enhancement of free radical formation due to a decrease in Km for hydrogen peroxide. Proc Natl Acad Sci U S A. 1996 Jun 11;93(12):5709-14.

40. Deng HX, Hentati A, Tainer JA, Iqbal Z, Cayabyab A, Hung WY, et al. Amyotrophic lateral sclerosis and structural defects in Cu,Zn superoxide dismutase. Science. 1993 Aug 20;261(5124):1047-51.

41. Yim MB, Chock PB, Stadtman ER. Copper, zinc superoxide dismutase catalyzes hydroxyl radical production from hydrogen peroxide. Proc Natl Acad Sci U S A. 1990 Jul;87(13):5006-10.

42. Wang J, Slunt H, Gonzales V, Fromholt D, Coonfield M, Copeland NG, et al. Copper-binding-site-null SOD1 causes ALS in transgenic mice: aggregates of non-native SOD1 delineate a common feature. Hum Mol Genet. 2003 Nov 1;12(21):2753-64.

43. Son M, Fathallah-Shaykh HM, Elliott JL. Survival in a transgenic model of FALS is independent of iNOS expression. Ann Neurol. 2001 Aug;50(2):273.

44. Shibata N, Hirano A, Kobayashi M, Dal Canto MC, Gurney ME, Komori T, et al. Presence of Cu/Zn superoxide dismutase (SOD) immunoreactivity in neuronal hyaline inclusions in spinal cords from mice carrying a transgene for Gly93Ala mutant human Cu/Zn SOD. Acta Neuropathol. 1998 Feb;95(2):136-42.

45. Bruijn LI, Becher MW, Lee MK, Anderson KL, Jenkins NA, Copeland NG, et al. ALS-linked SOD1 mutant G85R mediates damage to astrocytes and promotes rapidly progressive disease with SOD1-containing inclusions. Neuron. 1997 Feb;18(2):327-38.

46. Johnston JA, Dalton MJ, Gurney ME, Kopito RR. Formation of high molecular weight complexes of mutant Cu, Zn-superoxide dismutase in a mouse model for familial amyotrophic lateral sclerosis. Proc Natl Acad Sci U S A. 2000 Nov 7;97(23):12571-6.

47. Wang J, Xu G, Gonzales V, Coonfield M, Fromholt D, Copeland NG, et al. Fibrillar inclusions and motor neuron degeneration in transgenic mice expressing superoxide dismutase 1 with a disrupted copper-binding site. Neurobiol Dis. 2002 Jul;10(2):128-38.

48. Bruening W, Roy J, Giasson B, Figlewicz DA, Mushynski WE, Durham HD. Up-regulation of protein chaperones preserves viability of cells expressing toxic Cu/Zn-superoxide dismutase mutants associated with amyotrophic lateral sclerosis. J Neurochem. 1999 Feb;72(2):693-9.

49. Bruijn LI, Houseweart MK, Kato S, Anderson KL, Anderson SD, Ohama E, et al. Aggregation and motor neuron toxicity of an ALS-linked SOD1 mutant independent from wild-type SOD1. Science. 1998 Sep 18;281(5384):1851-4.

50. Niwa J, Ishigaki S, Hishikawa N, Yamamoto M, Doyu M, Murata S, et al. Dorfin ubiquitylates mutant SOD1 and prevents mutant SOD1-mediated neurotoxicity. J Biol Chem. 2002 Sep 27;277(39):36793-8.

51. Watanabe M, Dykes-Hoberg M, Culotta VC, Price DL, Wong PC, Rothstein JD. Histological evidence of protein aggregation in mutant SOD1 transgenic mice and in amyotrophic lateral sclerosis neural tissues. Neurobiol Dis. 2001 Dec;8(6):933-41.

52. Rothstein JD, Kuncl R, Chaudhry V, Clawson L, Cornblath DR, Coyle JT, et al. Excitatory amino acids in amyotrophic lateral sclerosis: an update. Ann Neurol. 1991 Aug;30(2):224-5.

53. Rothstein JD, Tsai G, Kuncl RW, Clawson L, Cornblath DR, Drachman DB, et al. Abnormal excitatory amino acid metabolism in amyotrophic lateral sclerosis. Ann Neurol. 1990 Jul;28(1):18-25.

54. Shaw PJ, Forrest V, Ince PG, Richardson JP, Wastell HJ. CSF and plasma amino acid levels in motor neuron disease: elevation of CSF glutamate in a subset of patients. Neurodegeneration. 1995 Jun;4(2):209-16.

55. Couratier P, Sindou P, Esclaire F, Louvel E, Hugon J. Neuroprotective effects of riluzole in ALS CSF toxicity. Neuroreport. 1994 Apr 14;5(8):1012-4.

56. Gibson SB, Bromberg MB. Amyotrophic lateral sclerosis: drug therapy from the bench to the bedside. Semin Neurol. 2012 Jul;32(3):173-8.

57. Heath PR, Shaw PJ. Update on the glutamatergic neurotransmitter system and the role of excitotoxicity in amyotrophic lateral sclerosis. Muscle Nerve. 2002 Oct;26(4):438-58.

58. Van Damme P, Van Den Bosch L, Van Houtte E, Callewaert G, Robberecht W. GluR2-dependent properties of AMPA receptors determine the selective vulnerability of motor neurons to excitotoxicity. J Neurophysiol. 2002 Sep;88(3):1279-87.

59. Fray AE, Ince PG, Banner SJ, Milton ID, Usher PA, Cookson MR, et al. The expression of the glial glutamate transporter protein EAAT2 in motor neuron disease: an immunohistochemical study. Eur J Neurosci. 1998 Aug;10(8):2481-9.

60. Maragakis NJ, Dykes-Hoberg M, Rothstein JD. Altered expression of the glutamate transporter EAAT2b in neurological disease. Ann Neurol. 2004 Apr;55(4):469-77.

61. Rothstein JD, Van Kammen M, Levey AI, Martin LJ, Kuncl RW. Selective loss of glial glutamate transporter GLT-1 in amyotrophic lateral sclerosis. Ann Neurol. 1995 Jul;38(1):73-84.

62. Sasaki S, Komori T, Iwata M. Excitatory amino acid transporter 1 and 2 immunoreactivity in the spinal cord in amyotrophic lateral sclerosis. Acta Neuropathol. 2000 Aug;100(2):138-44.

63. Rothstein JD, Patel S, Regan MR, Haenggeli C, Huang YH, Bergles DE, et al. Beta-lactam antibiotics offer neuroprotection by increasing glutamate transporter expression. Nature. 2005 Jan 6;433(7021):73-7.

64. Dal Canto MC, Gurney ME. Development of central nervous system pathology in a murine transgenic model of human amyotrophic lateral sclerosis. Am J Pathol. 1994 Dec;145(6):1271-9.

65. Liu J, Lillo C, Jonsson PA, Vande Velde C, Ward CM, Miller TM, et al. Toxicity of familial ALS-linked SOD1 mutants from selective recruitment to spinal mitochondria. Neuron. 2004 Jul 8;43(1):5-17.

66. Wong PC, Pardo CA, Borchelt DR, Lee MK, Copeland NG, Jenkins NA, et al. An adverse property of a familial ALS-linked SOD1 mutation causes motor neuron disease characterized by vacuolar degeneration of mitochondria. Neuron. 1995 Jun;14(6):1105-16.

67. Afifi AK, Aleu FP, Goodgold J, MacKay B. Ultrastructure of atrophic muscle in amyotrophic lateral sclerosis. Neurology. 1966 May;16(5):475-81.

68. Hirano A, Donnenfeld H, Sasaki S, Nakano I. Fine structural observations of neurofilamentous changes in amyotrophic lateral sclerosis. J Neuropathol Exp Neurol. 1984 Sep;43(5):461-70.

69. Hirano A, Nakano I, Kurland LT, Mulder DW, Holley PW, Saccomanno G. Fine structural study of neurofibrillary changes in a family with amyotrophic lateral sclerosis. J Neuropathol Exp Neurol. 1984 Sep;43(5):471-80.

70. Kong J, Xu Z. Massive mitochondrial degeneration in motor neurons triggers the onset of amyotrophic lateral sclerosis in mice expressing a mutant SOD1. J Neurosci. 1998 May 1;18(9):3241-50.

71. Higgins CM, Jung C, Xu Z. ALS-associated mutant SOD1G93A causes mitochondrial vacuolation by expansion of the intermembrane space and by involvement of SOD1 aggregation and peroxisomes. BMC Neurosci. 2003 Jul 15;4:16.

72. Beal MF, Hyman BT, Koroshetz W. Do defects in mitochondrial energy metabolism underlie the pathology of neurodegenerative diseases? Trends Neurosci. 1993 Apr;16(4):125-31.

73. Damiano M, Starkov AA, Petri S, Kipiani K, Kiaei M, Mattiazzi M, et al. Neural mitochondrial Ca2+ capacity impairment precedes the onset of motor symptoms in G93A Cu/Zn-superoxide dismutase mutant mice. J Neurochem. 2006 Mar;96(5):1349-61.

74. Richter C, Park JW, Ames BN. Normal oxidative damage to mitochondrial and nuclear DNA is extensive. Proc Natl Acad Sci U S A. 1988 Sep;85(17):6465-7.

75. Browne SE, Bowling AC, Baik MJ, Gurney M, Brown RH, Jr., Beal MF. Metabolic dysfunction in familial, but not sporadic, amyotrophic lateral sclerosis. J Neurochem. 1998 Jul;71(1):281-7.

76. Groeneveld GJ, Veldink JH, van der Tweel I, Kalmijn S, Beijer C, de Visser M, et al. A randomized sequential trial of creatine in amyotrophic lateral sclerosis. Ann Neurol. 2003 Apr;53(4):437-45.

77. Klivenyi P, Ferrante RJ, Matthews RT, Bogdanov MB, Klein AM, Andreassen OA, et al. Neuroprotective effects of creatine in a transgenic animal model of amyotrophic lateral sclerosis. Nat Med. 1999 Mar;5(3):347-50.

78. Shefner JM, Cudkowicz ME, Schoenfeld D, Conrad T, Taft J, Chilton M, et al. A clinical trial of creatine in ALS. Neurology. 2004 Nov 9;63(9):1656-61.

79. Manfredi G, Xu Z. Mitochondrial dysfunction and its role in motor neuron degeneration in ALS. Mitochondrion. 2005 Apr;5(2):77-87.

80. Hollenbeck PJ, Saxton WM. The axonal transport of mitochondria. J Cell Sci. 2005 Dec 1;118(23):5411-9.

81. Perlson E, Maday S, Fu MM, Moughamian AJ, Holzbaur EL. Retrograde axonal transport: pathways to cell death? Trends Neurosci. 2010 Jul;33(7):335-44.

82. Chevalier-Larsen E, Holzbaur ELF. Axonal transport and neurodegenerative disease. Bba-Mol Basis Dis. 2006 Nov-Dec;1762(11-12):1094-108.

83. Hirano A. Cytopathology of amyotrophic lateral sclerosis. Adv Neurol. 1991;56:91-101.

84. Murakami T, Nagano I, Hayashi T, Manabe Y, Shoji M, Setoguchi Y, et al. Impaired retrograde axonal transport of adenovirus-mediated E. coli LacZ gene in the mice carrying mutant SOD1 gene. Neurosci Lett. 2001 Aug 10;308(3):149-52.

85. Williamson TL, Cleveland DW. Slowing of axonal transport is a very early event in the toxicity of ALS-linked SOD1 mutants to motor neurons. Nat Neurosci. 1999 Jan;2(1):50-6.

86. Boillee S, Yamanaka K, Lobsiger CS, Copeland NG, Jenkins NA, Kassiotis G, et al. Onset and progression in inherited ALS determined by motor neurons and microglia. Science. 2006 Jun 2;312(5778):1389-92.

87. Philips T, Robberecht W. Neuroinflammation in amyotrophic lateral sclerosis: role of glial activation in motor neuron disease. Lancet Neurol. 2011 Mar;10(3):253-63.

88. Lee Y, Morrison BM, Li Y, Lengacher S, Farah MH, Hoffman PN, et al. Oligodendroglia metabolically support axons and contribute to neurodegeneration. Nature. 2012 Jul 26;487(7408):443-8.

89. Philips T, Bento-Abreu A, Nonneman A, Haeck W, Staats K, Geelen V, et al. Oligodendrocyte dysfunction in the pathogenesis of amyotrophic lateral sclerosis. Brain. 2013 Jan 31.

90. Gong YH, Parsadanian AS, Andreeva A, Snider WD, Elliott JL. Restricted expression of G86R Cu/Zn superoxide dismutase in astrocytes results in astrocytosis but does not cause motoneuron degeneration. J Neurosci. 2000 Jan 15;20(2):660-5.

91. Lino MM, Schneider C, Caroni P. Accumulation of SOD1 mutants in postnatal motoneurons does not cause motoneuron pathology or motoneuron disease. J Neurosci. 2002 Jun 15;22(12):4825-32.

92. Pramatarova A, Laganiere J, Roussel J, Brisebois K, Rouleau GA. Neuron-specific expression of mutant superoxide dismutase 1 in transgenic mice does not lead to motor impairment. J Neurosci. 2001 May 15;21(10):3369-74.

93. Beers DR, Henkel JS, Xiao Q, Zhao W, Wang J, Yen AA, et al. Wild-type microglia extend survival in PU.1 knockout mice with familial amyotrophic lateral sclerosis. Proc Natl Acad Sci U S A. 2006 Oct 24;103(43):16021-6.

94. Clement AM, Nguyen MD, Roberts EA, Garcia ML, Boillee S, Rule M, et al. Wild-type nonneuronal cells extend survival of SOD1 mutant motor neurons in ALS mice. Science. 2003 Oct 3;302(5642):113-7.

95. Yamanaka K, Chun SJ, Boillee S, Fujimori-Tonou N, Yamashita H, Gutmann DH, et al. Astrocytes as determinants of disease progression in inherited amyotrophic lateral sclerosis. Nat Neurosci. 2008 Mar;11(3):251-3.

96. Hanisch UK, Kettenmann H. Microglia: active sensor and versatile effector cells in the normal and pathologic brain. Nat Neurosci. 2007 Nov;10(11):1387-94.

97. Henkel JS, Beers DR, Zhao W, Appel SH. Microglia in ALS: the good, the bad, and the resting. J Neuroimmune Pharmacol. 2009 Dec;4(4):389-98.

98. Michelucci A, Heurtaux T, Grandbarbe L, Morga E, Heuschling P. Characterization of the microglial phenotype under specific pro-inflammatory and anti-inflammatory conditions: Effects of oligomeric and fibrillar amyloid-beta. J Neuroimmunol. 2009 May 29;210(1-2):3-12.

99. Almer G, Guegan C, Teismann P, Naini A, Rosoklija G, Hays AP, et al. Increased expression of the pro-inflammatory enzyme cyclooxygenase-2 in amyotrophic lateral sclerosis. Ann Neurol. 2001 Feb;49(2):176-85.

100. Alexianu ME, Kozovska M, Appel SH. Immune reactivity in a mouse model of familial ALS correlates with disease progression. Neurology. 2001 Oct 9;57(7):1282-9.

101. Hall ED, Oostveen JA, Gurney ME. Relationship of microglial and astrocytic activation to disease onset and progression in a transgenic model of familial ALS. Glia. 1998 Jul;23(3):249-56.

102. Engelhardt JI, Tajti J, Appel SH. Lymphocytic infiltrates in the spinal cord in amyotrophic lateral sclerosis. Arch Neurol. 1993 Jan;50(1):30-6.

103. Drachman DB, Frank K, Dykes-Hoberg M, Teismann P, Almer G, Przedborski S, et al. Cyclooxygenase 2 inhibition protects motor neurons and prolongs survival in a transgenic mouse model of ALS. Ann Neurol. 2002 Dec;52(6):771-8.

104. Kriz J, Nguyen MD, Julien JP. Minocycline slows disease progression in a mouse model of amyotrophic lateral sclerosis. Neurobiol Dis. 2002 Aug;10(3):268-78.

105. Van Den Bosch L, Tilkin P, Lemmens G, Robberecht W. Minocycline delays disease onset and mortality in a transgenic model of ALS. Neuroreport. 2002 Jun 12;13(8):1067-70.

106. Yrjanheikki J, Tikka T, Keinanen R, Goldsteins G, Chan PH, Koistinaho J. A tetracycline derivative, minocycline, reduces inflammation and protects against focal cerebral ischemia with a wide therapeutic window. Proc Natl Acad Sci U S A. 1999 Nov 9;96(23):13496-500.

107. Sofroniew MV, Vinters HV. Astrocytes: biology and pathology. Acta Neuropathol. 2010 Jan;119(1):7-35.

108. Howland DS, Liu J, She Y, Goad B, Maragakis NJ, Kim B, et al. Focal loss of the glutamate transporter EAAT2 in a transgenic rat model of SOD1 mutant-mediated amyotrophic lateral sclerosis (ALS). Proc Natl Acad Sci U S A. 2002 Feb 5;99(3):1604-9.

109. Levine JB, Kong J, Nadler M, Xu Z. Astrocytes interact intimately with degenerating motor neurons in mouse amyotrophic lateral sclerosis (ALS). Glia. 1999 Dec;28(3):215-24.

110. Gowing G, Philips T, Van Wijmeersch B, Audet JN, Dewil M, Van Den Bosch L, et al. Ablation of proliferating microglia does not affect motor neuron degeneration in amyotrophic lateral sclerosis caused by mutant superoxide dismutase. J Neurosci. 2008 Oct 8;28(41):10234-44.

111. Lepore AC, Dejea C, Carmen J, Rauck B, Kerr DA, Sofroniew MV, et al. Selective ablation of proliferating astrocytes does not affect disease outcome in either acute or chronic models of motor neuron degeneration. Exp Neurol. 2008 Jun;211(2):423-32.

112. Nagy D, Kato T, Kushner PD. Reactive astrocytes are widespread in the cortical gray matter of amyotrophic lateral sclerosis. J Neurosci Res. 1994 Jun 15;38(3):336-47.

113. Schiffer D, Cordera S, Cavalla P, Migheli A. Reactive astrogliosis of the spinal cord in amyotrophic lateral sclerosis. J Neurol Sci. 1996 Aug;139 Suppl:27-33.

114. Sasaki S, Warita H, Abe K, Iwata M. Inducible nitric oxide synthase (iNOS) and nitrotyrosine immunoreactivity in the spinal cords of transgenic mice with a G93A mutant SOD1 gene. J Neuropathol Exp Neurol. 2001 Sep;60(9):839-46.

115. Turner BJ, Ackerley S, Davies KE, Talbot K. Dismutase-competent SOD1 mutant accumulation in myelinating Schwann cells is not detrimental to normal or transgenic ALS model mice. Hum Mol Genet. 2010 Mar 1;19(5):815-24.

116. Lobsiger CS, Boillee S, McAlonis-Downes M, Khan AM, Feltri ML, Yamanaka K, et al. Schwann cells expressing dismutase active mutant SOD1 unexpectedly slow disease progression in ALS mice. Proc Natl Acad Sci U S A. 2009 Mar 17;106(11):4465-70.

117. Kang SH, Li Y, Fukaya M, Lorenzini I, Cleveland DW, Ostrow LW, et al. Degeneration and impaired regeneration of gray matter oligodendrocytes in amyotrophic lateral sclerosis. Nat Neurosci. 2013 May;16(5):571-9.

118. Nave KA. Myelination and support of axonal integrity by glia. Nature. 2010 Nov 11;468(7321):244-52.

119. Jahn O, Tenzer S, Werner HB. Myelin proteomics: molecular anatomy of an insulating sheath. Mol Neurobiol. 2009 Aug;40(1):55-72.

120. Sowell ER, Peterson BS, Thompson PM, Welcome SE, Henkenius AL, Toga AW. Mapping cortical change across the human life span. Nat Neurosci. 2003 Mar;6(3):309-15.

121. Meletis K, Barnabe-Heider F, Carlen M, Evergren E, Tomilin N, Shupliakov O, et al. Spinal cord injury reveals multilineage differentiation of ependymal cells. PLoS Biol. 2008 Jul 22;6(7):e182.

122. Jurynczyk M, Selmaj K. Notch: a new player in MS mechanisms. J Neuroimmunol. 2010 Jan 25;218(1-2):3-11.

123. Pierre K, Pellerin L. Monocarboxylate transporters in the central nervous system: distribution, regulation and function. J Neurochem. 2005 Jul;94(1):1-14.

124. Koehler-Stec EM, Simpson IA, Vannucci SJ, Landschulz KT, Landschulz WH. Monocarboxylate transporter expression in mouse brain. Am J Physiol. 1998 Sep;275(3 Pt 1):E516-24.

125. Pierre K, Pellerin L, Debernardi R, Riederer BM, Magistretti PJ. Cell-specific localization of monocarboxylate transporters, MCT1 and MCT2, in the adult mouse brain revealed by double immunohistochemical labeling and confocal microscopy. Neuroscience. 2000;100(3):617-27.

126. Halestrap AP, Price NT. The proton-linked monocarboxylate transporter (MCT) family: structure, function and regulation. Biochem J. 1999 Oct 15;343 Pt 2:281-99.

127. Rinholm JE, Hamilton NB, Kessaris N, Richardson WD, Bergersen LH, Attwell D. Regulation of oligodendrocyte development and myelination by glucose and lactate. J Neurosci. 2011 Jan 12;31(2):538-48.

128. Benarroch EE. Oligodendrocytes: Susceptibility to injury and involvement in neurologic disease. Neurology. 2009 May 19;72(20):1779-85.

129. Keirstead HS, Blakemore WF. Identification of post-mitotic oligodendrocytes incapable of remyelination within the demyelinated adult spinal cord. J Neuropathol Exp Neurol. 1997 Nov;56(11):1191-201.

130. Redwine JM, Armstrong RC. In vivo proliferation of oligodendrocyte progenitors expressing PDGFalphaR during early remyelination. J Neurobiol. 1998 Nov 15;37(3):413-28.

131. Rivers LE, Young KM, Rizzi M, Jamen F, Psachoulia K, Wade A, et al. PDGFRA/NG2 glia generate myelinating oligodendrocytes and piriform projection neurons in adult mice. Nat Neurosci. 2008 Dec;11(12):1392-401.

132. Zhao C, Deng W, Gage FH. Mechanisms and functional implications of adult neurogenesis. Cell. 2008 Feb 22;132(4):645-60.

133. Levine JM, Reynolds R, Fawcett JW. The oligodendrocyte precursor cell in health and disease. Trends Neurosci. 2001 Jan;24(1):39-47.

134. Keirstead HS, Levine JM, Blakemore WF. Response of the oligodendrocyte progenitor cell population (defined by NG2 labelling) to demyelination of the adult spinal cord. Glia. 1998 Feb;22(2):161-70.

135. Bergles DE, Roberts JD, Somogyi P, Jahr CE. Glutamatergic synapses on oligodendrocyte precursor cells in the hippocampus. Nature. 2000 May 11;405(6783):187-91.

136. Butt AM, Duncan A, Hornby MF, Kirvell SL, Hunter A, Levine JM, et al. Cells expressing the NG2 antigen contact nodes of Ranvier in adult CNS white matter. Glia. 1999 Mar;26(1):84-91.

137. Trotter J, Karram K, Nishiyama A. NG2 cells: Properties, progeny and origin. Brain Res Rev. 2010 May;63(1-2):72-82.

138. Pfeiffer SE, Warrington AE, Bansal R. The oligodendrocyte and its many cellular processes. Trends Cell Biol. 1993 Jun;3(6):191-7.

139. Kondo T, Raff M. Oligodendrocyte precursor cells reprogrammed to become multipotential CNS stem cells. Science. 2000 Sep 8;289(5485):1754-7.

140. Raff MC, Miller RH, Noble M. A glial progenitor cell that develops in vitro into an astrocyte or an oligodendrocyte depending on culture medium. Nature. 1983 Jun 2-8;303(5916):390-6.

141. Zhang SC. Defining glial cells during CNS development. Nat Rev Neurosci. 2001 Nov;2(11):840-3.

142. Niebroj-Dobosz I, Rafalowska J, Fidzianska A, Gadamski R, Grieb P. Myelin composition of spinal cord in a model of amyotrophic lateral sclerosis (ALS) in SOD1G93A transgenic rats. Folia Neuropathol. 2007;45(4):236-41.

143. Baumann N, Pham-Dinh D. Biology of oligodendrocyte and myelin in the mammalian central nervous system. Physiol Rev. 2001 Apr;81(2):871-927.

144. Sanchez-Abarca LI, Tabernero A, Medina JM. Oligodendrocytes use lactate as a source of energy and as a precursor of lipids. Glia. 2001 Dec;36(3):321-9.

145. Walz W, Mukerji S. Lactate production and release in cultured astrocytes. Neurosci Lett. 1988 Apr 12;86(3):296-300.

146. Funfschilling U, Supplie LM, Mahad D, Boretius S, Saab AS, Edgar J, et al. Glycolytic oligodendrocytes maintain myelin and long-term axonal integrity. Nature. 2012 May 24;485(7399):517-21.

147. Li H, Richardson WD. Genetics meets epigenetics: HDACs and Wnt signaling in myelin development and regeneration. Nat Neurosci. 2009 Jul;12(7):815-7.

148. Wang S, Sdrulla AD, diSibio G, Bush G, Nofziger D, Hicks C, et al. Notch receptor activation inhibits oligodendrocyte differentiation. Neuron. 1998 Jul;21(1):63-75.

149. Shawber C, Nofziger D, Hsieh JJ, Lindsell C, Bogler O, Hayward D, et al. Notch signaling inhibits muscle cell differentiation through a CBF1-independent pathway. Development. 1996 Dec;122(12):3765-73.

150. Kwon SM, Alev C, Lee SH, Asahara T. The molecular basis of Notch signaling: a brief overview. Adv Exp Med Biol. 2012;727:1-14.

151. Lathia JD, Mattson MP, Cheng A. Notch: from neural development to neurological disorders. J Neurochem. 2008 Dec;107(6):1471-81.

152. Louvi A, Artavanis-Tsakonas S. Notch and disease: a growing field. Semin Cell Dev Biol. 2012 Jun;23(4):473-80.

153. Bray SJ. Notch signalling: a simple pathway becomes complex. Nat Rev Mol Cell Biol. 2006 Sep;7(9):678-89.

154. Le Borgne R, Bardin A, Schweisguth F. The roles of receptor and ligand endocytosis in regulating Notch signaling. Development. 2005 Apr;132(8):1751-62.

155. Talora C, Campese AF, Bellavia D, Felli MP, Vacca A, Gulino A, et al. Notch signaling and diseases: an evolutionary journey from a simple beginning to complex outcomes. Biochim Biophys Acta. 2008 Sep;1782(9):489-97.

156. Ables JL, Breunig JJ, Eisch AJ, Rakic P. Not(ch) just development: Notch signalling in the adult brain. Nat Rev Neurosci. 2011 May;12(5):269-83.

157. Artavanis-Tsakonas S, Rand MD, Lake RJ. Notch signaling: cell fate control and signal integration in development. Science. 1999 Apr 30;284(5415):770-6.

158. Brou C, Logeat F, Gupta N, Bessia C, LeBail O, Doedens JR, et al. A novel proteolytic cleavage involved in Notch signaling: the role of the disintegrin-metalloprotease TACE. Mol Cell. 2000 Feb;5(2):207-16.

159. Selkoe D, Kopan R. Notch and Presenilin: regulated intramembrane proteolysis links development and degeneration. Annu Rev Neurosci. 2003;26:565-97.

160. Petcherski AG, Kimble J. Mastermind is a putative activator for Notch. Curr Biol. 2000 Jun 29;10(13):R471-3.

161. Borggrefe T, Oswald F. The Notch signaling pathway: transcriptional regulation at Notch target genes. Cell Mol Life Sci. 2009 May;66(10):1631-46.

162. Kovall RA. More complicated than it looks: assembly of Notch pathway transcription complexes. Oncogene. 2008 Sep 1;27(38):5099-109.

163. Jarriault S, Brou C, Logeat F, Schroeter EH, Kopan R, Israel A. Signalling downstream of activated mammalian Notch. Nature. 1995 Sep 28;377(6547):355-8.

164. Wu G, Lyapina S, Das I, Li J, Gurney M, Pauley A, et al. SEL-10 is an inhibitor of notch signaling that targets notch for ubiquitin-mediated protein degradation. Mol Cell Biol. 2001 Nov;21(21):7403-15.

165. Takahashi T, Nowakowski RS, Caviness VS, Jr. Early ontogeny of the secondary proliferative population of the embryonic murine cerebral wall. J Neurosci. 1995 Sep;15(9):6058-68.

166. Li HS, Wang D, Shen Q, Schonemann MD, Gorski JA, Jones KR, et al. Inactivation of Numb and Numblike in embryonic dorsal forebrain impairs neurogenesis and disrupts cortical morphogenesis. Neuron. 2003 Dec 18;40(6):1105-18.

167. Zhong W, Jiang MM, Weinmaster G, Jan LY, Jan YN. Differential expression of mammalian Numb, Numblike and Notch1 suggests distinct roles during mouse cortical neurogenesis. Development. 1997 May;124(10):1887-97.

168. Kageyama R, Ohtsuka T, Kobayashi T. Roles of Hes genes in neural development. Dev Growth Differ. 2008 Jun;50 Suppl 1:S97-103.

169. Presente A, Andres A, Nye JS. Requirement of Notch in adulthood for neurological function and longevity. Neuroreport. 2001 Oct 29;12(15):3321-5.

170. Berezovska O, Xia MQ, Hyman BT. Notch is expressed in adult brain, is coexpressed with presenilin-1, and is altered in Alzheimer disease. J Neuropathol Exp Neurol. 1998 Aug;57(8):738-45.

171. Ehm O, Goritz C, Covic M, Schaffner I, Schwarz TJ, Karaca E, et al. RBPJkappa-dependent signaling is essential for long-term maintenance of neural stem cells in the adult hippocampus. J Neurosci. 2010 Oct 13;30(41):13794-807.

172. Imayoshi I, Sakamoto M, Yamaguchi M, Mori K, Kageyama R. Essential roles of Notch signaling in maintenance of neural stem cells in developing and adult brains. J Neurosci. 2010 Mar 3;30(9):3489-98.

173. Antonini A, Stryker MP. Rapid remodeling of axonal arbors in the visual cortex. Science. 1993 Jun 18;260(5115):1819-21.

174. Carlisle HJ, Kennedy MB. Spine architecture and synaptic plasticity. Trends Neurosci. 2005 Apr;28(4):182-7.

175. Wong RO, Ghosh A. Activity-dependent regulation of dendritic growth and patterning. Nat Rev Neurosci. 2002 Oct;3(10):803-12.

176. Berezovska O, McLean P, Knowles R, Frosh M, Lu FM, Lux SE, et al. Notch1 inhibits neurite outgrowth in postmitotic primary neurons. Neuroscience. 1999;93(2):433-9.

177. Sestan N, Artavanis-Tsakonas S, Rakic P. Contact-dependent inhibition of cortical neurite growth mediated by notch signaling. Science. 1999 Oct 22;286(5440):741-6.

178. Wang Y, Chan SL, Miele L, Yao PJ, Mackes J, Ingram DK, et al. Involvement of Notch signaling in hippocampal synaptic plasticity. Proc Natl Acad Sci U S A. 2004 Jun 22;101(25):9458-62.

179. De Strooper B, Konig G. Alzheimer's disease. A firm base for drug development. Nature. 1999 Dec 2;402(6761):471-2.

180. Park HC, Appel B. Delta-Notch signaling regulates oligodendrocyte specification. Development. 2003 Aug;130(16):3747-55.

181. Mattson MP. Pathways towards and away from Alzheimer's disease. Nature. 2004 Aug 5;430(7000):631-9.

182. Ray WJ, Yao M, Nowotny P, Mumm J, Zhang W, Wu JY, et al. Evidence for a physical interaction between presenilin and Notch. Proc Natl Acad Sci U S A. 1999 Mar 16;96(6):3263-8.

183. Hassan BA, Bermingham NA, He Y, Sun Y, Jan YN, Zoghbi HY, et al. atonal regulates neurite arborization but does not act as a proneural gene in the Drosophila brain. Neuron. 2000 Mar;25(3):549-61.

184. Arumugam TV, Chan SL, Jo DG, Yilmaz G, Tang SC, Cheng A, et al. Gamma secretase-mediated Notch signaling worsens brain damage and functional outcome in ischemic stroke. Nat Med. 2006 Jun;12(6):621-3.

185. Woo HN, Park JS, Gwon AR, Arumugam TV, Jo DG. Alzheimer's disease and Notch signaling. Biochem Biophys Res Commun. 2009 Dec 25;390(4):1093-7.

186. Fleisher AS, Raman R, Siemers ER, Becerra L, Clark CM, Dean RA, et al. Phase 2 safety trial targeting amyloid beta production with a gamma-secretase inhibitor in Alzheimer disease. Arch Neurol. 2008 Aug;65(8):1031-8.

187. Charil A, Filippi M. Inflammatory demyelination and neurodegeneration in early multiple sclerosis. J Neurol Sci. 2007 Aug 15;259(1-2):7-15.

188. John GR, Shankar SL, Shafit-Zagardo B, Massimi A, Lee SC, Raine CS, et al. Multiple sclerosis: re-expression of a developmental pathway that restricts oligodendrocyte maturation. Nat Med. 2002 Oct;8(10):1115-21.

189. Jurynczyk M, Jurewicz A, Bielecki B, Raine CS, Selmaj K. Inhibition of Notch signaling enhances tissue repair in an animal model of multiple sclerosis. J Neuroimmunol. 2005 Dec 30;170(1-2):3-10.

190. Livak KJ, Schmittgen TD. Analysis of relative gene expression data using real-time quantitative PCR and the 2(-Delta Delta C(T)) Method. Methods. 2001 Dec;25(4):402-8.

191. Kolly C, Suter MM, Muller EJ. Proliferation, cell cycle exit, and onset of terminal differentiation in cultured keratinocytes: pre-programmed pathways in control of C-Myc and Notch1 prevail over extracellular calcium signals. J Invest Dermatol. 2005 May;124(5):1014-25.

192. Vogl MR, Reiprich S, Kuspert M, Kosian T, Schrewe H, Nave KA, et al. Sox10 Cooperates with the Mediator Subunit 12 during Terminal Differentiation of Myelinating Glia. J Neurosci. 2013 Apr 10;33(15):6679-90.

193. Dadon-Nachum M, Melamed E, Offen D. The "dying-back" phenomenon of motor neurons in ALS. J Mol Neurosci. 2011 Mar;43(3):470-7.

194. Woodhoo A, Alonso MB, Droggiti A, Turmaine M, D'Antonio M, Parkinson DB, et al. Notch controls embryonic Schwann cell differentiation, postnatal myelination and adult plasticity. Nat Neurosci. 2009 Jul;12(7):839-47.